Aus dem Max von Pettenkofer-Institut für
Hygiene und Medizinische Mikrobiologie
der Ludwig-Maximilians-Universität München
Lehrstuhl: Bakteriologie
Komm. Vorstand: Prof. Dr. Rainer Haas

Modulation of host cell migration by *Legionella pneumophila* effectors and signaling compounds

Dissertation zum Erwerb des Doktorgrades
der Naturwissenschaften an der Medizinischen Fakultät
der Ludwig-Maximilians-Universität zu München

vorgelegt von

Sylvia Simon

aus Wissembourg, Frankreich

2015

Gedruckt mit Genehmigung der Medizinischen Fakultät der
Ludwig-Maximilians-Universität München

Betreuer: Prof. Dr. Hubert Hilbi
Zweitgutachter: Prof. Dr. Alexander Dietrich

Dekan
Prof. Dr. med. Dr. h.c. Maximilian Reiser, FACR, FRCR

Tag der mündlichen Prüfung: 23.09.2015

Summary

The opportunistic bacterium *Legionella pneumophila* causes a severe pneumonia termed „Legionnaires disease" and employs a conserved mechanism to replicate within a specific vacuole in macrophages or protozoa such as the social soil amoeba *Dictyostelium discoideum*. *L. pneumophila* interacts with host cells via the Icm/Dot type IV secretion system (T4SS), which translocates approximately 300 different effector proteins.

In the first part of this thesis, the effects of *L. pneumophila* on migration and chemotaxis of amoebae, macrophages or neutrophils were assessed. Using different migration assays, a dose- and T4SS-dependent inhibition of *D. discoideum* migration towards folic acid was observed as well as the abrogation of starvation-induced aggregation of the social amoebae. Similarly, *L. pneumophila* impaired migration of murine macrophages and neutrophils towards the cytokines CCL5 and TNFα or the peptide fMLP, respectively. *L. pneumophila* lacking LegG1, a T4SS-translocated effector and activator of the small GTPase Ran, caused a hyper-inhibition of *D. discoideum*, macrophage and neutrophil migration. The phenotype was reverted by providing LegG1 on a plasmid to a similar extent as observed for mutant bacteria lacking a functional Icm/Dot T4SS. Likewise, LegG1 promoted random migration of infected macrophages and epithelial cells in a Ran-dependent manner. Single-cell tracking and real-time analysis of *L. pneumophila*-infected phagocytes revealed that the velocity and directionality of the cells were decreased. Moreover, the cell motility as well as microtubule dynamics were impaired. Taken together, these findings suggest that Ran activation by the *L. pneumophila* effector LegG1 and subsequent microtubule polymerization are implicated in Icm/Dot-dependent inhibition of phagocyte migration.

Small molecule signaling promotes the communication between bacteria as well as among bacteria and eukaryotes. *L. pneumophila* employs the autoinducer LAI-1 (3-hydroxypentadecane-4-one) for cell-cell communication. LAI-1 is produced and detected by the Lqs (*Legionella* quorum sensing) system, which regulates a variety of processes including pathogen-host cell interactions and natural competence for DNA uptake. In the second part of this thesis, the role of LAI-1 in inter-kingdom signaling was analyzed.

Summary

Using migration assays, it was shown that *L. pneumophila* lacking the autoinducer synthase LqsA no longer impeded the migration of infected cells and synthetic LAI-1 dose-dependently inhibited cell migration, without affecting uptake, cytotoxicity or intracellular bacterial replication. The forward migration index but not the velocity of LAI-1-treated cells was reduced. Moreover, the microtubule and actin cytoskeleton appeared strongly destabilized. LAI-1-dependent inhibition of cell migration involved the scaffold protein IQGAP1, the small GTPases RhoA and Cdc42 as well as the Cdc42-specific guanine nucleotide exchange factor ARHGEF9. Upon treatment with LAI-1, Cdc42 was inactivated and IQGAP1 redistributed to the cell cortex independently of Cdc42. Thus, under these conditions, IQGAP1 functions upstream of Cdc42. Furthermore, LAI-1 reversed the inhibition of cell migration by *L. pneumophila* in a Cdc42-dependent manner, suggesting that the compound and the bacteria reciprocally target the same signaling pathway. Collectively, the results indicated that the *L. pneumophila* quorum sensing compound LAI-1 inhibits chemotactic and random migration of eukaryotic cells through a signaling pathway comprising IQGAP1, Cdc42 and ARHGEF9.

In summary, the results described in this thesis led to new insights regarding the effect of *L. pneumophila* on host cell migration and identified the effector protein LegG1 as well as the signaling molecule LAI-1 as modulators of chemotaxis processes of phagocytes.

Zusammenfassung

Das opportunistische Bakterium *Legionella pneumophila* infiziert Umweltamöben und verursacht eine schwere Lungenentzündung, die „Legionärskrankheit“ indem es alveolare Makrophagen infiziert. Die intrazelluläre Replikation erfolgt in einer Vakuole mittels des Icm/Dot Typ IV Sekretionssystems (T4SS), durch welches bis zu 300 verschiedene „Effektor“-Proteine in die Wirtszelle eingeschleust werden.

Im ersten Teil dieser Arbeit werden die Effekte einer *L. pneumophila* Infektion auf die Migration und Chemotaxis von Amöben, Makrophagen und Neutrophilen analysiert. Mittels verschiedener Migrationsversuche wurde eine Dosis- und T4SS-abhängige Chemotaxis Inhibition von *D. discoideum* zu Folsäure festgestellt sowie auch der Aushungerungs-induzierten Aggregation. Ebenso wurde eine Hemmung der Chemotaxis von Makrophagen zu CCL5 oder TNFα und von Neutrophilen zu fMLP ermittelt. Eine Infektion mit *L. pneumophila* Mutanten-Stämmen mit fehlendem LegG1 Effektor führte zu einer verstärkten Inhibition der Migration von *D. discoideum*, Makrophagen und Neutrophilen. Dieser Phänotyp konnte revertiert werden, indem LegG1 durch ein Plasmid produziert wurde. Das Migrationsverhalten war vergleichbar mit Zellen, die mit einer Mutante, die kein funktionelles T4SS mehr besitzt, infiziert wurden. Des Weiteren wurde nachgewiesen dass LegG1 die nicht-gerichtete Migration von Epithelzellen in Abhängigkeit der Ran GTPase fördert. Jedoch haben Einzelzellanalysen gezeigt, dass die Geschwindigkeit und die gerichtete Migration von infizierten Phagozyten, durch Beeinträchtigung des Microtubuli-Netzwerkes, reduziert wurden. Diese Experimente liessen den Schluss zu, dass LegG1, welches die GTPase Ran aktiviert, als Antagonist der Icm/Dot-abhängigen Inhibition der Zellmigration wirkt.

L. pneumophila ist in der Lage Zell-Zell-Kommunikation durchzuführen mittels des α-Hydroxyketon (AHK) Autoinduktormoleküls 3-Hydroxypentadekan-4-on (LAI-1: *Legionella* Autoinducer-1). LAI-1 wird produziert und erkannt durch das Lqs (*Legionella* quorum sensing) System, welches wichtige Prozesse reguliert wie Pathogen-Wirtszell-Interaktionen und die natürliche Kompetenz für DNA-Aufnahme. Im zweiten Teil dieser Arbeit wurden die Signaltransduktion und Effekte von LAI-1 auf Wirtszellmigration untersucht.

Zusammenfassung

Anhand verschiedener Migrationsversuche wurde gezeigt, dass eine Infektion mit einem *L. pneumophila* Stamm, welcher die Autoinduktorsynthase LqsA nicht mehr produziert, keine Inhibition der Migration mehr verursacht.

Des Weiteren wurde eine Dosis-abhängige Hemmung der Zellmotilität durch LAI-1 entdeckt, die keine Auswirkung auf Zytotoxizität und bakterielle Aufnahme oder intrazelluläre Replikation hatte. Sowohl die gerichtete Zellmigration als auch das Aktin und Mikrotubuli Netzwerk wurden durch die LAI-1 Zugabe beeinträchtigt. Die LAI-1-abhängige Inhibition der Motilität erfolgt über das Gerüstprotein IQGAP1, ebenso wie über die kleinen GTPasen RhoA und Cdc42 zusammen mit dem spezifischen Aktivator ARHGEF9. Nach LAI-1 Behandlung wurde Cdc42 inaktiviert und IQGAP1 relokalisierte in der Zelle vom Zytoplasma zum Zellkortex. Unter diesen Bedingungen wirkte IQGAP1 hierarschich oberhalb von Cdc42 in der Signalkaskade. Zudem wurde gezeigt, dass LAI-1 die von *L. pneumophila* verursachte Inhibition der Zellmigration in Abhängigkeit von Cdc42 revertiert und somit den selben Signalübertragungsweg reziprok beeinflusste. Zusammengefasst zeigen diese Daten dass LAI-1 die Migration von Wirtszellen inhibiert, indem das Molekül eine Signalkaskade aktiviert, welche IQGAP1, Cdc42 und ARHGEF9 beinhaltet.

Die im Rahmen dieser Arbeit präsentierten Ergebnisse liefern neue Erkenntnisse bezüglich des Einflusses von *L. pneumophila* Effektor Proteinen und Signalmolekülen auf die Zellmigration.

Contents

Contents

List of figures

Contents

List of tables

I. Introduction

A. Pathogenesis of *Legionella pneumophila*

1. From environmental sources to disease

In the summer of 1976, over 200 persons attending the 58th American Legion´s convention in Philadelphia began to fall ill presenting mysterious symptoms ranging from fever to coughing over breathing difficulties [1, 2]. Serum analysis and infected lung extracts allowed the identification of the Gram-negative bacterium *Legionella pneumophila* to be responsible for this explosive outbreak of pneumonia [3]. Besides causing pneumonia, an infection with *L. pneumophila* does not have to be life-threatening and can also cause influenza-like symptoms termed Pontiac fever. The family *Legionellaceae* comprises over 50 species with several serogroups; yet over 90% of human infections are caused by *L. pneumophila* [4, 5]. The exception is Australia and New Zealand, where *Legionella longbeachae,* found also associated with plants and soil, is the most common causative agent [6].

The aerobic bacterium can survive and replicate in biofilms as well as in free living protozoa including *Dictyostelium discoideum*, *Acanthamoeba castellanii* and *Hartmanella vermiformis* as well as in man-made aquatic systems, such as cooling towers, whirlpools and showers [7, 8]. To date, no transmission between humans has been reported. Evolutionary adaptation, based on horizontal gene transfer, allows *L. pneumophila* to persist in a variety of extra- and intracellular niches [9, 10]. The environment inside protozoa or biofilms protect the bacteria from physical and chemical threats, such as antibiotics, radiation, high temperatures, biocides and detergents [11]. The temperature range of replication is between 25 – 42 °C, where 35 °C is the optimal growth condition [12]. Upon inhalation of contaminated aerosols, the bacterium employs a conserved mechanism to replicate within alveolar macrophages of the innate immune system. *L. pneumophila* possesses a biphasic life cycle and alternates between a replicative, non virulent and a transmissive, virulent phase (Figure 1) [13].

The opportunistic pathogen uses a type IV secretion system (T4SS; section A.2) to secrete a plethora of effector proteins, which guarantee intracellular replication by subverting host signaling pathways (section A.3).

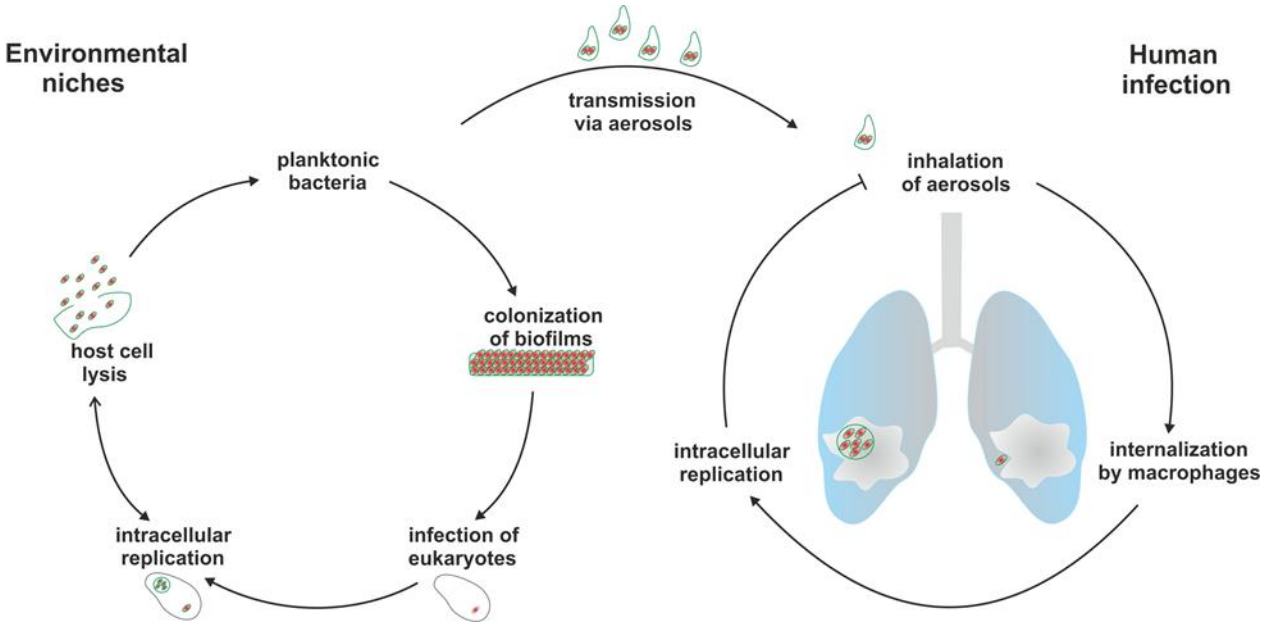

Figure 1. Environmental cycle of *Legionella* spp. and human infection.
Legionella spp. survive in the environment as planktonic bacteria, colonize biofilms and multiply in free-living protozoa. After release from their replicative niches, transmission happens via inhalation of bacteria-containing aerosols. Highly virulent bacteria infect and replicate in alveolar macrophages, thus triggering inflammation and the severe pneumonia called "Legionnaires' disease".

2. The Icm/Dot type IV secretion system

T4SS are employed by many pathogenic bacteria to govern virulence, DNA transfer [14], conjugation [15] and transport of effector proteins [16, 17]. Bacterial uptake and growth as well as the subversion of host cell processes are promoted by the translocation of so-called effector proteins. Numerous proteins have been described to interfere with cellular pathways, such as small GTPase activation [18], retrograde trafficking [19] or ubiquitinylation and apoptotis [20]. The key virulence component of *L. pneumophila* is the Icm/Dot (intracellular multiplication/defective for organelle trafficking) system exporting over 300 different effector proteins into the host cell [21, 22]. Those proteins are able to interfere with numerous pathways by targeting small GTPases, microtubule-dependent cascades as well as phosphoinositide (PI) metabolism.

The T4SS is composed of two large subcomplexes including 27 proteins. Five cytoplasmic and 17 inner membrane associated proteins have been identified as well as one periplasmic and four outer membrane proteins (Figure 2). The first complex consists of DotC, DotD, DotF (IcmG), DotG (IcmE) and DotH (IcmK) and connects the inner and outer membrane of *L. pneumophila*. DotF and DotG represent inner membrane proteins whereas DotC and DotD are two outer membrane lipoproteins interacting with DotH [17, 23]. The second subcomplex, localized at the inner membrane, consists of five proteins: DotL (IcmO), DotM (IcmP), DotN (IcmJ), IcmS and IcmW [24]. DotL regulates the secretion apparatus and creates a link between the subtrates and the transport machinery. IcmS and IcmW are adaptor proteins controlling the selection of secreted proteins [25, 26]. Those chaperone-like proteins are required for the export of SdeA, SidA, SidB, SidD, SidF, SidG and SidH [23]. Furthermore, three supplementary cytoplasmic proteins, DotB, IcmQ and IcmR, were described to be involved in the assembly of the T4SS and formation of pores in the cell membrane. In addition to the T4SS, *L. pneumophila* harbors four other secretion systems [27]. The Lss T1SS consists of three proteins; the ABC (ATP binding cassette) transporter, a membrane fusion protein and an outer membrane protein [28]. No substrates have been identified for the T1SS yet. The type II Lsp system consists of a membrane spanning apparatus and translocates several enzymes such as phosphatases, lipases or chitinases [27]. Together with the T4SS, the T2SS represents the most important system required for infection and modulation of host cell immune responses. The Lvh T4SS contains 11 genes homologous to other T4SS and is implicated in conjugation and DNA transfer [27, 29]. Last, a putative T5SS was identified in the *L. pneumophila* Paris strain [27, 30]. Composition or substrates of this secretion system have not been identified yet.

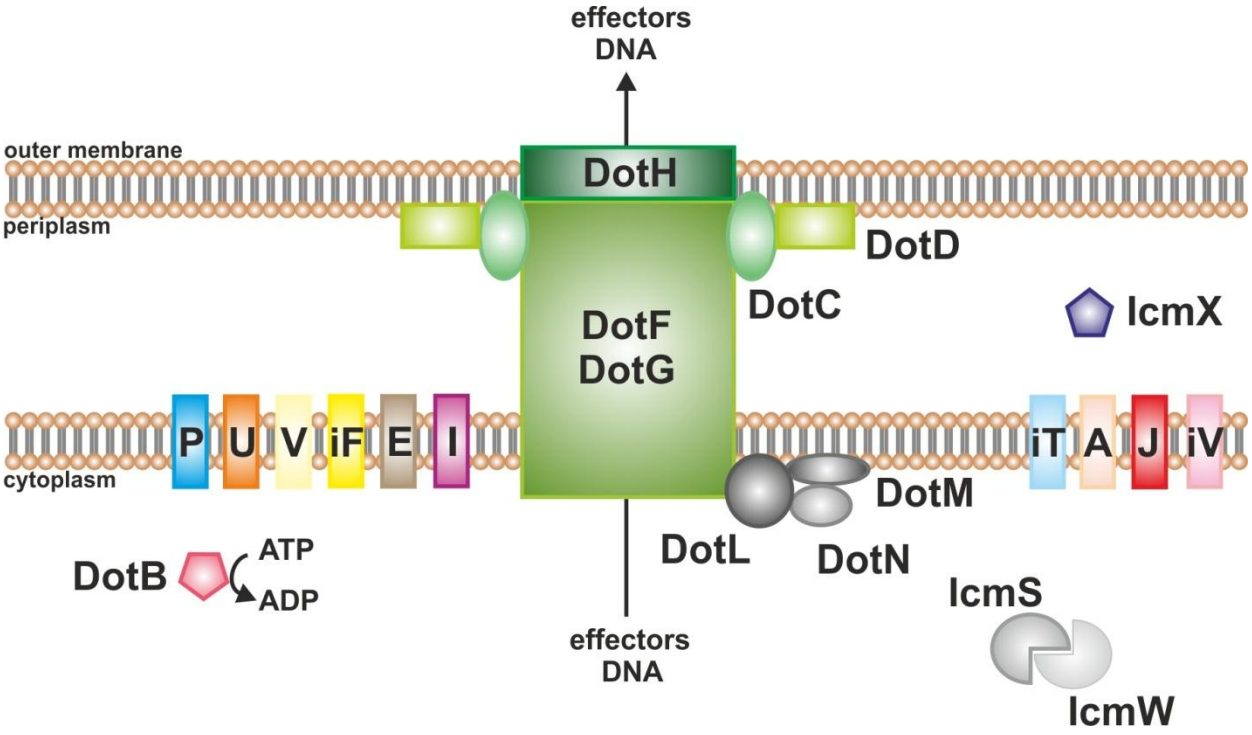

Figure 2. The Icm/Dot T4SS.
The T4SS is composed of 27 proteins divided in two main complexes allowing the transport of bacterial proteins and DNA. The core subcomplex includes DotF, DotG, DotH, DotC and Dot D (green). The second complex is composed of the coupling protein DotL bridging the effector proteins with the transport apparatus, DotM, DotN, IcmS and IcmW (grey). IcmX was identified as a periplasmic protein and DotB as a hexameric ATPase regulating the assembly of the T4SS and the selection of effector proteins. Model adapted from [25, 26].

3. Host cell infection

L. pneumophila enters the host cell through actin-dependent phagocytosis, a process in which the T4SS plays an essential role (Figure 3) [31, 32]. Adhesion and entry are the primary steps of the infection conducted by several effectors including SdeA (LaiA), LadC, EnhC and LpnE [33, 34, 35, 36]. Immediately after internalization, the bacterium resides in a membrane-bound compartment termed the *Legionella*-containing vacuole (LCV) and avoids fusion with lysosomes in an Icm/Dot T4SS-dependent manner [37]. Numerous Icm/Dot substrates of *L. pneumophila* are involved in this important step. For example, SidK inhibits phagosomal acidification required for bacterial lysis by targeting VatA, the catalytic subunit of the vacuolar H^+-ATPase, which is necessary to establish an acidic environment [38]. Furthermore, the effector LegC3 was proposed to counteract membrane fusion events thus protecting the bacteria [39, 40].

In addition, vacuole protein sorting (VPS) inhibitors such as VipA, VipD and VipF are able to block lysosomal trafficking through multiple mechanisms [41]. Moreover, bacterial lipopolysaccharide (LPS) molecules circumvent lysosomal killing in an effector-independent way [42]. Shorlty after LCV formation, many docking events take place leading to the recruitment of mitochondria, smooth vesicles from the endoplasmic reticulum (ER) and later ribosomes [43, 44].

Establishement of LCVs is coordinated by the use of PIs, phosphorylated derivates of phosphatidylinositol (PtdIns) and small GTPases [45, 46]. Proteome analysis revealed that over 560 host proteins decorate the LCV including small GTPases of the secretory (Arf1, Rab1, Rab8) or endosomal (Rab7, Rab14) vesicle trafficking cascades [47].

PtdIns(3)P and PtdIns(4)P represent relevant PIs involved in endosomal and secretory trafficking. The effector protein SidC is localized on the LCV and was described to promote LCV/ER fusion and bind to PtdIns(4)P via its N-terminal and C-terminal part, respectively [48, 49, 50]. LidA promotes the recruitment of early secretory vesicles to the LCV and interacts with Rab1, Rab6 and Rab8 as well as with PtdIns(3)P and PtdIns(4)P [51, 52]. Moreover, the effector protein LpnE binds PtdIns(3)P and host enzymes like human OCRL1 as well as the *D. discoideum* homologue Dd5P4, which is involved in PI metabolism [52, 53, 54]. Notably, the phosphoinositide 3-kinase (PI3K) also plays a role in bacterial uptake and vesicle trafficking [48]. The Icm/Dot substrate SidM also interacts with PtdIns(4)P, exhibits Rab1 guanine nucleotide exchange factor (GEF) activity and catalyses the AMPylation of Rab1, Rab8 and Rab14 [46, 52, 55]. This effector creates a link between the exploitation of small GTPases and PI lipids. Lastly, RalF was identified as an Icm/Dot T4SS effector protein, which is not binding PIs but is responsible for the recruitment and activation of the ADP-ribosylation factor 1 (Arf1), thus influencing membrane transport and organelle structure [56, 57].

After LCV formation is completed, *L. pneumophila* switches from a transmissive into a replicative phase allowing proliferation of the bacteria. The substrate AnkB was described to be essential for intravacuolar replication by subverting the polyubiquinylation machinery. The proteolytic removal of effectors from the LCV favors intracellular propagation [58]. Also, the effector RavZ inhibits autophagy during *L. pneumophila* infection by targeting autophagy related proteins (Atg8), thus allowing intracellular replication [59].

For termination of the replicative cycle, the bacteria might be released by non-lytic egress via the effectors LepA and LepB or pore formation [60, 61]. Subsequently, *L. pneumophila* can start a new infection cycle and persist in the environment by colonizing biofilms or reinfect host cells.

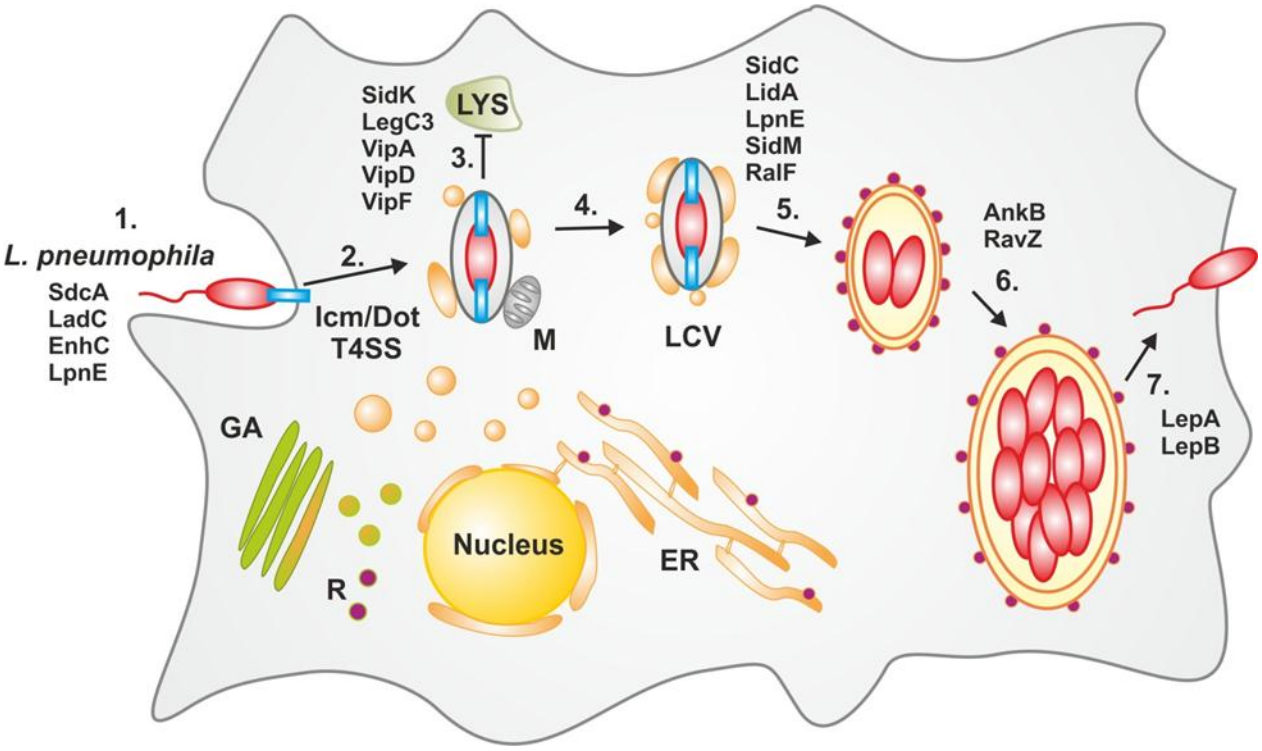

Figure 3. Infection cycle of *L. pneumophila*.
The intracellular transmissive and replication phases of *L. pneumophila* can be divided in seven main steps: 1. Adhesion and entry into the host cell via phagocytosis; 2. Formation of the LCV in an Icm/Dot T4SS-dependent manner and recruitement of vesicles from the ER as well as mitochondria; 3. Evasion from the lysosomal trafficking; 4. Fusion of surrounding ER vesicles with the LCV; 5. The compartment becomes a rough-ER-like vacuole and 6. allows bacterial replication; 7. *L. pneumophila* is released and can reinfect new host cells or be transmitted to other environmental niches. Relevant Icm/Dot-translocated effectors involved in the different steps are indicated in black. Model adapted from [25].
Abbreviations: ER: endoplasmic reticulum; GA: Golgi apparatus; LCV: *Legionella*-containing vacuole; LYS: lysosome; M: mitochondria; R: ribosomes; T4SS: type IV secretion system.

B. Effect of *L. pneumophila* on microtubule dynamics and cell migration

1. Microtubule polymerization and function in eukaryotic cell processes

a. Microtubule organization

The cytoskeleton is composed of microtubules, microfilaments and intermediate filaments. Microtubule dynamics are essential for various vital cell processes including cell adhesion, protrusion formation, mitosis and cell migration. Microtubules, found in all dividing eukaryotic cells, are long cylindrical polymers formed of α– and β–tubulin monomers. They are arranged into protofilaments in a head-to-tail fashion which bind laterally to create a hollow tube. Two ends are discernable; a plus-end where β-tubulin is exposed and faster assembled and a minus-end characterized by the exposure of slowly assembled α-tubulin [62]. The centrosome is the main microtubule organization center (MTOC) responsible for the assembly of tubulin into microtubules. Their intrinsic dynamic behaviour is regulated at the plus-end by microtubule associated proteins (MAPs), influencing thereby multiple steps in cell migration, numerous signaling pathways and interactions with organelles or other cytoskeletal components. Furthermore, microtubule-associated motor proteins like kinesin and dynein as well as transport vesicles mediate the function of microtubules. The regulation of microtubule dynamics also implicates a transition between polymerization (growth) and depolymerization (shrinkage). A „microtubule catastrophe" reflects an interruption in growth, caused by a sudden loss of protection, possibly age- or length-dependent [63]. The switch depends on the presence of a GTP-cap at the end of the microtubule. Incorporation of a GTP-tubulin allows polymerization, whereas one of a GDP-tubulin, triggered through GTP hydrolysis, more likely promotes depolymerization of the microtubule [64]. Numerous different rescue events can be initialized through various rescue sites, e.g., mediated by GTP-islands hidden in the lattice structure of the microtubule [65].

b. Role in mitosis

Mitosis corresponds to the segregation of chromosomes into two daughter cells. This process happens during each cell cycle and is dependent on the formation of a mitotic apparatus.

The separation requires a proper positioning of the mitotic spindle composed of microtubules, motors and associated proteins. Plus-ends of microtubules attach to chromosomes through a protein structure localized on chromatin centromeres, called kinetochores. There are three groups of spindle microtubules: kinetochores fibers with their plus-ends attached to chromosomes, interpolar microtubules arising from one spindle pole to the other and astral microtubules pointing to the cortex via their plus-end [66]. Microtubule dynamics (growth and shrinkage) allow a lateral and end-on cell attachment and transport of kinetochores to the spindle pole. This happens on both sides of the cell and is termed bi-orientation. Microtubule forces permit the chromosomal alignment of the spindle to the center allowing chromatid separation. This is guided by the recruitment of plus-ending tracking proteins termed TIPs [67]. The microtubule-dependent cell division is essential for homeostasis and tissue development.

c. Implication in cell adhesion

The capacity of cells to interact with the underlying extracellular matrix (ECM) at so called „focal adhesions" (FA) sites generates the required force for directed cell migration. FA, formed at the leading edge of a cell, are targeted by microtubules. They are responsible for the delivery of receptors involved in cell adhesion like integrins [68]. These transmembrane proteins couple the ECM to the actin network and recruit FA components to modulate microtubules and the activity of RhoGTPases. In return, microtubule dynamics are able to influence FA by controlling their disassembly and thus creating mechanical forces [69]. Interplay between adhesion sites, force generation, contractility and cytoskeletal components are vital for correct directed cell motility.

d. Role in cell migration

Cell migration is a fundamental multistep process present in single cells as well as in multicellular organisms and describes random and directed movement through the body. It is essential in immune responses, cancer, wound healing and tissue development/renewal [62]. Directed cell migration can be induced by surface-bound stimuli, a gradient of soluble chemoattractants or by the presence of intracellular signals.

Eukaryotic immune cells use chemotaxis to move from the blood to site of infections as well as between the vascular and lymphatic system. Upon stimulation of membrane receptors by chemoattractive coumpounds such as pro-inflammatory cytokines or bacterial components (LPS, flagellin), the cell polarizes by forming a distinct front and rear side, dependent on the creation of a protrusion at the leading edge, positioning of the nucleus and reorientation of the MTOC [70, 71]. In response to such signals, an actin-dependent extension of the cell membrane (protrusion) is formed at the cell front (lamellipodium or filopodium) and allows the cell to move forward. Furthermore, in order to create a cell protrusion, most cells rely on actin polymerization and microtubule dynamics through their signaling properties and crosslinking with intermediate filaments. Microtubules can act directly or indirectly by delivering small RhoGTPases like the cell division control protein (Cdc42) and the Ras-related-activating protein (Rac1) together with their regulators to the cell membrane and influencing their activities [72]. Indeed, the activity of Cdc42 in association with an intracellular PI gradient regulate the polarization pathway during motility.

A rise of phosphatidylinositol-3,4,5-triphosphate (PIP3) is generated by the activation of PI3K at the leading edge and the phosphatase and tensin homolog (PTEN) at the back [73]. A polarity center is formed at the plasma membrane between the master regulator Cdc42-GTP and the partitioning defective (Par) complex composed of Par6/atypical protein kinase C (aPKC)/Par3 [74]. Additionally, the formation of a front-rear axis is promoted by the Cdc42-dependent regulation of microtubule plus end tracking protein (CTIPs) like the cytoplasmic linker protein of 170 kDa (CLIP-170). The interaction between Rac1/Cdc42 with CLIP-170 and the Ras GTPase-activating-like protein (IQGAP1, section A.2.a.) at the leading edge contributes to a polarized microtubule array [75]. Cell adhesion, contraction and retraction represent key steps of the migration cycle. As described above, microtubules control dynamics of focal adhesion complexes and integrin-mediated adhesion. In concert with cell retraction regulated by the small GTPase Ras homolog gene family member A (RhoA) located at the rear edge and retraction of the cell body, the required force for pulling the rear of the cell forward is generated.

D. discoideum amoebae represent a powerful tool in the analysis of directed migration. Indeed, the social amoebae produce cyclic adenosine 3′,5′-monophosphate (cAMP) and aggregate chemotactically under starvation conditions [76, 77].

In order to survive, fruiting bodies and spores can then be formed. Genes encoding components necessary for the signaling cascade are up-regulated such as cAMP receptors. Four have been identified and termed cAR1-4. cAR1 and cAR3 are involved in early developmental states whereas cAR2 and cAR4 are important during late developmental phases [78]. As described for eukaryotic cells, the signaling cascade comprises a stimulation of membrane receptors, the production of PIP3 by PI3K as well as the activation of Ras and small GTPases [79, 80, 81]. This leads to the formation of pseudopods and subsequent directed migration. During a normal life cycle, *D. discoideum* amoebae sense folic acid gradients allowing their movement in search of bacteria [82]. As mentioned, actin polarization is essential and causes through polymerization pseudopod formation at the leading edge and via depolymerization retraction at the trailing edge [78].

In summary (Figure 4), the bidirectional organization of the microtubule network ranging from the leading edge to the rear edge and the activity of small GTPases coordinate cell protrusion, polarization, adhesion, contraction and retraction necessary for directed cell migration [62].

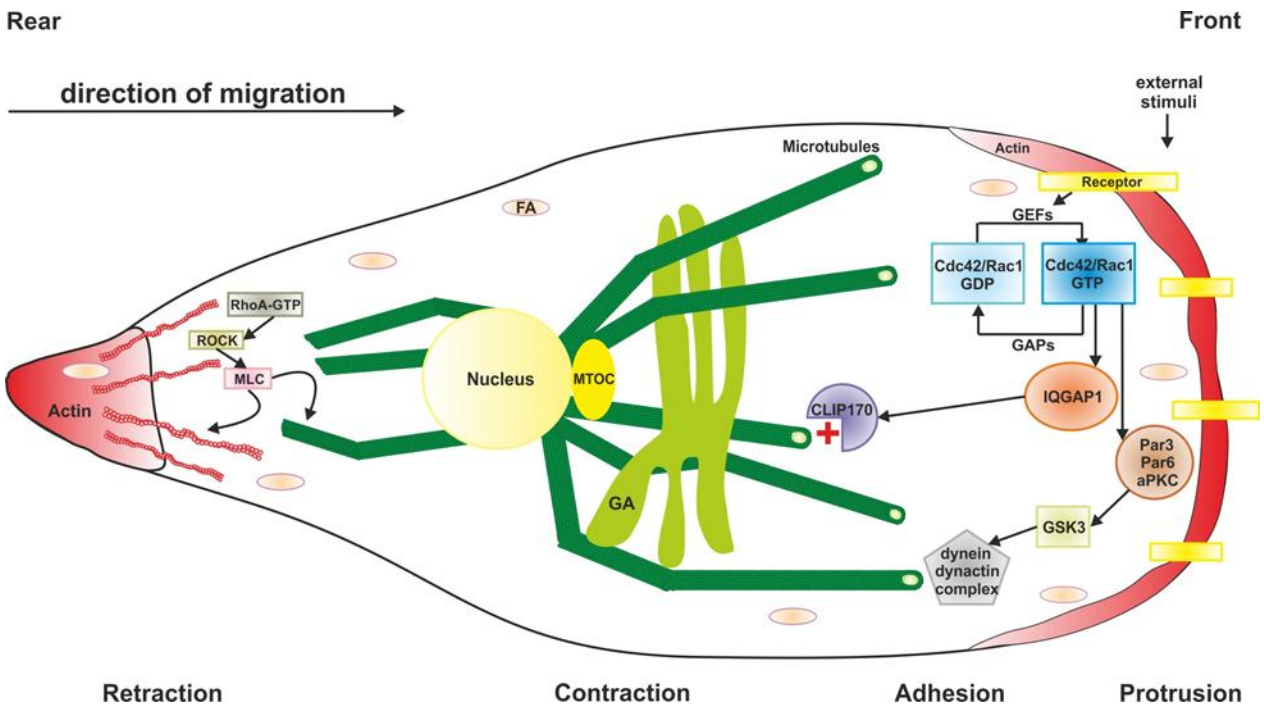

Figure 4. Schematic representation of cell migration.
The migration cycle can be divided into four major steps: protrusion at the leading edge, cell adhesion and contraction to generate the required forces and retraction at the rear edge. Microtubule dynamics and the actin cytoskeleton in concert with RhoGTPases are fundamental components of each phase. Abbreviations: aPKC: atypical protein kinase C; Cdc42: cell division control protein 42; CLIP170: cytoplasmic linker protein 170; FA: focal adhesion; GA: Golgi apparatus; GAP: GTPase activating protein; GEF: guanine nucleotide exchange factor; GSK3: glycogen synthase kinase 3; IQGAP1: Ras GTPase-activating protein; MLC: myosin light chain; MTOC: microtubule organizing center; Par3/6: partitioning defective 3/6 homolog; Rac1: Ras-related C3 botulinum toxin substrate 1; RhoA: Ras homolog gene family member A; ROCK: Rho-associated protein kinase.

2. The bacterial effector LegG1 stabilizes microtubule polymerization

a. The Ran cycle

Recent proteomics studies of purified LCVs identified over 560 host proteins including a plethora of small GTPases. Among those, the Ras-related nuclear protein (Ran) and its effector RanBP1 were found to be LCV components. Ran is a member of the Ras superfamily of small GTPases and regulates many essential functions like nucleo-cytoplasmic transport, mitosis and regulation of microtubule dynamics. Like other GTPases, Ran exists in an activated GTP-bound and in an inactivated GDP-bound form.

Activation happens in the nucleus via the Ran guanine nucleotide exchange factor (RanGEF) termed RCC1 (regulator of chromosome condensation 1). The cytoplasmic Ran GTPase activating protein (RanGAP1), together with RanBP1, orchestrates the inactivation of Ran [83]. As mentioned, Ran plays a crucial role in nuclear transport during interphase. Over 20 nuclear transport receptors (NTRs) have been identified, among them importin-α, importin-β and exportin, controlled by RanGTP, which are the main factors regulating cargo delivery. A gradient of RanGTP and RanGDP is maintained at high levels in the nucleus and the cytosol, respectively, and is the driving mechanism for nuclear transport. Cargo proteins leaving the nucleus are associated with exportins and those imported are combined with importins via their nuclear localization signal (NLS) and nuclear export signal (NES) tags, respectively. In the nucleus, RanGTP is maintained at a high concentration by RCC1 and dissociated from the formed nuclear import signal [84, 85]. Furthermore, RanGTP forms in the nucleus a complex with proteins exhibiting leucine-rich nuclear export signals. After translocation of the complex through the nuclear pore, RanGTP is released from its cargo proteins in the cytosol through GTP hydrolysis converting Ran into its inactivated RanGDP form. In the cytosol, the gradient is preserved by RanGAP in combination with RanBP1 and RanBP2 [86].

Besides its main role in nuclear transport, RanGTP is essential for the regulation of the mitotic spindle assembly in dividing cells. Early findings using fluorescence energy transfer (FRET) in *Xenopus laevis* eggs revealed RCC1 to possess high affinity for chromatin and to maintain a gradient of RanGTP around the mitotic chromosomes.

Nuclear export and import signals dissociated from RanGTP function as SAFs (spindle assembly factors) and allow the recruitment of proteins to specific sites of the spindle apparatus during mitosis [87]. Additionally, the high RanGTP concentration leads to microtubule nucleation close to chromatin whereas low concentrations located further away stabilizes the centrosomal microtubules [88]. These data indicate that Ran activation in mitotic cells controls the assembly of microtubule spindles and the nucleo-cytoplasmic transport.

b. LegG1, a novel RanGTPase activator

Recently, the Icm/Dot-translocated effector *Legionella* eukaryotic gene 1 (LegG1) was identified as the first prokaryotic Ran activator (Figure 5). The *L. pneumophila* protein LegG1 (alias PieG, Lpg1976) is encoded in the plasticity island of effectors (Pie) gene cluster and possesses an amino acid homology to the RanGEF RCC1 [89, 90]. The *legG1* gene is conserved among all *L. pneumophila* strains sequenced to date. The C-terminal CAAX tetrapeptide motif of LegG1 is lipidated by the host prenylation machinery to accomodate the targeting of bacterial protein to host membranes [91]. Proteomics data and fluorescence microscopy show that Ran, its effector RanBP1 and LegG1 localize to LCVs in an Icm/Dot-dependent manner. Using LCVs harboring Δ*legG1* mutant bacteria, LegG1 was identified to be able to catalyze the activation of Ran and to promote the accumulation of RanBP1 on LCVs. Moreover, LegG1 is a virulence factor which promotes intracellular replication of *L. pneumophila* and LCV motility [18, 92]. As Ran controls microtubule assembly and microtubule-dependent trafficking, LegG1 influences microtubule dynamics. Different approaches including siRNA treatment to knock-out LegG1 and microbial microinjection of the effector protein using the *Yersinia* T3SS toolbox confirmed that the *L. pneumophila* effector is implicated in microtubule polymerization in amoebae and macrophages [18]. These findings paved the way for new studies to elucidate the effect of LegG1 on host cell migration.

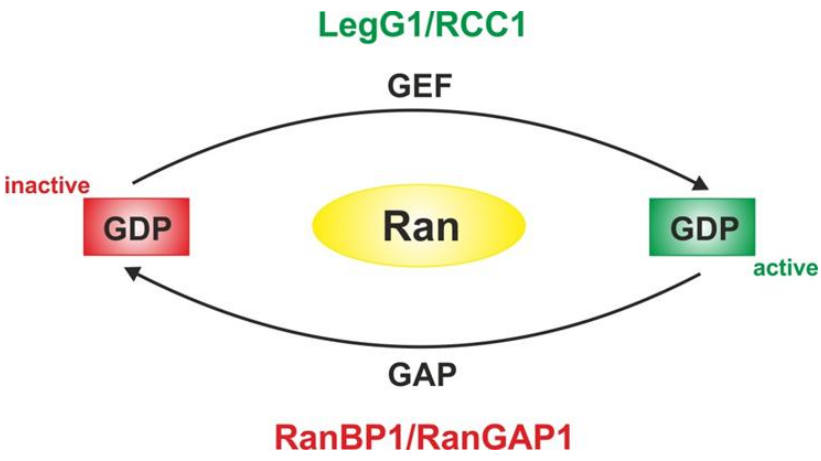

Figure 5. The Ran cycle.
The small GTPase Ran switches between two forms: an active GTP-bound and an inactive GDP-bound form. RanGEFs such as RCC1 mediate the conversion of RanGDP into RanGTP. RanGAPs for example RanBP1 or RanGAP1 converse RanGTP in its inactive mode through GTP-hydrolysis. LegG1 has been identified as a *L. pneumophila* effector able to activate Ran.
Abbreviations: GAP: GTPase activating protein; GEF: guanine nucleotide exchange factor.

C. Pathogen-host cell interaction

1. Quorum sensing systems in bacteria

Research in quorum sensing (QS) started in the late 1960s and was described as a process allowing bacteria to perform cell-cell communication. The system is ubiquitously found in bacteria and frequently comprises a two-component system (TCS) using a sensor histidine kinase and a response regulator [93]. Around 1970, the groups of Nealson and Eberhard identified the first density sensing mechanism in the Gram-negative marine bacterium *Vibrio fischeri* reviewed in reference [94]. This led to the establishment of a basic model incorporating the production, detection and integration of signaling molecules termed autoinducers (AIs). A certain threshold concentration is required for response, which is dependent on the cell density of the bacterial population called the quorum. The AI concentration increases simultaneously with the growing bacterial population. Bacteria use QS to track changes in cell density and coordinate gene expression for many processes including virulence, biofilm formation, sporulation, competence and bioluminescence [95]. QS systems can be divided into two major groups: the oligopeptide system employed by Gram-positive bacteria and the LuxI-LuxR system used by Gram-negative bacteria (Figure 6).

a. Quorum sensing in Gram-positive bacteria

Gram-positive bacteria employ autoinducer peptides (AIPs) which can modify the expression of genes involved in competence, e.g., in *Streptococcus pneumonia* or *Bacillus subtilis*, or virulence, e.g., in *Listeria monocytogenes*, *Enterococcus faecalis*, *Staphylococcus aureus* or *Bacillus cereus* [96]. *S. aureus*, present in the skin flora and responsible for pneumonia and sepsis, employs a QS system encoded by the *agr* (accessory gene regulator) operon and can be described as a model for Gram-positive bacteria [97]. It is composed of four essential components; the propeptide AgrD encodes the proAIP processed to its active form by a multifunctional endopeptidase, AgrB. AgrC is the membrane-bound histidine kinase and binds the extracellularly accumulating AIP and autophosphorylates it.

A phosphate group is transferred from a conserved histidine of AgrC to a conserved aspartate of AgrA, thereby activating AgrA. The resulting activation of the promoters P2 and P3 triggers the up-regulation of the *agr* operon and promotes the expression of virulence factors [98].

b. Quorum sensing in Gram-negative bacteria

The QS circuit of the bacterium *V. fischeri* is responsible for the induction of lumiscence and produces a diffusible autoinducer molecule (*N*-(3-oxohexanoyl)-homoserine lactone (3-oxo-C6-HSL)) via the LuxI-LuxR system [94]. Furthermore, two additional QS systems have been described, the AinS-AinR and the LuxS-LuxP/Q systems producing C8-HSL and AI-2, respectively. However, most Gram-negative bacteria use homologues of the LuxI-LuxR QS system to perform cell-cell communication. This is the case for the bacterium *Vibrio cholerae*, the causative agent of the disease cholera. The main symptoms are diarrhea and dehydration triggered by the cholera toxin, the production of which is dependent on QS. Two autoinducer molecules are synthesized: (S)-3-hydroxytridecan-4-one (CAI-1) and a furanosyl borate diester (AI-2) produced by the kinases CqsA and LuxS, respectively [95]. The signals are detected by CqsS and LuxPQ, thus triggering the phosphorylation of the common response regulator LuxO. Consequently, the expression of *qrr1-4* (quorum regulatory sRNAs) genes is activated, which positively regulates biofilm formation at low cell density in *V. cholera*e [99].

During the last decade, QS has been well described in the bacterium *Pseudomonas aeruginosa*, which is an opportunistic, highly adaptable pathogen causing chronic and acute infections in immune-deficient humans and is found in lungs from persons suffering from cystic fibrosis. This bacterium harbors two LuxI-LuxR homologous QS systems and one PQS circuit which integrate two chemically distinct classes of signaling molecules, the *N*-acylhomoserine lactones (AHLs) and the quinolones [100]. The first pathway comprises the LuxI homologue LasI which synthesizes the homoserine lactone 3O-C_{12}-HSL detected by the cytoplasmic LuxR homologue LasR. The second pathway includes a LuxI homologue termed RhlI responsible for the production of C4-HSL detected by RhlR. Additionally, *P. aeruginosa* employs a third circuit, the *Pseudomonas* quinolone system (PQS) to control cooperative responses and biofilm formation [101].

This system comprises the autoinducer synthase *pqsABCDH* synthetizing PQS and the transcription regulator PqsR binding the AI molecule. The different QS molecules target genes including those encoding virulence factors like elastase, rhamnosyltransferase, proteases, the stationary phase sigma factor σ^S and toxic lectins. Besides promoting host cell interactions and regulating virulence, the Vikstrom group showed that AHL molecules from *P. aeruginosa* influence epithelial cell migration in an IQGAP1-dependent manner (section C.2.c) [102]. Furthermore, AHL-12 was described to induce neutrophil migration by altering the phosphorylation state of p38 (mitogen-activated protein kinase) and LSP1 (leukocyte specific protein 1) crucial for actin polymerization [103]. The AHLs, PQS and quinolone signaling molecules possess immune-modulatory functions by inhibiting cytokine release and immune cell activation [104]. Clear evidence has now been obtained that prokaryotes and eukaryotes communicate via signaling molecules through a process called inter-kingdom signaling.

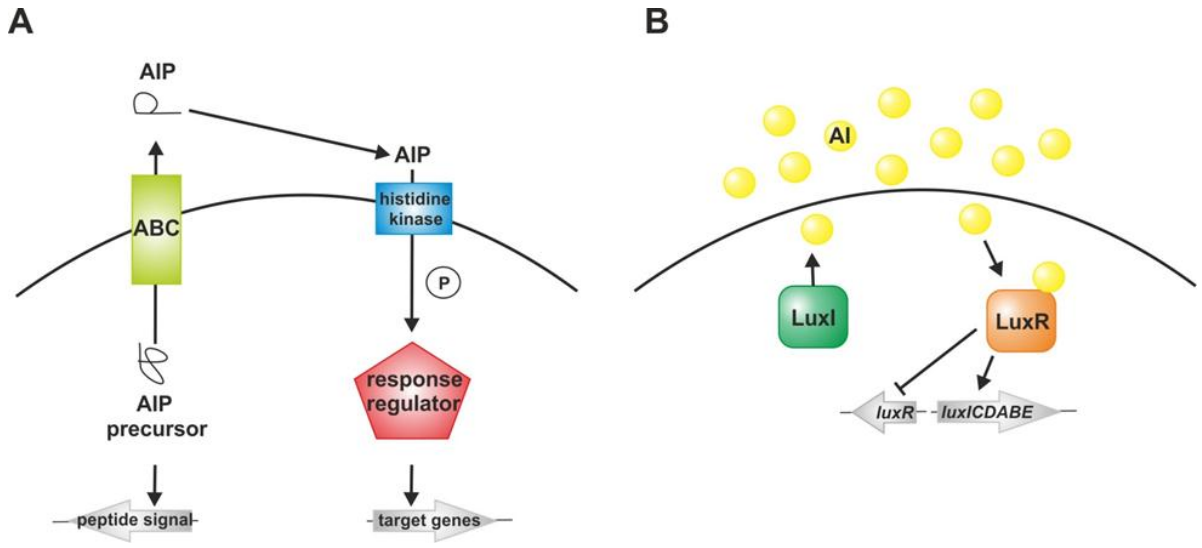

Figure 6. Representative models for QS systems in Gram-positive and -negative bacteria.
A. In Gram-positive bacteria, an AIP molecule is synthesized, processed into its active form and transported out of the cell via the ABC transporter. Once the threshold concentration is reached, the signal is detected by a histidine sensor kinase which auto-phosphorylates and transfers the phospho-group to the conserved aspartate of the response regulator. This leads to the transcription activation of various target genes.
B. The QS circuit of the Gram-negative *V. fischeri* comprises two proteins, LuxI and LuxR encoded by the *luxI* and *luxR* genes, respectively. LuxI synthesizes the AI molecule 3-oxo-C6-HSL. At high bacterial density, the intra- and extracellular AI concentration increases and allows the formation of a LuxR-HSL complex. The transcription of the *luxICDABE* operon induces light production and activates through the binding of this complex the corresponding promoter.
Abbreviations: ABC: ATP-binding cassette; AI: autoinducer; AIP: autoinducer peptide.

c. Quorum sensing in *L. pneumophila*

L. pneumophila uses an endogenously synthetized AHK (alpha-hydroxyketone) autoinducer molecule to perform cell-cell communication during the stationary growth phase. The components of the *L. pneumophila* QS circuit are encoded by the *Legionella* quorum sensing (*lqs)* gene cluster (*lpg2731-2734*) and composed of the autoinducer synthase LqsA producing the AI molecule *Legionella* autoinducer-1 (LAI-1), the sensor kinase LqsS and the response regulator LqsR. Furthermore, LqsT (*lpg2506*) was recently described as a novel LAI-1 responsive sensor kinase during AHK signaling (Figure 7) [105].

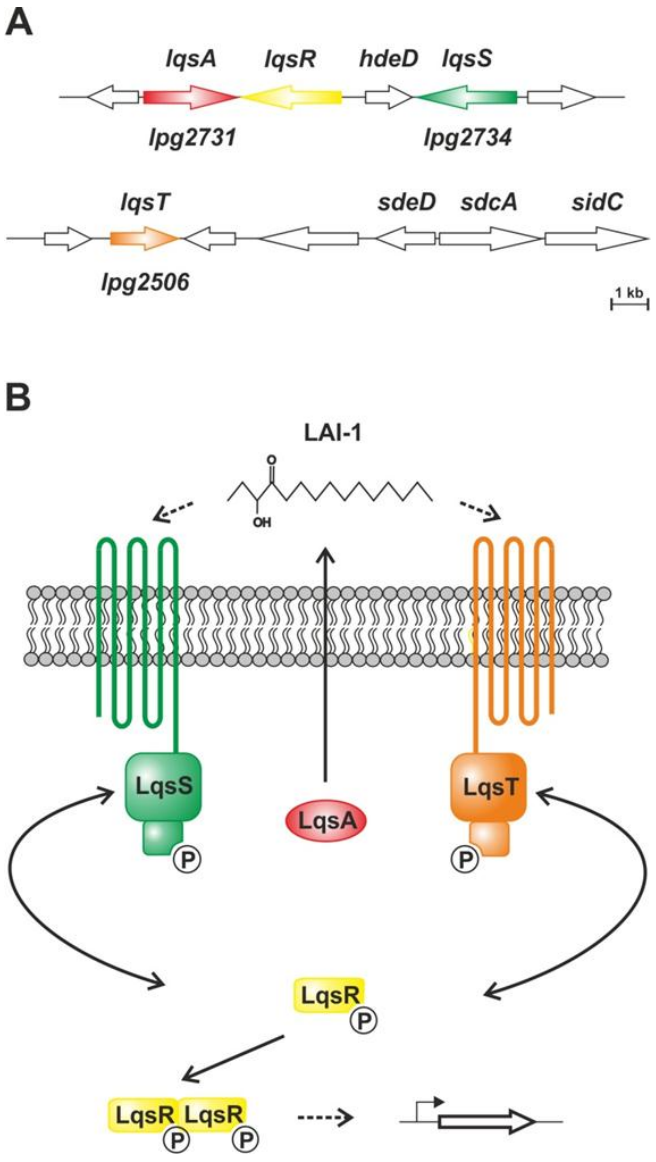

Figure 7. The *L. pneumophila lqs* gene cluster and LAI-1 signaling circuit.
A. The autoinducer synthase LqsA, the response regulator LqsR and the cognate sensor kinase LqsS are located in the *lqs* gene cluster *(lpg2731-lpg2734*). The orphan sensor kinase *lqsT* is located close to the effector genes *sdeD*, *sdcA* and *sidC*.
B. The autoinducer signaling molecule 3-hydroxypentadecane-4-one LAI-1 is produced by LqsA and detected by LqsS and LqsT. The signal is transmitted through the response regulator LqsR. Phosphorylation reactions lead to the dimerization of LqsR. Dashed arrows represent hypothetical interactions.
Abbreviations: LAI-1: *Legionella* autoinducer 1; Lqs: *Legionella* quorum sensing.

LqsA shares 45% homology with CqsA and can partially complement the depletion of *cqsA* in *V. cholera*, thus displaying functional similarities. The autoinducer synthase LqsA exhibits a conserved lysine residue which binds to pyridoxal-5´-phosphate. Strains lacking *lqsA* are mildly defective for pathogen-host interactions [106]. LqsS is 29% identical to CqsS and a member of the six transmembrane helix two component sensor histidine kinases family. Mutant strains lacking *lqsS* show impairment in salt resistance and virulence. Also, the up-regulation of a „fitness island" encoding metal ion transport systems and pilus components was described for Δ*lqsS* strain [107]. Interestingly, it was recently observed that this phenotype can be reversed by an overexpression of *lqsA*, leading to the identification of a novel sensor kinase LqsT. The orphan *lqsT* gene (*lpg2506*) located near the effector genes *sdeD*, *sdcA* and *sidC*, is expressed from its own promoter and shares 31% homology to LqsS. In comparison to wild-type *L. pneumophila*, strains lacking *lqsS* or *lqsT* displayed enhanced salt resistance and alterations in uptake by phagocytes. Additionally, LqsS and LqsT are antagonistic sensors; indeed, 90% of genes down-regulated in Δ*lqsT* strains were up-regulated in strains lacking *lqsS* [105]. The response regulator LqsR, also encoded in the *lqs* cluster, stimulated host-pathogen interactions, suppressed replication and is an element of the stationary phase regulatory network. Its production is dependent on the LetA/LetS two-component system and the sigma factor RpoS (σ38). LetA induces the expression of small non-coding RNAs which sequester the repressor of virulence traits CsrA. RpoS in concert with LetA positively acts on LqsR by inducing the transmission phenotype (virulence and motility). Compared to wild-type, strains lacking *lqsR* and/or *lqsS* presented a reduced sedimentation due to the formation of extracellular filaments [108]. Furthermore, it was recently shown that phosphorylation signaling via LqsS and LqsT converges on LqsR. LqsS and LqsT are autophosphorylated and are bound by LqsR or phospho-LqsR. After phosphorylation on its conserved aspartate residue (D108), LqsR was able to form dimers [109]. QS autoinducers regulate a plethora of signaling pathways including eukaryotic cell migration as described in *P. aeruginosa*. These findings led us to address the question of whether LAI-1 might affect host cell motility.

2. Involvment of IQGAP1 in cell migration and quorum sensing signaling

a. The IQGAP family of proteins and interacting targets

The IQGAP family of proteins was identified in numerous organisms ranging from yeast to mammals. Three IQGAPs have been isolated in humans, termed IQGAP1, IQGAP2 and IQGAP3 [110]. Described for the first time in 1994, IQGAP1 is the best-studied family member and a ubiquitously expressed scaffold protein. Numerous functions have been associated with IQGAP1, for example the regulation of the cytoskeleton, microbial infection, cell-cell contact and cell migration. Furthermore, changes in expression levels of IQGAP1 have been related to cancer progression. IQGAP1 is a multidomain protein (Figure 8) which can bind to over 90 different interaction partners. Binding occurs through five main domains. First, the calponin homology domain in the N-terminal part associates reversibly with F-actin, thus enhancing actin polymerization. The WW domain of IQGAP1 is involved in the mitogen-activated protein kinase (MAPK) cascade and oncogenic signaling in cancer by modulating epidermal growth factor receptor (EGFR) activation. The IQ motif targets calmodulin, a calcium-binding protein and reduces the interaction with other IQGAP1 targets. A Ras GTPase-activating protein related domain (GRD) is responsible for the modulation of the cytoskeleton by interacting with two Rho GTPases, Cdc42 and Rac1. Finally, the C-terminal domain termed RasGAP C-terminal (RCG) binds to E- and β-cadherin as well as CLIP-170 a microtubule-binding protein affecting cell adhesion and capture of microtubules [111]. IQGAP2 and IQGAP3 share 62% and 57% identity with IQGAP1, respectively. IQGAP2, predominantly confined to the liver, has been associated with gastric cancer. Similarly, IQGAP3 expression is mainly localized to the brain, lung and intestines and contributes to tumorgenesis by interacting with the EGFR signaling pathway, modulating target partners like Ras and Cdc42. Homologues of IQGAP proteins have been identified in yeast and amoebae [112]. The fission yeast *Schizosaccharomyces pombe* possesses a single IQGAP, termed Rng2, which is involved in the formation and contraction of the actomyosin ring during cytokinesis. Rng2 together with other kinases allows the maturation of cytokinesis proteins, called nodes, which results in the recruitment of actin and myosin to the contractile ring.

The localization of Rng2 to the nodes is dependent on the GRD and RCG domain in the C-terminal part of the IQGAP protein. Nodes condense into bundles, reorganize the plasma membrane and permit the separation of the cell into two daughter cells [113, 114, 115]. Likewise, in the budding yeast *Saccharomyces cerevisiae*, Iqg1/Cyk1 is the only member of the IQGAP family. Iqg1 is also responsible for the recruitment of actin and myosin to the contractile ring at the cell division site [116, 117]. Interestingly, in *D. discoideum*, three of four identified proteins have been characterized and termed DdIQGAP1, DdIQGAP2 and DdIQGAP3. DdIQGAP1 has an impact on cell polarity and regulation of the actin cytoskeleton by modulating the Rho GTPase Rac1 [118]. DdIQGAP2, together with DdIQGAP1 and DdIQGAP3, which have overlapping functions, is implicated in chemotaxis and cell motility [119].

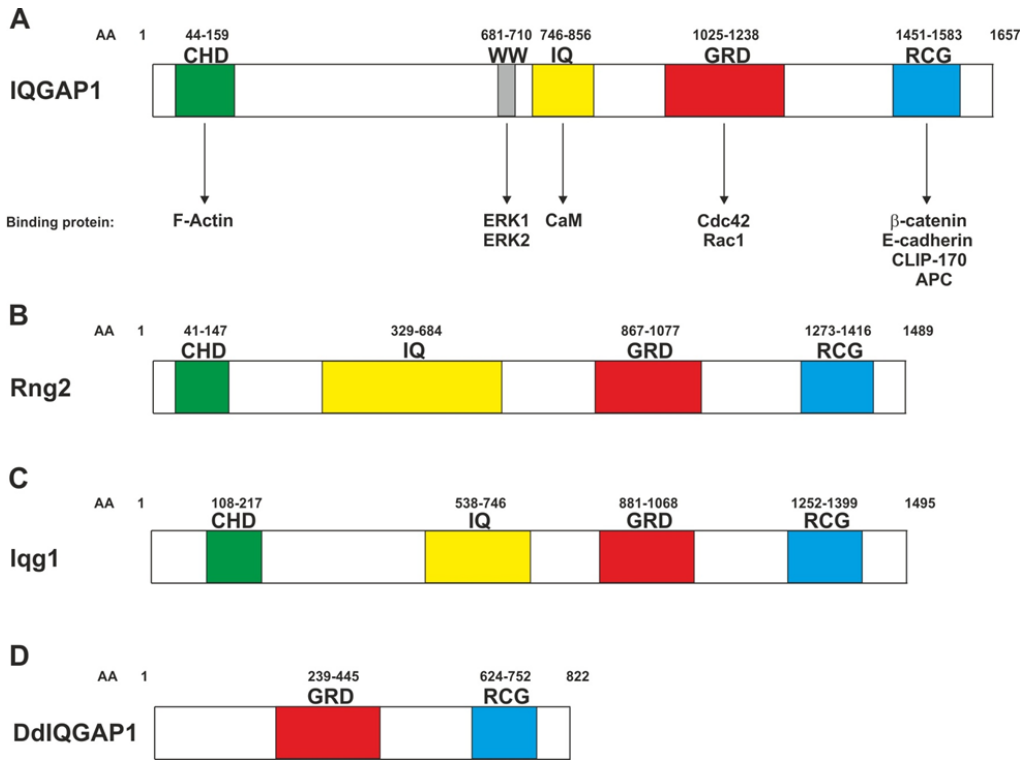

Figure 8. The domain structure of IQGAP proteins in mammals, yeast and amoebae.
Schematic diagrams of human IQGAP1 and homologues are represented showing the regions of interactions with *in vitro* identified target proteins.
Abbreviations: AA: amino acid; CHD: calponin homology domain; GRD: Ras GTPase-activating protein-related domain; IQ: IQ domain containing four IQ motifs; RCG: RasGAP C-terminal; WW: polyproline binding domain. Numbers correspond to amino acid residues. Homologues of IQGAP proteins have been identified in other species: B, Rng2 in *S. pombe*; C, Iqg1 in *S. cerevisiae* and D, DdIQGAP1 in *D. discoideum*.

b. The Rho family of GTPases

IQGAP1 is a Ras GTPase activating protein which can bind to many target proteins and regulate several cell functions. It targets Rho GTPases like Cdc42 (Cdc42-GTP), Rac1, but also E- and β-cadherin, CLIP170 as well as actin. Rho family GTPases are key regulators in cell migration, polarization and reorganization in the microtubule and actin network, essential steps during inflammation reactions, wound healing, development and tumor invasion.

Cdc42, Rac1 and RhoA are the best characterized and most important small GTPases during cell migration [120]. These GTPases cycle between an inactive GDP-bound form and an active GTP-form. The GTPase activity is regulated through GEFs, GAPs and GDIs (GDP dissociation inhibitors). Approximately 80 GEFs have been identified in the human genome and can be classified into two families, the Dbl family with 69 members and the DOCK family with 11 members [121]. Proteins of the Dbl family, which function upstream of Rho GTPases, share a Dbl homology (DH) catalytic domain responsible for the GDP-GTP exchange reaction and a pleckstrin homology (PH) domain located C-terminally to the DH domain. β-PIX (PAK interacting exchange factor) is the best described family member and activates Cdc42 and Rac1 [122]. DOCK family proteins, divided into four groups (DOCK A-D), contain a Dock homology region 1 and 2, DHR1 and DHR2, which play a similar role as the PH-DH domain of Dbl proteins. DHR1 is essential for phospholipid binding and DHR2 for the GEF activity. DOCK A and B members possess a N-terminal Src homology (SH3) domain and mostly act on Rac1 (DOCK180), whereas DOCK D members (DOCK9 and 10) preferentially activate Cdc42 [123, 124]. Little is known about members of the DOCK C group. Table 1 summarizes the Rho-GEFs, GAPs and GDIs most significant for cell migration [112, 125, 126, 127, 128, 129]. Importantly, however, IQGAP1 does not function as a normal GAP by ending the signaling activity of RhoGTPases, but is able to inhibit the GTPase activity of Cdc42 and stabilizing it in its active GTP-bound form [130].

	Target	Localization	Function
RhoGEF-Bcl family			
Asef1 (ARHGEF4)	Cdc42/RhoA/Rac1	cytoplasma	migration/adhesion
α-PIX (ARHGEF6)	Rac1	cell projection	migration
β-PIX (ARHGEF7)	Rac1	cell junction/cytoplasma	migration/attachement
RhoGEF9 (ARHGEF9)	Cdc42	cytoplasma	migration
Ephexin4 (ARHGEF16)	Cdc42/Rac1	cytoplasma	chemotactic migration
FGD1	Cdc42	cell projection/cytoplasma	regulation of the actin cytoskeleton
Ect2	Cdc42/RhoA/Rac1	nucleus/cytoplasma/cell junction	cytokinesis/cell polarity
Tiam1	Rac1/(Cdc42)	membrane/cytoplasma/cell junction	migration/adhesion
RhoGEF-DOCK family			
DOCK1	Rac1	membrane/cytoplasma	polarization
DOCK2	Rac1	membrane/cytoplasma	polarization
DOCK3	Rac1	membrane/cytoplasma	migration/polarization
DOCK10/DOCK11	Cdc42	membrane/cytoplasma	migration/contractility
RhoGAPs			
RhoGAP1 (ARHGAP1)	Cdc42/RhoA/Rac1	cytoplasma	convert GTP to GDP
RhoGAP15 (ARHGAP15)	Rac1	membrane/cytoplasma	"
RhoGAP17 (ARHGAP17)	Cdc42/(Rac1)	membrane/cytoplasma/cell junction	polarization/adhesion
RhoGAP21 (ARHGAP21)	Cdc42/RhoA	cytoplasma/cell junction	adhesion
RhoGAP31 (ARHGAP21)	Cdc42/Rac1	cell projection/cell junction	polarization/migration
RhoGDIs			recycling of GTPases/migration
Rho dissociation inhibitor 1 (ARHGDIA)	Cdc42/RhoA/Rac1	cytoplasma	
Rho dissociation inhibitor 2 (ARHGDIB)	RhoA	cytoplasma	
Rho dissociation inhibitor 3 (ARHGDIG)	RhoB	cytoplasma	

Table 1. RhoGEFs, GAPs and GDIs involved in cell migration.
Abbreviations: Asef: APC-stimulated guanine exchange factor 1; Cdc42: cell division control protein 42; DOCK: dedicator of cytokinesis; Ect2: epithelial cell transforming sequence 2 oncogene; GAP: GTPase activating protein; GDI: guanosine nucleotide dissociation inhibitor; GEF: guanine nucleotide exchange factor; PIX: PAK interacting exchange factor; Rac1: Ras-related C3 botulinum toxin substrate 1; Tiam1: T-lymphoma invasion and metastasis-inducing protein1.

c. Effect of quorum sensing signals on cell migration

Recently, it was described that bacterial QS signals (section C.2.a.) have an impact on the behavior of human cells. The QS AHL molecule N-acylhomoserine lactone from the Gram-negative bacterium *P. aeruginosa* impaires the migration of intestinal epithelial cells by interacting with IQGAP1 and inducing changes in the phosphorylation pattern of Cdc42 and Rac1. Furthermore, the AHL signal influences the localization of IQGAP1 in the cell and also colocalizes with the protein. Cdc42- and Rac1-dependent dynamics of the actin cytoskeleton are altered and help the bacterium to invade and infect more efficiently the cell itself and neighbouring cells. Only cell migration seems to be modified and not cell proliferation or viability [102].

The immune-modulatory effect of AHL is reflected by an up-regulation of the production of pro-inflammatory cytokines like IL-6 (interleukin-6) in bronchial epithelial cells of a cystic fibrosis lung [131]. Additionally, AHL molecules induce apoptosis coordinated by an increase of cytosolic calcium [132]. Surprisingly, the effect of homoserine lactone molecules depends on the exposed cell type. Paes *et al*., describe a positive influence of the QS signal from *P. aeruginosa* regarding re-epithelialization [133]. Migration of keratinocytes is improved during wound healing due to an enhanced expression of the matrix metallopeptidase 13 (Mmp13) gene dependent on the activator protein 1 (AP1) signaling pathway. In conclusion, QS molecules trigger, through inter-kingdom signaling, essential changes in the migration behavior of immune cells by altering crucial steps during the regulation of actin cytoskeleton, calcium signaling and immune responses in which IQGAP1 and RhoGTPases seem to be main actors.

D. Aims of the thesis

Cell migration and chemotaxis play major roles in a broad range of physiological events including immune responses against bacterial invaders. *L. pneumophila* is able to translocate approximately 300 different effector proteins into host cells, thus influencing their migration behavior. The aim of this thesis was to gain insights into the modulation of immune cell migration after a *L. pneumophila* infection. By the use of murine macrophages, neutrophils and *D. discoideum* amoebae, the influence of the bacteria on directed migration was to be examined through the analysis of the forward migration index and velocity in chemotactic under-agarose assays. Previous work demonstrated that the effector protein LegG1 is able to activate the small Ran GTPase and to interfere with the microtubule network. Another goal was to test the possible Ran-dependent effect of LegG1 on cell motility and thus on microtubule polymerization.

Furthermore, *L. pneumophila* is capable to perform cell-cell communication via the production and sensing of the signaling molecule LAI-1. An additional aspect analyzed in this work was the influence of LAI-1 on host cell migration. The aim was to increase our knowledge regarding the motility parameters affected and host cell proteins involved in the signaling cascade of LAI-1. This thesis provides new insights into these processes and allowed the identification of implicated bacterial effector proteins and compounds involved in inter-kingdom signaling.

II. Materials and Methods

A. Materials

1. Laboratory equipment

Table 2. Equipment

Equipment	Manufacturer
Autoclave Varioklav classic	H+P (Oberschleißheim)
Benchtop centrifuge 5417R	Eppendorf (Hamburg)
Confocal microscope Leica TCS SP5	Leica (Mannheim)
Culture microscope Primo Vert	Zeiss (Oberkochen)
Electrophoresis chamber Mini-Protean 3	Bio-Rad (Munich)
Gel imaging system ChemiDoc MP System	Bio-Rad (Munich)
Gel imaging system GelDoc EQ	Bio-Rad (Munich)
Hot plate magnetic stirrer RCT basic	IKA (Staufen)
Ice maker AF30	Scotsman (Vernon Hills)
Incubator Heraeus BR6000	Thermo (Waltham)
Incubator Heraeus Function Line	Thermo (Waltham)
Incubator IPP500	Memmert (Schwabach)
pH-meter Level 1	inoLab (Weilheim)
Pipettes Pipetman	Gilson (Middleton)
Pipettor Pipetus	Hirschmann (Eberstadt)
Power supply PAC100	Bio-Rad (Munich)
Precision balance BP61-S	Sartorius (Goettingen)
Precision balance PG2002-S	Mettler-Toledo (Greifensee)
Spectrophotometer Helios Epsilon	Thermo (Waltham)
Water bath 1005	GFL (Burgwedel)

2. Chemicals and consumables

Table 3. Chemicals and consumables

Material	Manufacturer
ACES	AppliChem (Darmstadt)
Acrylamid/bisacrylamid	Serva (Heidelberg)
Activated charcoal powder	Fluka (Buchs)
Agar	BD Biosciences (Franklin Lakes)
Agarose Ultra Pure	Life Technologies (Darmstadt)
Alexa Fluor 488 Phalloidin Molecular Probes	Life Technologies (Darmstadt)
Bacteriological peptone	BD Difco (Heidelberg)
Bacteriological peptone	Oxoid (Wesel)
Bacto proteose peptone	BD Biosciences (Franklin Lakes)
Bacto yeast extract	BD Biosciences (Franklin Lakes)
BBL yeast extract	BD Biosciences (Franklin Lakes)
Bovine serum albumin (BSA)	AppliChem (Darmstadt)
β-mercaptoethanol	AppliChem (Darmstadt)
CCL5 recombinant protein	Life Technologies (Darmstadt)
D(+)-glucose monohydrate	Fluka (Buchs)
ECL detection kit	GE Healthcare (Chalfont St Giles)
FCS (fecal calf serum)	Life Technologies (Grand Island)
FeN_3O_9 x 9 H_2O	Sigma (St. Louis)
fMLP	provided by AG Haas (Munich)
Folic acid	Sigma (St. Louis)
Glycine	MP Biomedicals (Eschwege)
HBSS	Life Technologies (Grand Island)
HiPerFect Transfection Reagent	Qiagen (Hilden)
Histopaque 1077	Sigma (St. Louis)

Histopaque 1119	Sigma (St. Louis)
IL-8 recombinant protein	Life Technologies (Darmstadt)
K_2HPO_4	Fluka (Buchs)
KH_2PO_4	Fluka (Buchs)
LB agar	Life Technologies (Grand Island)
LB broth base	Life Technologies (Grand Island)
L-cysteine	Sigma (St. Louis)
L-glutamine	Life Technologies (Grand Island)
MES Buffer	Sigma (St. Louis)
$MgSO_4$	Fluka (Buchs)
Na_2HPO_4	Fluka (Buchs)
PFA	Sigma (St. Louis)
Plastic luer lock syringes (10 mL)	BD Biosciences (Franklin Lakes)
poly-L-lysine	Sigma (St. Louis)
Protein A/G PLUS-agarose reagent	Santa Cruz (Heidelberg)
Protein ladder (PageRuler prestained 10-190K)	Thermo (Waltham)
RPMI 1640	Life Technologies (Grand Island)
SDS	Serva (Heidelberg)
TNFα recombinant protein	Life Technologies (Darmstadt)
TEMED	Biomol Feinchemikalien (Hamburg)
TRIS MP	Biomedicals (Santa Ana)
Trypsin	Life Technologies (Grand Island)
Vectashield mounting medium	Vector Laboratories (Cambridgeshire)

3. Medium and buffer composition

a. Media

Table 4. AYE (ACES yeast extract) medium

Component	Per Liter medium	Supplier
ACES	10 g	AppliChem
Bacto yeast extract	10 g	BD biosciences
L-cysteine	0.4 g	Sigma
FeN_3O_9 x $9H_2O$	0.25 g	Sigma

ACES and yeast extract were dissolved in 900 mL H_2O, cysteine and iron separately in 10 mL H_2O. First, the cysteine solution and iron were added slowly while stirring. The pH was adjusted to 6.9 with 10 M KOH. Then, H_2O was added to reach end volume. The medium was sterilized through glass fiber filter 2 times and stored at 4 °C [43].

Table 5. CYE (charcoal yeast extract) agar plates

Component	Per Liter medium	Supplier
ACES	10 g	AppliChem
Bacto yeast extract	10 g	BD biosciences
Activated charcoal puriss p.a. ; powder	2 g	Fluka
Agar	15 g	BD biosciences
L-cysteine	0.4 g 10 mL^{-1}	Sigma
FeN_3O_9 x $9H_2O$	0.25 g 10 mL^{-1}	Sigma

ACES and yeast extract were mixed in H_2O and the pH was adjusted to 6.9 with 10 M KOH. H_2O was added to reach end volume. After the addition of activated charcoal and agar, the medium was autoclaved and cooled to 50 °C. The filter-sterilized L-cysteine and iron were added. If necessary, chloramphenicol was supplemented to an end concentration of 5 mg L^{-1}. Plates were stored at 4 °C [134].

Table 6. HL5 medium

Component	Per Liter medium	Supplier
D(+)-glucose monohydrate	11 g	Fluka
BBL yeast extract	5 g	BD Biosciences
Bacto proteose peptone	5 g	BD Biosciences
Bacteriological peptone	5 g	Oxoid
Na_2HPO_4	0.355 g	Fluka
KH_2PO_4	0.34 g	Fluka

The pH was adjusted to 6.5 with 1 M KOH or 1 M HCl. The medium was autoclaved and stored at 4°C [135].

Table 7. MB medium

Component	Per Liter medium	Supplier
BBL yeast extract	7 g	BD Biosciences
Bacteriological peptone	14 g	Oxoid
MES buffer	4.26 g	Sigma

The pH was adjusted to 6.9 with 1 M KOH or 1 M HCl. The medium was autoclaved and stored at 4 °C [136].

Table 8. SM medium

Component	Per Liter medium	Supplier
Bacteriological peptone	10 g	Oxoid
BBL yeast extract	1 g	BD Biosciences
KH_2PO_4	1.9 g	Fluka
K_2HPO_4	0.6 g	Fluka
$MgSO_4$	0.43 g	Fluka

After adjusting the pH to 6.0 with KOH, the medium was stored at 4 °C [137].

b. Buffers

Table 9. PBS (phosphate-buffered saline) 10 x

Component	Per Liter buffer	Supplier
NaCl	80 g	Roth
KCl	2 g	Roth
Na_2HPO_4	14.2 g	Fluka
KH_2PO_4	2.4 g	Fluka

The pH was adjusted to 7.4 with 1 M NaOH or 1 M HCl. The buffer autoclaved and stored at room temperature.

Table 10. SorC

Component	Per Liter buffer	Supplier
Na_2HPO_4	0.28 g	Fluka
KH_2PO_4	2.04 g	Fluka
$CaCl_2$ x 2 H_2O	0.00735 g	Roth

After adjusting the pH to 6.0 with 1 M KOH or 1 M HCl, the buffer was autoclaved and stored at room temperature [138].

Table 11. TBS (TRIS-buffered saline) 10 x

Component	Per Liter buffer	Supplier
TRIS	6.5 g	MP Biomedicals
NaCl	80 g	Roth

The pH was adjusted to 7.5 with HCl and the buffer autoclaved and stored at 4°C.

4. Strains and plasmids

Table 12. Mammalian cells lines and bacterial strains

Strain	Properties	Reference
Mammalian cell lines		
A549	Human alveolar basal epithelial cells	gift from U. Greber (Zurich)
HeLa	Human cervix adenocarcinoma cells	gift from U. Greber (Zurich)
RAW 264.7	Murine macrophage cell line	ATCC TIB-71
Dictyostelium discoideum		
Ax3 pSW102	G418 resistant (^{R})	[53]
Ax2/ GFP-α-tubulin	G418^{R}	[139]
Bacteria		
L. longbeachae		
NSW150	*L. longbeachae* sg 1 clinical isolate, Australia	[140]
NSW150Δ*dotA*	NSW *dotA*::Kan^{R}	[140]

L. pneumophila

AK01 (Δ*lqsT*)	JR32 *lqsT*::Kan^R	105
AK02 (Δ*lqsS/lqsT*)	JR32 *lqsS*::Km *lqsT*::Gen^R	105
CR01 (Δ*sidC-sdcA*)	JR32 *sidC-sdcA*::Kan^R	50
CR04 (Δ*sidM/drrA*)	JR32 *sidM/drrA*::Kan^R	52
ER01 (Δ*legG1*)	JR32 *legG1*::Kan^R	18
GS3011 (Δ*icmT*)	*L. pneumophila* *JR32 icmT3011*::Kan^R	141
JR32	*L. pneumophila* *sg 1 Philadelphia*	142
MW635 (Δ*icmG*)	JR32 *icmG*::Kan^R	143
NT02 (Δ*lqsA*)	JR32 *lqsA*:: Kan^R	107
NT03 (Δ*lqsR*)	JR32 *lqsR*:: Kan^R	107
NT05 (Δ*lqsS*)	JR32 *lqsS*:: Kan^R	107

Table 13. Plasmids

Plasmid	Characterization	Sequence
pCR33	pMMB207C-M45, Cam^R	48
pCR34	pMMB207C-M45-*sidC*	48
pCR76	pMMB207C-P$_{tac}$-RBS-*gfp*-RBS-MCS	19
pCR77	pMMB207C-P$_{tac}$-RBS-*dsred*-RBS-MCS	19
pEB201	pMMB207C-M45-*sidM*	52
pER4	pCR76-M45-*legG1*	18
pER5	pCR77-M45-*legG1*	18
pER22	pSW001-P$_{lpg1775}$-*lpg1775-lpg1776*	144
pGP3	pCJYE53-G3-*legG1*, Cam^R	18
pGP4	pCJYE138-G3-*legG1*, Cam^R	18
pSW001	pMMB207-C-RBS-*dsred* (constitutive *dsred*)	145

5. Antibodies

a. Primary antibodies

Table 14. Primary antibodies

Antibody	Origin	Supplier
anti-ARHGAP1	rabbit	Abcam (Cambridge)
anti-ARHGAP17	rabbit	Abcam (Cambridge)
anti-ARHGEF9	rabbit	Abcam (Cambridge)
anti-Cdc42	rabbit	Abcam (Cambridge)
anti-Cdc42(GTP)	mouse	Biomol (Hamburg)
anti-Cdc42/Rac1-phosphoS71	rabbit	Abcam (Cambridge)
anti-GAPDH	rabbit	Cell Signaling (Leiden)
anti-IQGAP1	rabbit	Abcam (Cambridge)
anti-Rac1	rabbit	Abcam (Cambridge)
anti-Ran	rabbit	Abcam (Cambridge)
anti-RanBP1	rabbit	Abcam (Cambridge)
anti-RhoA	rabbit	Abcam (Cambridge)
anti-tubulin WA3	mouse	AG Taubenberger (Munich)

b. Secondary antibodies

Table 15. Secondary antibodies

Antibody	Origin	Label	Supplier
anti-rabbit IgG	goat	FITC	Jackson ImmunoResearch (West Grove)
anti-rabbit IgG	goat	Cy5	Life Technologies (Darmstadt)
anti-mouse IgG	goat	FITC	Jackson ImmunoResearch (West Grove)
anti-mouse IgG	goat	Cy5	Jackson ImmunoResearch (West Grove)

6. Oligonucleotides used for RNAi

Table 16. Oligonucleotides

Target gene	Gene description	Entrez Gene ID	Product name	Product ID
ARHGAP1	Rho GTPase activating protein 1	392	Hs_ARHGAP1_5	SI03233797
			Hs_ARHGAP1_6	SI04144126
			Hs_ARHGAP1_7	SI0416481
			Hs_ARHGAP1_8	SI04177754
ARHGAP17	Rho GTPase activating protein 17	70497	Hs_ARHGAP17_1	SI00302001
			Hs_ARHGAP17_3	SI00302036
			Hs_ARHGAP17_4	SI00302043
			Hs_ARHGAP17_5	SI02780449
ARHGEF9	Cdc42 guanine nucleotide exchange factor	23229	Hs_ARHGEF9_5	SI04138498
			Hs_ARHGEF9_7	SI04210689
			Hs_ARHGEF9_10	SI05428654
			Hs_ARHGEF9_11	SI05428661
Cdc42	Cell division cycle protein 42	998	Hs_CDC42_4	SI00028413
			Hs_CDC42_7	SI02757328
			Hs_CDC42_15	SI04381671
			Hs_CDC42_17	SI04948440
DOCK11	Dedicator of cytokinesis 11	139818	Hs_DOCK11_5	SI04157202
			Hs_DOCK11_6	SI04257743
			Hs_DOCK11_7	SI04277035
			Hs_DOCK11_8	SI04330795

FGD1	FYVE, RhoGEF and PH domain containing 1	2245	Hs_FGD1_2	SI00386568
			Hs_FGD1_5	SI03170818
			Hs_FGD1_7	SI04203192
			Hs_FGD1_9	SI04280087
IQGAP1	IQ motif containing GTPase activating protein 1	8826	Hs_IQGAP1_1	SI00057036
			Hs_IQGAP1_2	SI00057043
			Hs_IQGAP1_3	SI00057050
			Hs_IQGAP1_5	SI02655268
Rac1	Ras-related C3 botulinum toxin substrate 1	5879	Hs_RAC1_5	SI02638293
			Hs_RAC1_6	SI02655051
			Hs_RAC1_7	SI03037524
			Hs_RAC1_8	SI03040884
Ran	Ras-related nuclear protein	5901	Hs_RAN_7	SI04950498
			Hs_RAN_8	SI04950505
			Hs_RAN_9	SI04950512
			Hs_RAN_10	SI04950519
RanBP1	Ras binding protein 1	5902	Hs_RANBP1_3	SI00698201
			Hs_RANBP1_4	SI00698208
			Hs_RANBP1_6	SI03188381
			Hs_RANBP1_7	SI04142089
RhoA	Ras homolog family member A	387	Hs_RHOA_1	SI00702695
			Hs_RHOA_6	SI02654211
			Hs_RHOA_7	SI02654267
			Hs_RHOA_8	SI02776907

B. Methods

1. Cultivation of *L. pneumophila and L. longbeachae*

L. pneumophila and *L. longbeachae* strains were grown at 37 °C on CYE agar plates containing charcoal and yeast extract buffered with ACES [134]. After 3 days of cultivation on plates, 3 mL of AYE liquid medium were inoculated with *L. pneumophila* at a starting OD_{600} of 0.1 and aerobically grown at 37 °C on a turning wheel. Chloramphenicol (5 µg mL^{-1}) or IPTG (1 mM) were added for selection. After 21-22 h and at an OD_{600} of 3.0, the bacteria reached their most infectious state. After 18 h at 37 °C, liquid cultures of *Legionella spp*. reached an OD_{600} of 2.5 and were mixed 1:1 with sterile 50% glycerol and permanently stored at -80 °C.

2. Cell cultivation and storage

a. Mammalian cells

Murine RAW 264.7 macrophages, human A549 lung epithelial cells and HeLa cervix carcinoma cells were cultivated in RPMI 1640 medium amended with 10% FCS (heat inactivated fetal calf serum) and L-glutamine (2 mM) at 37 °C under 5% CO_2. For passaging, cells were scratched with a cell scraper or detached with trypsin from the surface (3 mL for one 75 cm^2 flask). 80% confluent cells were harvested and resuspended in 3 mL freezing medium (70% RPMI 1640, 20% FCS, 10% DMSO). Cryogenic vials were filled with 1 mL of cells and placed in a freezing box (containing isopropanol, precooled for 1 h at 4 °C). After freezing overnight at -80 °C, they were stored in liquid N_2. For thawing, cells were centrifuged and replaced by RPMI 1640 culture medium to eliminate toxic DMSO present in the freezing solution.

b. *Dictyostelium discoideum*

The *D. discoideum* Ax3 pSW102 strain was grown in HL5 medium at 23 °C and supplemented with G418 (20 µg mL^{-1}) for selection. Amoebae were detached mechanically [135].

Confluent *D. discoideum* cells were resuspended in 1 mL freezing medium (80% HL5, 10% FCS, 10% DMSO) and filled into cryogenic vials. Storage and thawing was performed as described for mammalian cells (section B.1.)

3. Neutrophil isolation

The HISTOPAQUE reagents (1119 and 1077, Sigma-Aldrich) were used for leukocyte separation and isolation of neutrophils. 3 mL of HISTOPAQUE-1119 was added, carefully layered by 3 mL of HISTOPAQUE-1077 and 6 mL of freshly isolated human blood in a 15 mL conical centrifuge tube. The tube was centrifuged at 700 x g without brake at room temperature for 30 min. Layers could be observed, in the following order from the top to the bottom of the tube: blood plasma, mononuclear cells/platelets, HISTOPAQUE-1077, granulocytes (including neutrophils), HISTOPAQUE-1119 and erythrocytes. Fluid remaining on the top of the cells of interest was aspirated and discarded. Granulocytes were then transferred to a new tube and washed with 10 mL of isotonic PBS. After centrifugation (200 x g, 10 min, 3 times), the cells were resuspended in buffered saline [146]. This step was repeated three times. After the final centrifugation step, neutrophils were resuspended in RPMI medium and used for migration assays.

4. Aggregation assay

For starvation/aggregation assays, *D. discoideum* Ax3 cells (5×10^6) were grown in 6-well plates in HL5 medium the day before infection. Cells were washed two times with SorC and infected with the indicated *L. pneumophila strains* at an MOI of 10. After 1 h, extracellular bacteria were removed by washing two times with SorC. To permit aggregation and development, cells were further incubated in SorC at 23 °C for 12 to 48 h and stained with propidium iodide (PI, 2.5 µg mL^{-1}, 10 min, 23 °C) prior to fluorescence microscopy.

5. Migration assays

a. Under-agarose assay and single cell tracking

Under-agarose assays were performed as previously described [147, 148]. *D. discoideum* cells, murine RAW 264.7 macrophages and human neutrophils were used for the assay.

For Ax3 pSW102 (GFP) amoebae, microscopy dishes (µ-Dish, 35 mm, Ibidi) were filled with a mixture of melted agarose in SM medium. After solidification (30 min), parallel slots (2 x 4 mm, 5 mm apart) were cut into the agarose. The chemoattractant solution, folic acid (1 mM) diluted in SM medium, was filled into the central slot. After 30 min, *D. discoideum* cells (30 µL) were filled into the neighboring slots. Prior to the experiment, 1 x 10^6 cells were seeded into a 6-well plate in HL5 medium, treated and/or infected with *L. pneumophila*. For the migration assay, cells were washed once with MB medium. The infection was performed for 1 h at an MOI of 10 at 23 °C. After the incubation time and two washing steps with MB to remove extracellular bacteria, the amoebae were detached by scratching in 500 µL MB medium. Then, the dishes were incubated in a humid chamber to allow cell migration at 23°C for 4 h.

For under-agarose assays using RAW 264.7 macrophages, the dishes were incubated with 10% FCS solution at room temperature for 30 min. After two washing steps with PBS, the dishes were filled with a mixture of 1% UltraPure Agarose/RPMI/HBSS (Life Technologies). Three parallel wells (5 mm apart) were formed using a template. Before the cells were filled into the neighbouring slots, the chemoattractant solution (CCL5 or TNFα 100 ng mL^{-1} for macrophages and the peptide formyl-methionyl-leucyl-phenylalanine (fMLP) 100 ng mL^{-1} for neutrophils, Invitrogen) was prefilled in the middle well for 45 min. The day before the infection with *L. pneumophila* (1 h, 37 °C), 1 x 10^6 macrophages or neutrophils were seeded into a 6-well plate in RPMI medium. Cells were washed once with RPMI, incubated for 45 min with a CellTracker Green BODIPY and after another washing step kept in 3 mL medium for the infection. Cells were washed twice with RPMI to remove extracellular bacteria, detached by scratching and resuspended into 500 µL RPMI medium. 150 µL of the cell suspension was filled into the slots. The dishes were incubated in a humid chamber at 37 °C for 4 h.

Under-agarose cell migration was monitored by detecting the green BODIPY fluorescence of macrophages or the GFP fluorescence of *D. discoideum* with the 10x objective of a Leica TCS SP5 microscope. The tile scan function of the Leica software allowed us to obtain merged overview pictures. The quantification of cell migration was documented with the ImageJ software using the plot profile function. The fluorescence intensities of infected cells relative to uninfected cells were plotted against the migration distance.

Tracking of migrating *D. discoideum*, RAW 264.7 macrophages or human neutrophils was recorded 1 h after the cells were filled into the slots by confocal microscopy (HCX PL APO CS 40x/1.25 oil UV objective). Migrating *D. discoideum* cells were recorded for 15 min within a 2 h time window by taking 1 frame per 25 sec. Macrophages and human neutrophils were followed for 1 h with 1 frame per 35 sec at 2 h post infection. Cells were tracked using the ImageJ manual tracking plugin and analyzed with the Chemotaxis and Migration Tool 2.0 (Ibidi).

b. Boyden chamber assay

One day prior to the experiment, cells were seeded into a 6 well plate in RPMI medium. Cells were washed once and detached by scratching. In this assay, inserts with a pore size of 8 µm were placed into a 24-well plate. The chemoattractant solution (fMLP for neutrophils) was placed into the lower part, whereas cells were placed in the upper part of the well. Cells were allowed to migrate towards the chemoattractant for 3-4 h. In order to determine the number of transmigrating cells, a Neubauer chamber was used.

c. Scratch assay

In vitro scratch assays were performed as described before (Liang et al., 2007). Briefly, A549 epithelial cells were seeded into 35 mm µ-Dishes (Ibidi) at a density of 1.5×10^5 cells mL^{-1} (3×10^5 cells $dish^{-1}$) and incubated for 24 h at 37 °C. Confluent cell layers were washed with fresh RPMI medium and infected with *L. pneumophila* strains at an MOI of 10 and/or treated with 10 µM LAI-1 for 90 min. After the infection and/or compound treatment, the cell layer was scratched with a sterile pipette tip and washed with fresh medium to remove detached cells.

Images of the scratched positions were taken with a Leica SP5 confocal microscope (HCX PL APO CS 10×/ 0.40 dry UV objective) 0 h and 24 h after.

The percentage of scratch closure was quantified with the ImageJ software (function analyze particles) by comparing the remaining scratch area with the initial cell-free scratch area.

6. RNA interference

For RNA interference experiments in scratch assays, A549 cells were grown in 35 mm µ-Dishes (Ibidi) and treated for 48 h with a mixture of four siRNA (Qiagen) oligonucleotides with the final concentration of 10 nM [149]. The siRNA stock (10 µM) was diluted 1:15 in RNase-free water and 22.5 µL of diluted siRNA was added in each well. Allstars negative control siRNA was used as a negative control. Subsequently, 181.9 µL RPMI medium without FCS were mixed with 5.6 µL HiPerFect transfection reagent (Qiagen), added to the well, mixed and incubated for 5-10 min at room temperature. In the meantime, cells were diluted in RPMI medium (with 10% FCS) and 1.312 mL (1.5×10^5 cells mL^{-1}) were added on top of each siRNA-HiPerFect transfection complex and incubated for 48 h. After a washing step with RPMI medium, cells were infected with *L. pneumophila* strains and/or treated with 10 µM LAI-1. The scratch assay was performed as described above (section B.5.c). The depletion efficiency of all siRNA oligonucleotides was assessed by Western blot. In growth assays, A549 cells were grown in 96-well plates and treated for 48 h with a final concentration of 10 nM of the siRNA oligonucleotides. The siRNA stock (10 µM) was diluted 1:15 in RNase-free water, and 3 µL of the diluted siRNA was added in each well. Allstars siRNA was used as a negative control. Subsequently, 24.25 µL RPMI medium without FCS was mixed with 0.75 µL HiPerFect transfection reagent (Qiagen), added to each well, mixed and incubated for 5-10 min at RT. In the meantime, cells were diluted in RPMI medium (with 10% FCS), 175 µL of the diluted cells (2×10^4 cells) was added on top of each siRNA-HiPerFect transfection complex and incubated for 48 h. The cells were then infected at an MOI of 10 with GFP-producing *L. pneumophila* grown for 21 h, diluted in RPMI, centrifuged and incubated for 1 h at 37 °C. After three washing steps with RPMI medium (containing 10% FCS), the cells were incubated for 48 h. Intracellular bacterial growth was analyzed by measuring fluorescence using a plate reader (FluoStar Optima, BMG Labtech).

7. Immuno-fluorescence

For immunofluorescence analysis, A549 cells were seeded onto coverslips in 24 well plates and treated with LAI-1 (10 µM). Non-treated A549 cells served as control. *L. pneumophila* overnight cultures (wild-type or Δ*icmT)* were diluted in RPMI medium and used for infection at an MOI of 10 at 37 °C for 1 h. Cells were fixed with 3% paraformaldehyde for 15 min, washed three times with PBS, permeabilized with 0.1% Triton X-100 (in PBS) and blocked with 1% BSA. Cells were incubated with primary antibodies diluted in blocking buffer against IQGAP1, Cdc42(GTP/GDP) or Cdc42-Ser71 (each 1:2500, overnight at 4°C). Cells were incubated (1 h, at room temperature, in the dark) with appropriate secondary antibodies diluted (1:500) in blocking buffer and coupled to FITC or Cy5. After three washing steps, coverslips were mounted with Vectashield supplemented with 1 µg mL^{-1} DAPI to stain the nucleus and analyzed with a Leica TCS SP5 confocal microscope. Microtubule cytoskeleton examination was performed with RAW 264.7 macrophages, infected or not with *L. pneumophila* (MOI 10, 1 h). After a washing step with Brb80, cells were fixed (50% Brb80, 0.1% Triton X-100, 0.5% glutaraldehyde) for 5 min. After washing with SorC, samples were blocked with 1 mg ml^{-1} sodium borohydrate in SorC for 10 min, subsequently stained with the anti-α -tubulin antibody WA3 (provided by M. Schleicher). And appropriate secondary antibodies (1:200). RAW 264.7 macrophages were seeded on coverslips in a 24 well-plate and stained with Texas red-phalloidin. Actin was visualized after washing steps with PBS, permeabilization with cold 1% Triton X-100/PBS for 3-5 min and blocking with 1% BSA. Nuclei were stained with DAPI (0.1 µg mL^{-1}). Imaging was accomplished by confocal microscopy.

8. Pulldown experiments and Western Blot

In order to identify Cdc42(GTP) and Cdc42(GDP) in epithelial cells, pulldown experiments using reagents from Santa Cruz (Protein A/G PLUS-Agarose) were performed.

A549 cells were treated with ice cold RIPA buffer and incubated at 4 °C for 10 min. Cellular debris were precipitated by centrifugation (10 min, 10000 x g, 4 °C).

The supernatant was transferred to a fresh tube on ice, together with 20 µL of resuspended volume of Protein A/G PLUS Agarose and incubated for 30 min at 4 °C. Beads were precipitated by centrifugation (5 min, 2000 x g, 4 °C) and 1 mL (approximately 100 – 500 µg total cell protein) of the supernatant was incubated for 1 h at 4 °C with the primary antibody (Abcam, 1:1000) anti-Cdc42(GTP/GDP). 20 µL of resuspended AG PLUS Agarose was added followed by an incubation step on a rotating device for 1 h at 4 °C. Immunoprecipitates were collected by centrifugation (2000 x g) for 5 min at 4 °C and the pellet was washed 4 times with 1 mL of RIPA buffer. After the final washing step, the pellet was resuspended in 40 µL of loading buffer. After a boiling step of 2-3 min, samples were subjected to SDS-PAGE and analyzed by Western Blot analysis using antibodies against anti-Cdc42(GTP/GDP) or anti-Cdc42(GTP), (both 1:1000). A GAPDH control (Abcam, 1:1000) was used to test the initial amount of protein [18].

9. Uptake and cytotoxicity assays

For uptake experiments, *D. discoideum* cells (5×10^5), RAW 264.7 macrophages or human neutrophils (2.5×10^5) were infected at an MOI of 10 for 1 h with GFP producing *L. pneumophila* wild-type or Δ*icmT* mutant bacteria and/or treated with different concentrations of LAI-1 (1, 5 or 10 µM). Fluorescence of GFP-positive phagocytes harboring *L. pneumophila* was determined by flow cytometry. The percentage of cells with GFP fluorescence above the defined threshold was depicted. The cytotoxicity of *L. pneumophila* (MOI 10, 4 h) strains using different concentrations of LAI-1 was examined for *D. discoideum*, macrophages or neutrophils in 24 well plates. Cells were collected into 15 mL tubes and resuspended in 500 µL SorC (*D. discoideum*) or PBS (macrophages and neutrophils) after centrifugation (240 × g, 10 min). PI (2.5 µg μL^{-1}) was added to the tubes and incubated for 10 min in the dark. PI-positive cells were quantified by flow cytometry [150].

III. Results

A broad range of intracellular pathogens have been described to modulate immune cell migration in order to ensure their own survival and replication. For instance, the bacterium *Yersinia pestis* can act to inhibit neutrophils and dendritic cells chemotaxis by altering early host inflammatory responses [151, 152]. The enteropathogen *Salmonella enterica* inhibits, via the type III secreted effector SseI, the migration of dendritic cells and primary macrophages [153]. Furthermore, *Shigella flexneri* and bacteria of the genus *Chlamydia* impair the migration of CD4+ T lymphocytes. Additionaly, the motility of vascular smooth muscle cell is increased by the up-regulation of IQGAP1 [154]. However, at the onset of this thesis, nothing was known about the influence of *L. pneumophila* on host cell migration. In order to promote their own growth, the invading bacteria modulate cell motility, chemotaxis and immune function by targeting, amongst other proteins, the action of small GTPases. Recent studies identified the *L. pneumophila* effector protein LegG1 as an activator of the host small GTPase Ran. The resulting major downstream effect is the stabilization of microtubule polymerization which is, together with cell polarization, crucial for proper chemotaxis [18].

The data presented in the first part (A) of this thesis show that the Ran activator LegG1, an Icm/Dot translocated *L. pneumophila* protein, influences host cell migration and chemotaxis by interfering with microtubule polymerization [144]. The second aspect of this work (B) contains an investigation of the effect of LAI-1, a *L. pneumophila* QS signal employed for cell-cell communication, on host cell chemotaxis and migration [206].

A. Icm/Dot-dependent inhibition of phagocyte migration by *L. pneumophila* is antagonized by a translocated Ran GTPase activator

1. Icm/Dot-dependent inhibition of *D. discoideum* and immune cell migration by *L. pneumophila*

The first question which needed to be answered was whether *Legionella* affects host cell migration. To this end, *D. discoideum* cells producing the green fluorescent protein GFP (Ax3, pSW102) were infected with *L. pneumophila* wild-type or with a mutant strain lacking a functional Icm/Dot T4SS termed Δ*icmT* for 1 h at different multiplicities of infection (MOIs). In an under-agarose migration assay, the infected amoebae migrated towards folic acid (1 mM) for an additional 4 h (Figure 9A). The results showed that uninfected cells migrated over 1500 µm towards the chemoattractant. An infection with the wild-type strain inhibited the migration in a MOI-dependent manner (approximately 1300 µm for an MOI of 1 and nearly no migration for an MOI of 50). In contrast, an infection with the Δ*icmT* strain did not alter the chemotaxis of *D. discoideum* cells, similar to the migration of uninfected cells (Figure 9B). Furthermore, the effect of *L. pneumophila* at early steps of the developmental process of *D. discoideum* was observed. Cells, normaly grown in rich HL5 medium, were transferred to nutrient poor SorC-buffer and infected with *L. pneumophila* wild-type and Δ*icmT* (MOI 10, 1 h). After 12, 24 and 48 h, aggregation of starved amoebae was determined following staining with propidium iodide (PI, Figure 9C). Uninfected and Δ*icmT* infected cells aggregated, formed streams and slugs which develop into stalks and fruiting bodies. This was not observed after an infection with the wild-type strain. These initial results suggest that *L. pneumophila* inhibits chemotaxis and aggregation of *D. discoideum* cells in an Icm/Dot- and MOI-dependent manner.

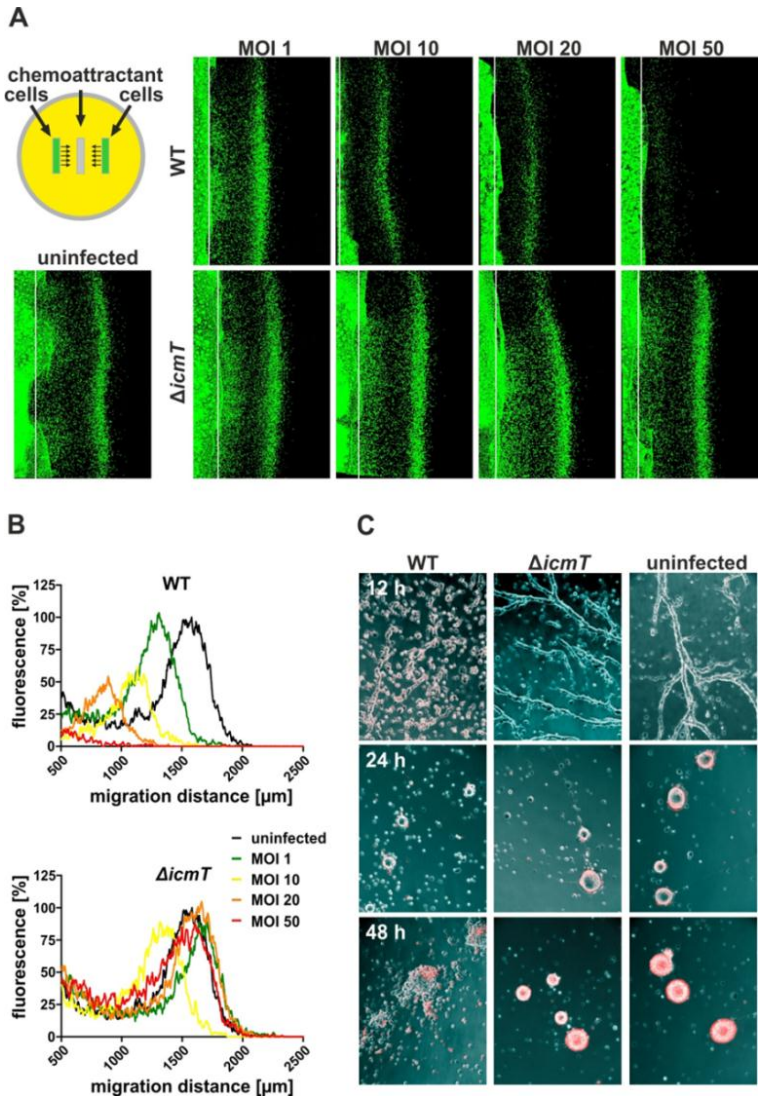

Figure 9. Icm/Dot-dependent inhibition of *D. discoideum* chemotaxis and aggregation by *L. pneumophila*.

A. *D. discoideum* cells Ax3 harboring pSW102 (GFP) were infected with *L. pneumophila* wild-type or Δ*icmT* at different MOIs (1-50) for 1 h. Migration towards folic acid (1 mM) was monitored in an under-agarose assay for 4 h. The white lines represent the edge of the sample wells.

B. Graph of the data from (A) represents the percentage of GFP fluorescence intensity versus migration distance. The data shown are representative of at least three independent experiments.

C. *D. discoideum* cells grown in rich HL5 medium were placed in SorC buffer and infected for 1 h at an MOI of 10 with *L. pneumophila* wild-type or Δ*icmT*. Upon starvation and following staining with PI (2.5 µg mL^{-1}), aggregation of the cells was recorded after 12, 24 and 48 h of incubation at 23 °C.

As *L. pneumophila* is also able to infect mammalian phagocytes, the effect on immune cell migration was investigated. Murine RAW 264.7 macrophages (Figure 10A-B) and primary human neutrophils (PMN, Figure 10C) were first stained with a CellTracker Green BODIPY and infected with *L. pneumophila* wild-type or Δ*icmT*. Migration of the cells to different chemoattractants (CCL5 or TNFα for macrophages and fMLP for neutrophils) was analyzed in an under-agarose assay 4 h post-infection. For both cell types, the migration distance of uninfected cells and cells infected with the Δ*icmT* strain was approximately 500 µm. In contrast, migration of cells infected with wild-type *L. pneumophila* was completely abolished as observed for *D. discoideum* amoebae. Similar results were obtained for the Boyden chamber assay (Figure 10D).

More than 1 x 10^6 uninfected or neutrophils infected with the Δ*icmT* mutant strain migrated through a culture insert (8 µm pore size) towards fMLP, whereas only approximately 2.5 x 10^5 wild-type infected immune cells passed.

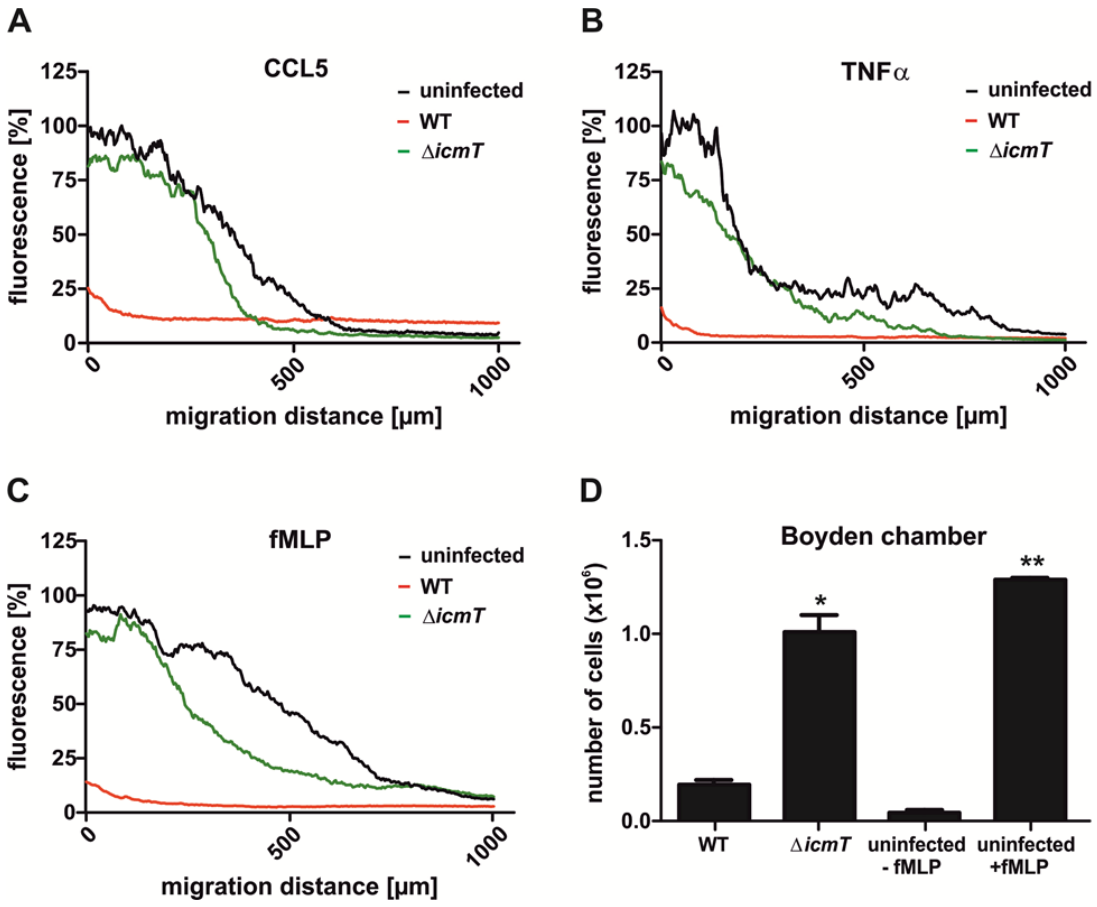

Figure 10. Icm/Dot-dependent inhibition of macrophage and neutrophil migration by *L. pneumophila*.

A. Murine RAW 264.7 macrophages were stained with CellTracker Green (BODIPY) and infected (MOI 10, 1 h) with *L. pneumophila* wild-type or Δ*icmT* mutant strain. Cells migrated towards CCL5 (100 ng mL^{-1}) in an under-agarose assay for 4 h. Graphs depict the percentage of fluorescence intensity versus migration distance.

B. A similar experiment as described in (A) was performed using macrophages migrating towards TNFα (100 ng mL^{-1}).

C. Freshly isolated human neutrophils were infected (MOI 10, 1 h) and migrated in an under-agarose assay for another 4 h towards fMLP (100 ng mL^{-1}).

D. Human neutrophils were infected with *L. pneumophila* wild-type or Δ*icmT* and migration towards fMLP was analyzed in a Boyden chamber assay for 3 h using cell culture insert with a pore size of 8 µm. Means and standard deviations of three independent experiments are shown. Student´s t-test; * $p < 0.05$, ** $p < 0.01$.

Additionally, the migration of murine macrophages infected with *L. longbeachae* wild-type or a T4SS deficient Δ*dotA* mutant showed the same effect as observed for *L. pneumophila*. The migration was also inhibited in an Icm/Dot-dependent manner (Figure 11).

Taken together, these data revealed an Icm/Dot-dependent inhibition of *D. discoideum* and leukocyte chemotaxis by *L. pneumophila and L. longbeachae*.

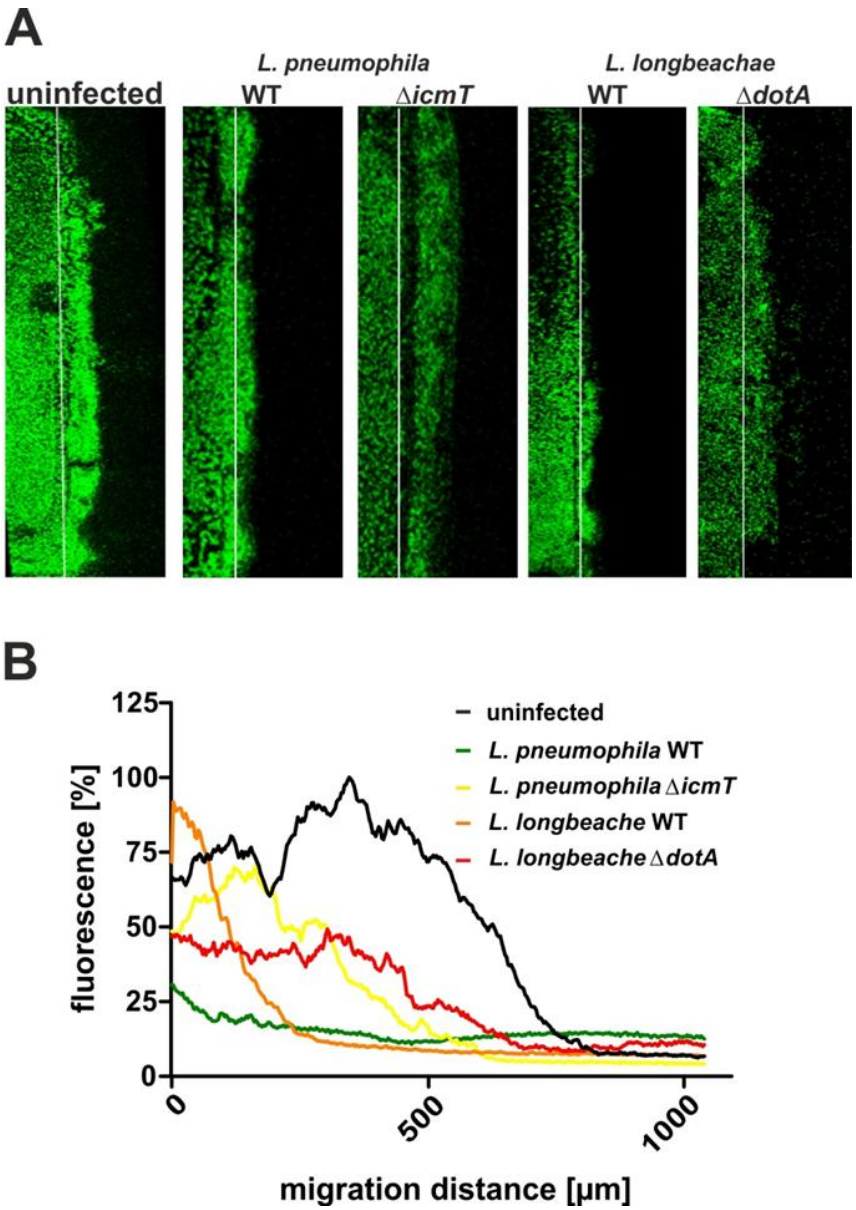

Figure 11. Icm/Dot-dependent inhibition of macrophage migration by *L. longbeachae*.
A. Murine macrophages were infected (MOI 10, 1 h) with *L. longbeachae* wild-type or a Δ*dotA* mutant. For comparison, cells were infected with *L. pneumophila* wild-type or Δ*icmT* mutant. Cells were stained with the CellTracker Green BODIPY and allowed to migrate in an under-agarose assay for another 4 h towards TNFα (100 ng mL^{-1}). The white lines represent the edge of the sample wells.
B. Graph of the data from (A) plotted as the percentage of BODIPY-fluorescence intensity versus migration distance.
Representative data of two independent experiments are shown.

2. The *L. pneumophila* Ran activator LegG1 modulates phagocyte chemotaxis

Based on recent findings that the Icm/Dot translocated effector protein LegG1 acts as a bacterial activator of Ran and stabilizes microtubules [18], the effect of LegG1 on host cell migration was analyzed.

To this end, *D. discoideum* cells were infected with *L. pneumophila* strains (MOI 10, 1 h) lacking LegG1 (Δ*legG1*) or overexpressing LegG1 (Δ*legG1*/+*legG1*). Results, represented in Figure 12A-B, revealed that the migration of *D. discoideum* cells infected with the wild-type strain was inhibited and even more following an infection with the Δ*legG1* strain. This hyper-inhibition phenotype was reverted by complementing LegG1 to a similar extent as observed for mutant bacteria lacking a functional Icm/Dot T4SS.

Additionally, the same effect was observed using murine macrophages (Figure 12C and D) and freshly isolated human neutrophils (Figure 12E and F). Similar to amoebae, the *L. pneumophila* strain lacking LegG1 caused a hyper-inhibition of directed cell migration of these immune cells, which was complemented and reverted by inserting LegG1 on a plasmid.

Furthermore, the influence of other *L. pneumophila* effectors was analyzed. Strains lacking the ER interactor SidC (Figure 13A), the Rab1 GEF SidM (Figure 13B) or the Icm/Dot component IcmG (alias DotF, Figure 13C) were used to test their effect on amoebae migration in comparison to LegG1. All mutants inhibited chemotaxis to a similar extent as the wild-type strain; Δ*icmG* only partially decreased migration. The phenotypes were reverted by providing the effector genes on plasmids.

In summary, the absence of the Ran activator LegG1 specifically hyper-inhibits migration of cells infected with Icm/Dot-proficient *L. pneumophila*. The impairment of directed cell migration by strains lacking LegG1 was even more pronounced than after infection with wild-type bacteria.

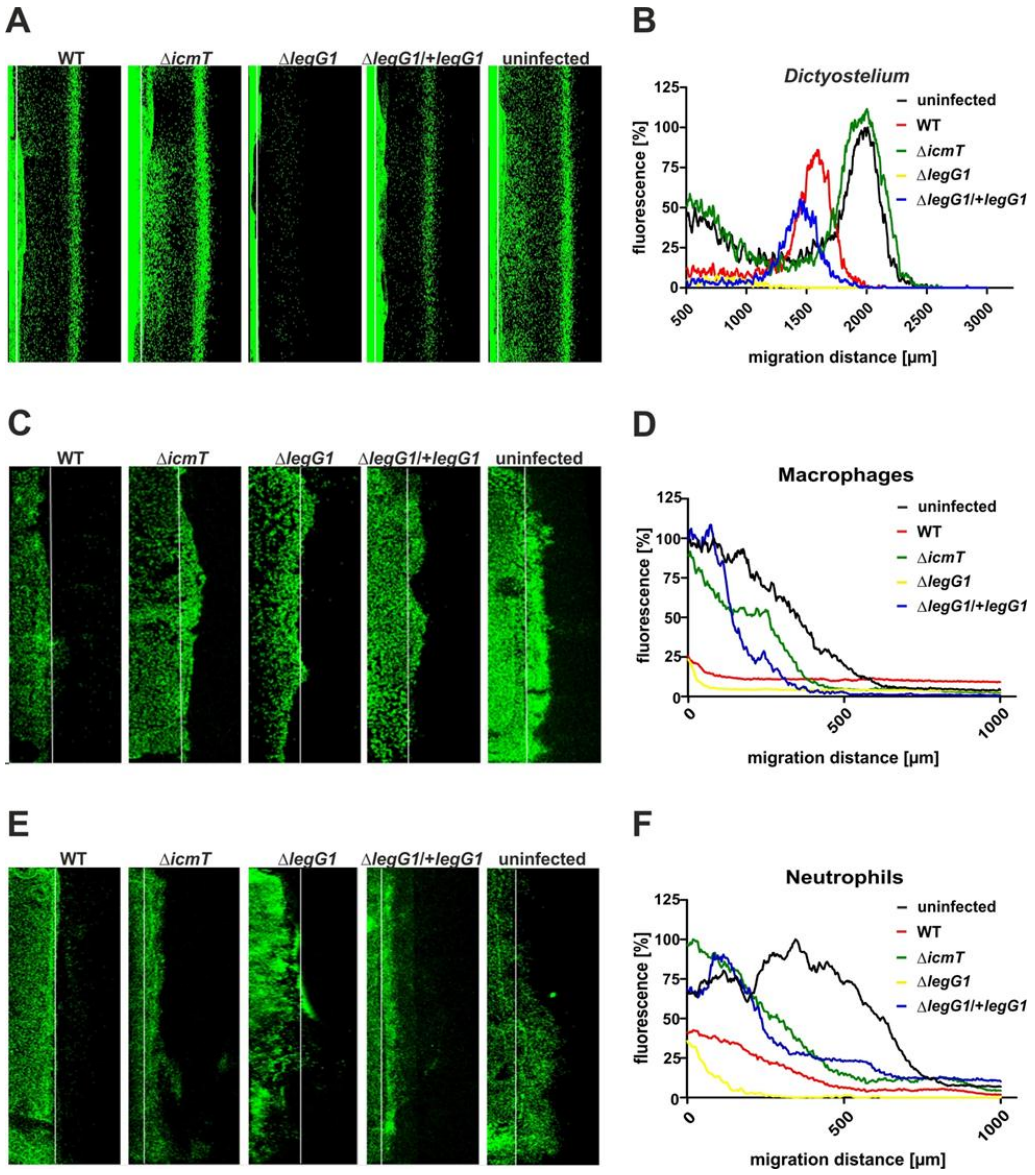

Figure 12. The *L. pneumophila* Ran activator LegG1 modulates phagocyte migration.
A. *D. discoideum* strain Ax3 harboring pSW102 (GFP) was infected for 1 h at an MOI of 10 with DsRed-labelled *L. pneumophila* wild-type, Δ*icmT*, Δ*legG1* or Δ*legG1/+legG1* strains. Cell migration towards folic acid (1 mM) was followed for another 4 h in an under-agarose assay.
B. Data from (A) were plotted as the percentage of GFP fluorescence intensity versus migration distance.
C. Murine RAW 264.7 macrophages were infected (MOI 10, 1 h) with the same *L. pneumophila* strains as described in (A). Cells were stained with the CellTracker Green BODIPY and allowed to migrate towards CCL5 (100 ng mL^{-1}) in an under-agarose assay for another 4 h.
D. Graph of the data from (C) plotted as percent green fluorescence intensity versus migration distance.
E. Freshly isolated human neutrophils were infected (MOI 10, 1 h) with *L. pneumophila* (wild-type, Δ*icmT*, Δ*legG1* or Δ*legG1/+legG1*), stained with CellTracker BODIPY and migration towards fMLP (100 ng mL^{-1}) was followed in an under-agarose assay for 4 h.
F. Graph of the data from (E) plotted as the percentage of green fluorescence intensity versus migration distance. The white lines represent the boundary of the sample wells. The data shown are representative of at least three independent experiments.

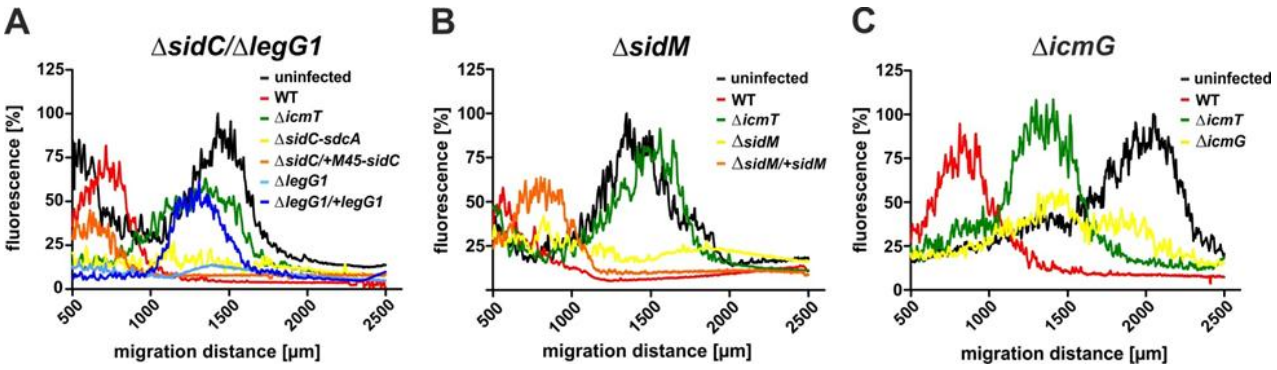

Figure 13. Effect of *L. pneumophila* effectors on *D. discoideum* migration.
D. discoideum amoebae harboring pSW102 (GFP) were infected with *L. pneumophila* wild-type, Δ*icmT*, Δ*sidC*, Δ*sidC/+M45-sidC* (A), Δ*sidM*, Δ*sidM/+sidM* (B) or Δ*icmG* (C) for 1 h at an MOI of 10. Migration towards folic acid (1 mM) was monitored for 4 h. Graphs represent the data plotted as the percentage of GFP fluorescence intensity versus migration distance. Data are representative of at least two independent experiments.

To confirm that the effects of *L. pneumophila* on cell migration were not caused by trivial bacterial impacts, uptake efficiency or cytotoxicity of wild-type, Δ*icmT*, Δ*legG1* or Δ*legG1/legG1* *L. pneumophila* strains were determined by flow cytometry or microscopy. The uptake efficiency (Figure 14A) of GFP-labelled bacteria by *D. discoideum* amoeba was comparable for all strains. The measured cytotoxicity (PI-positive cells) was in a low range (2-7%, Figure 14B). Thus, the *L. pneumophila* infection was not toxic for host cells.

Furthermore, LCV formation (Figure 14C), morphology (Figure 14D) and transient polarization dynamics through the localization of PIP3 (Figure 14E) of *D. discoideum* cells were assayed by immunofluorescence. No significant differences were observed after an infection (MOI 10, 1 h) with the wild-type, Δ*legG1* or Δ*legG1/+legG1* strain. Likewise, no distinguishable alterations were observed for uptake efficiency and cytotoxicity of the *L. pneumophila* strains in infected murine macrophages or human neutrophils (Figure 15A-D).

These data are in agreement with the notion that the inhibition of migration is governed by a specific Icm/Dot- dependent process.

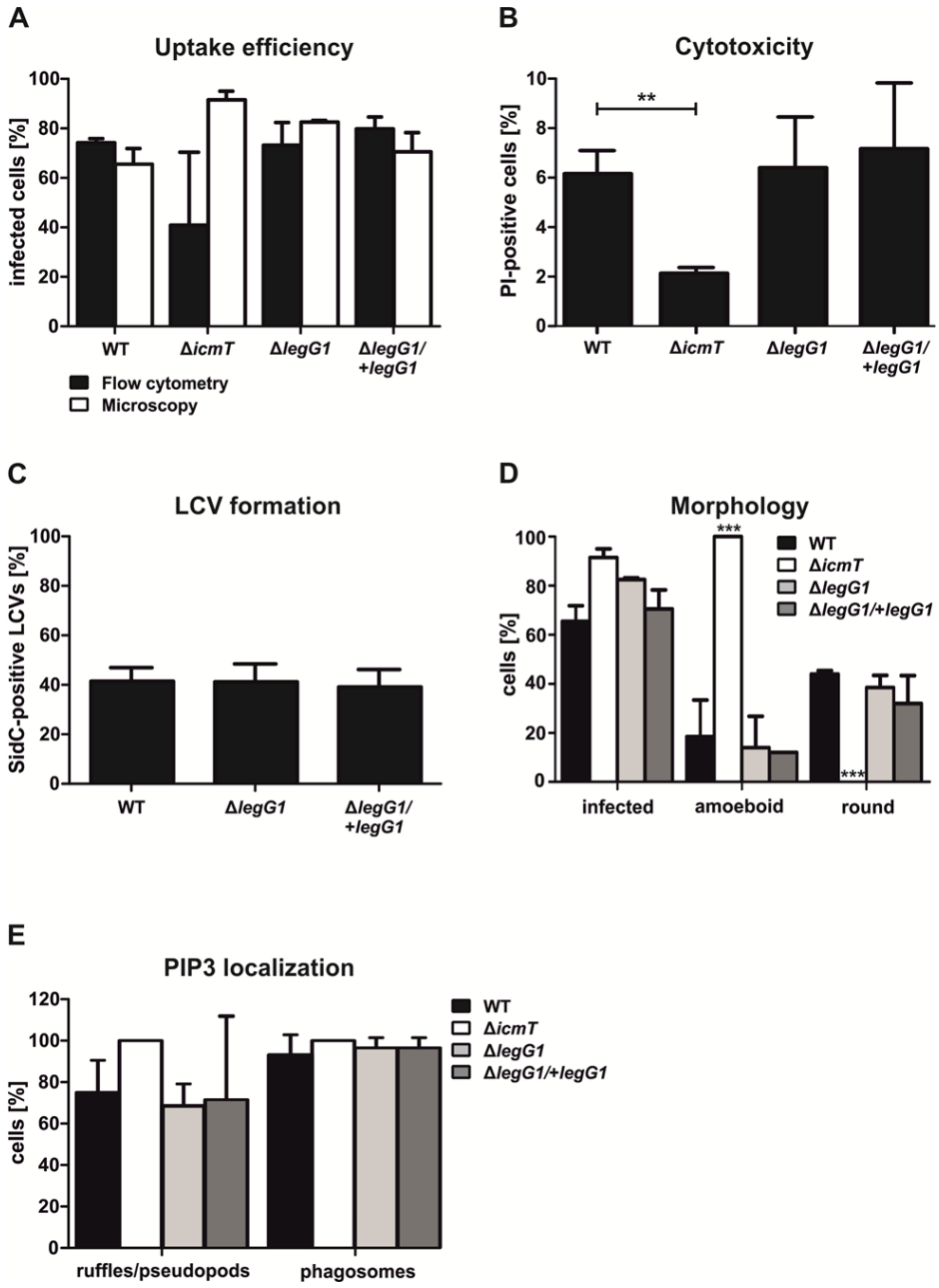

Figure 14. Morphological and physiological features of infected amoebae.

D. discoideum cells, grown in MB medium, were infected (MOI 10, 23 °C) with *L. pneumophila* wild-type, Δ*icmT*, Δ*legG1* or ΔlegG1/+*legG1*.

A. Uptake efficiency was determined 1 h post-infection by flow cytometry or microscopy.

B. Cytotoxicity was assessed by flow cytometry after infection (4 h) and subsequent PI staining (2.5 µg mL^{-1}).

C. LCV formation was determined by fluorescence microscopy using an anti-SidC antibody (n = 400 cells per strain).

D. Morphology of amoebae cells producing GFP was analyzed by microscopy.

E. Cell polarity was analyzed using the *D. discoideum* strain producing the PtdIns(3,4,5)P3 probe GFP-PH_{Crac} (PIP3). Data represent means and standard deviations of 3 (A, B) or 2 (D, E) independent experiments. Student´s t-test; ** $p < 0.01$, *** $p < 0.001$.

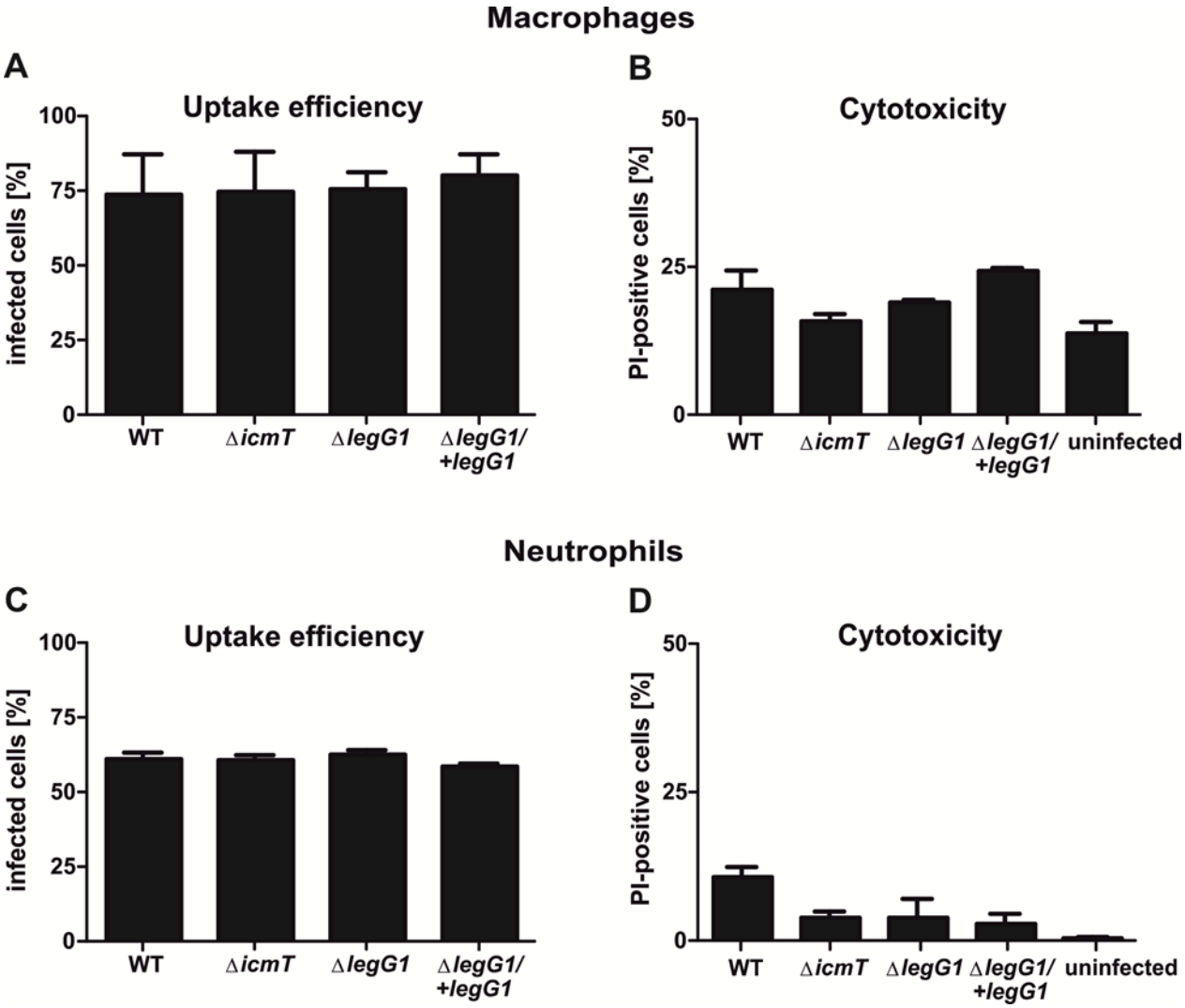

Figure 15. Uptake efficiency and cytotoxicity of *L. pneumophila*-infected macrophages and human neutrophils.

A, C. Murine RAW 264.7 macrophages or human neutrophils were infected (MOI 10, 1 h) with GFP-labelled *L. pneumophila* wild-type, Δ*icmT*, Δ*legG1* or Δ*legG1/+legG1*. Uptake efficiency was determined as the percentage of GFP-positive cells.

B, D. Cytotoxicity of *L. pneumophila* wild-type, Δ*icmT*, Δ*legG1* or Δ*legG1/+legG1* was analyzed after 4 h of infection by PI staining (2.5 µg mL^{-1}) of the infected phagocytes (macrophages and neutrophils). Graphs indicate means and standard deviations of three independent experiments.

3. Single cell tracking of *L. pneumophila*-infected phagocytes

The impacts of *L. pneumophila* and its effector LegG1 on phagocyte migration were analyzed in more detail. Cells were tracked on a single cell level using an under-agarose assay and appropriate tracking software. First, *D. discoideum* cells were infected (MOI 10, 1 h) with DsRed-labelled *L. pneumophila* strains (wild-type, Δ*icmT*, Δ*legG1* or Δ*legG1/+legG1*). Infected cells were tracked for 15 min within a 2 h window (Figure 16A), then forward migration index (FMI) and velocity were calculated. Compared to Δ*icmT*-infected cells, the FMI was reduced threefold for cells infected with *L. pneumophila* wild-type or Δ*legG1* mutant strain. The FMI of amoebae infected with the Δ*legG1/+legG1* strain was decreased twofold. Velocity was diminished twofold for wild-type, Δ*legG1* or Δ*legG1/+legG1*- but not for Δ*icmT*-infected cells. No differences were observed between uninfected (data not shown) and Δ*icmT*-infected cells (Figure 16B). Small changes in FMI and velocity attributable to the absence or overexpression of LegG1 were not statistically significant.

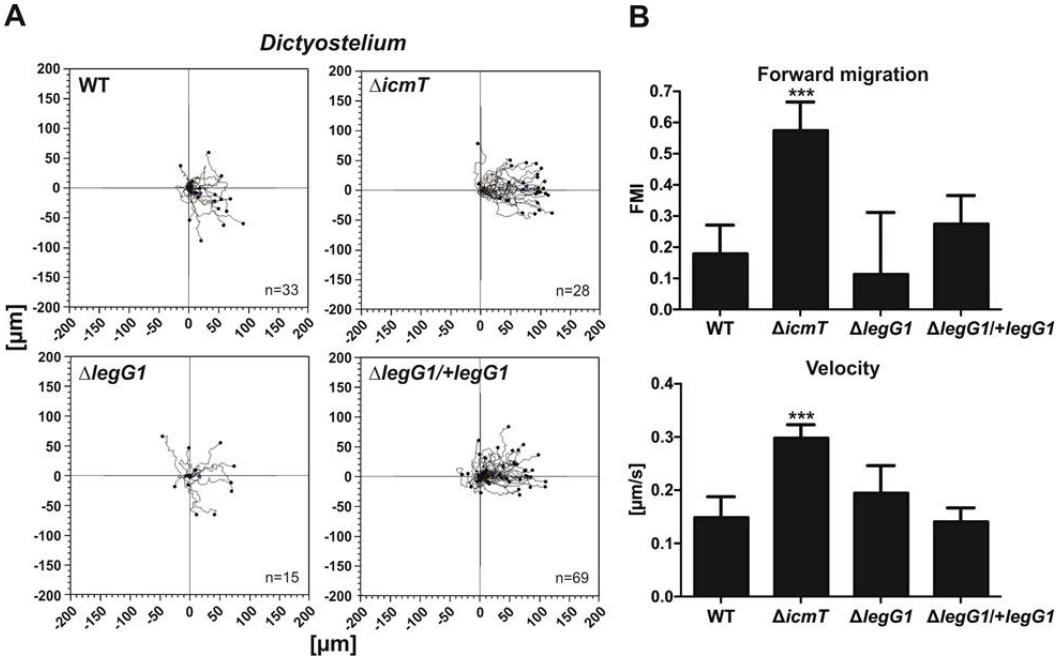

Figure 16. LegG1 affects forward migration and velocity of infected *D. discoideum* cells.
A. *D. discoideum* Ax3 cells harboring pSW102 (GFP) were infected (MOI 10, 1 h) with DsRed-labelled *L. pneumophila* wild-type, Δ*icmT*, Δ*legG1* or Δ*legG1*/+legG1. Infected cells were tracked in an under-agarose assay towards folic acid for 15 min in a 2 h time window. The corresponding plots were established using the ImageJ manual tracker.
B. The motility parameters FMI and velocity were analyzed using the Ibidi chemotaxis software. Student´s t-test; ** $p < 0.01$, *** $p < 0.001$.

Similar experiments were performed using murine RAW 264.7 macrophages and freshly isolated human neutrophils. After staining with CellTracker Green BODIPY, cells were tracked for 1 h at 2h post-infection in an under-agarose assay. Figure 17A and C show representative tracking plots of macrophages and neutrophils, respectively. Compared to Δ*icmT*-infected or uninfected cells (data not shown), the FMI for macrophages (Figure 17B) and neutrophils (Figure 17D) infected with wild-type bacteria or lacking the protein LegG1 was reduced by half. Again, no differences were observed between uninfected cells or cells lacking a functional Icm/Dot secretion system (Δ*icmT*).

Contrary to *D. discoideum* amoebae, both the FMI and the velocity of macrophages (Figure 17B) and neutrophils (Figure 17D) infected with the complementation strain of *L. pneumophila* (Δ*legG1/+legG1*) were significantly increased. The speed of wild-type or Δ*legG1*-infected immune cells was similarly decreased (1.25 fold) when compared to Δ*icmT*-infected cells, although to a lesser degree as *D. discoideum* cells.

These findings suggest that the *L. pneumophila* effector LegG1 affects directionality and speed of infected amoebae and leukocytes, thereby modulating chemotaxis and migration of infected cells.

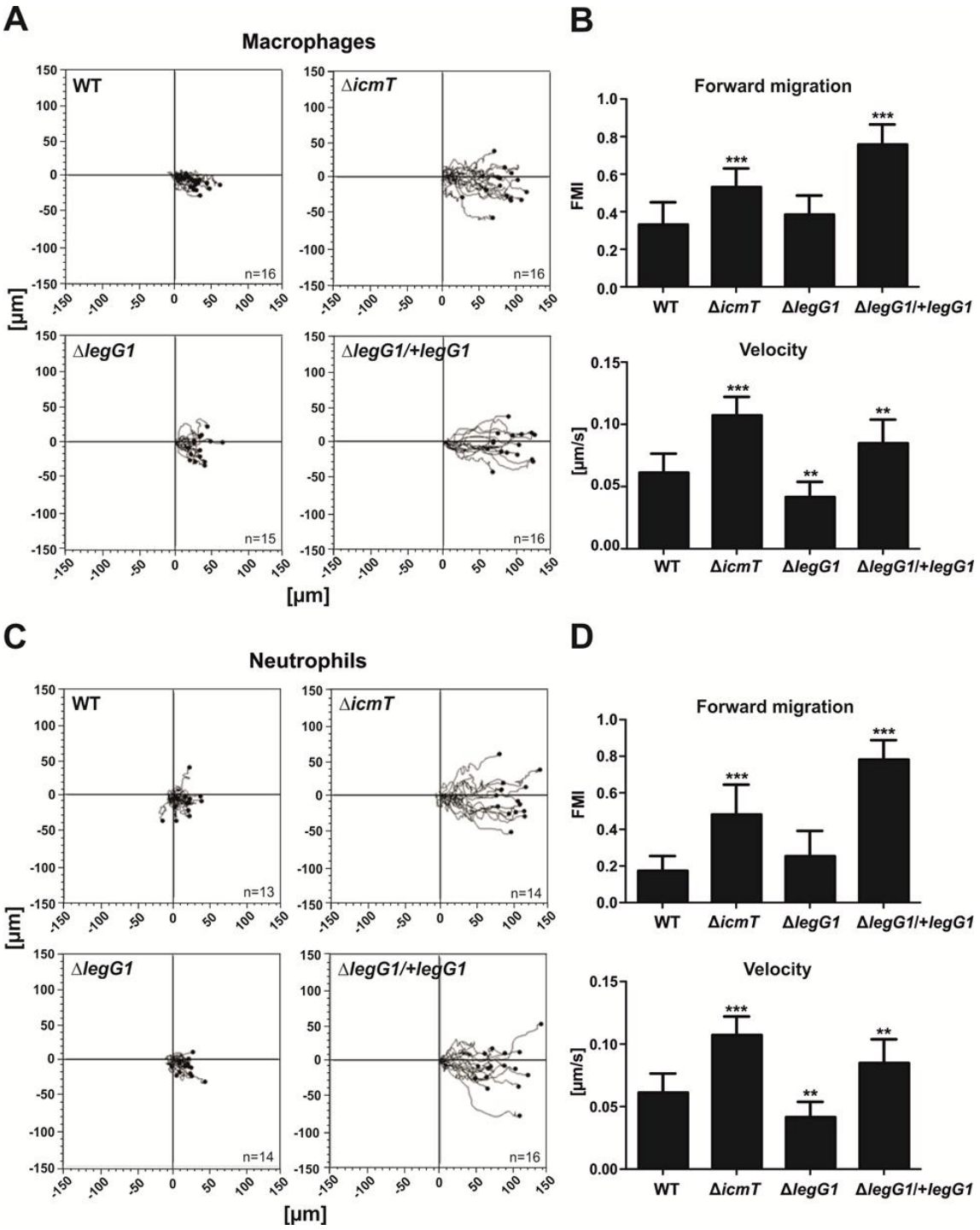

Figure 17. LegG1 alters motility parameters of infected immune cells.

A, C. Murine RAW 264.7 macrophages or human neutrophils were stained with CellTracker Green BODIPY and infected with DsRed-labelled *L. pneumophila* (MOI 10, 1 h) wild-type, Δ*icmT*, Δ*legG1* harboring or Δ*legG1*/+*legG1*. Macrophages or neutrophils motility towards CCL5 (100 ng mL^{-1}) or fMLP (100 ng L^{-1}), respectively, was tracked in an under-agarose assay for 1 h. The corresponding plots were made using the ImageJ manual tracker.

B. The motility parameters FMI and velocity were determined using the Ibidi chemotaxis software. Student´s t-test; ** $p < 0.01$, *** $p < 0.001$.

4. *L. pneumophila* LegG1 promotes random cell migration dependent on the small GTPase Ran

Having determined that *L. pneumophila* affects directed migration, the effect of *L. pneumophila* wild-type, Δ*icmT*, Δ*legG1* and Δ*legG1/+legG1* on random cell migration was examined. For this purpose, the scratch assay, also known as wound-healing assay, was used. Confluent cell layers were scratched and monitored over 24 h after bacterial infection. In order to underpin earlier results, layers of murine macrophages were infected (MOI 10, 1 h) with the *L. pneumophila* strains listed above. Images of the scratched positions were taken 0 h and 24 h after infection (Figure 18A). After 24 h, the scratch of wild-type or Δ*legG1*-infected cells was closed to 25% whereas no wound (100% scratch closure) was left for uninfected cells or cells infected with Δ*icmT* or Δ*legG1/+legG1* mutant bacteria (Figure 18B).

Since LegG1 is an activator of the Ran GTPase, the role of Ran on LegG1-dependent modulation of cell migration was analyzed. To this end, a scratch assay was performed using epithelial A549 cells pretreated for 48 h with small interfering (siRNA) to knockdown Ran. Cells were then infected with *L. pneumophila* wild-type, Δ*icmT*, Δ*legG1* or Δ*legG1/+legG1*. Cells (mock or scrambled) treated only with transfection reagent or negative siRNAs served as controls. Images of the scratched positions were taken 0 h and 24 h after the infection (Figure 18C). The scratch was closed to a similar extent for untreated (no bacterial infection or siRNA treatment), Δ*icmT* or Δ*legG1/+legG1*-infected epithelial cells (100% closure) and for wild-type or Δ*legG1*-infected cells (approximately 30% closure). Upon siRNA treatment, the scratch closure was comparable to control cells, for each condition, except for cells infected with the complementation strain of LegG1 (Δ*legG1/+legG1)*. The scratch closure was approximately 30% as observed for cells infected with *L. pneumophila* wild-type or Δ*legG1* (Figure 18D). This result suggests that LegG1 requires Ran to exhibit its effect. Efficiency of Ran depletion was controlled by Western Blot (data not shown).

Furthermore, in a similar approach, confluent cell layers of HeLa cells were subjected to „microbial microinjection" with LegG1. The effect of a single effector protein on host cell migration could be performed using *Yersinia enterocolitica* strains WA (pT3SS) lacking endogenous effectors but producing $YopE_{1-53}$, $YopE_{1-53}$-LegG1, $YopE_{1-138}$ or $YopE_{1-138}$-LegG1.

The N-terminal fragments of YopE are not cytotoxic and allow the secretion and translocation of hybrid proteins through the T3SS. Following cell contact, these *Y. enterocolitica* strains directly inject LegG1 into the host cell and promote microtubule polymerization [18]. The confluent cell layers were infected (MOI 10, 90 min) and scratched. Images were taken 0 h and 24 h after infection (Figure 18E). As expected, the N-terminal fragments $YopE_{1-53}$ and $YopE_{1-138}$ did not promote random cell migration as indicated by the scratch closure being below 25%. HeLa cells infected with *Yersinia* strains producing YopE-LegG1 fusion proteins migrated and significantly reduced the wound over time. The scratch closure was between 80 – 100% similar to uninfected cells (Figure 18F).

Taken together, these results suggest that the positive effect of LegG1 on random cell migration is dependent on Ran. Additionally, the bacterial effector is required and sufficient to promote cell motility of macrophages and epithelial cells.

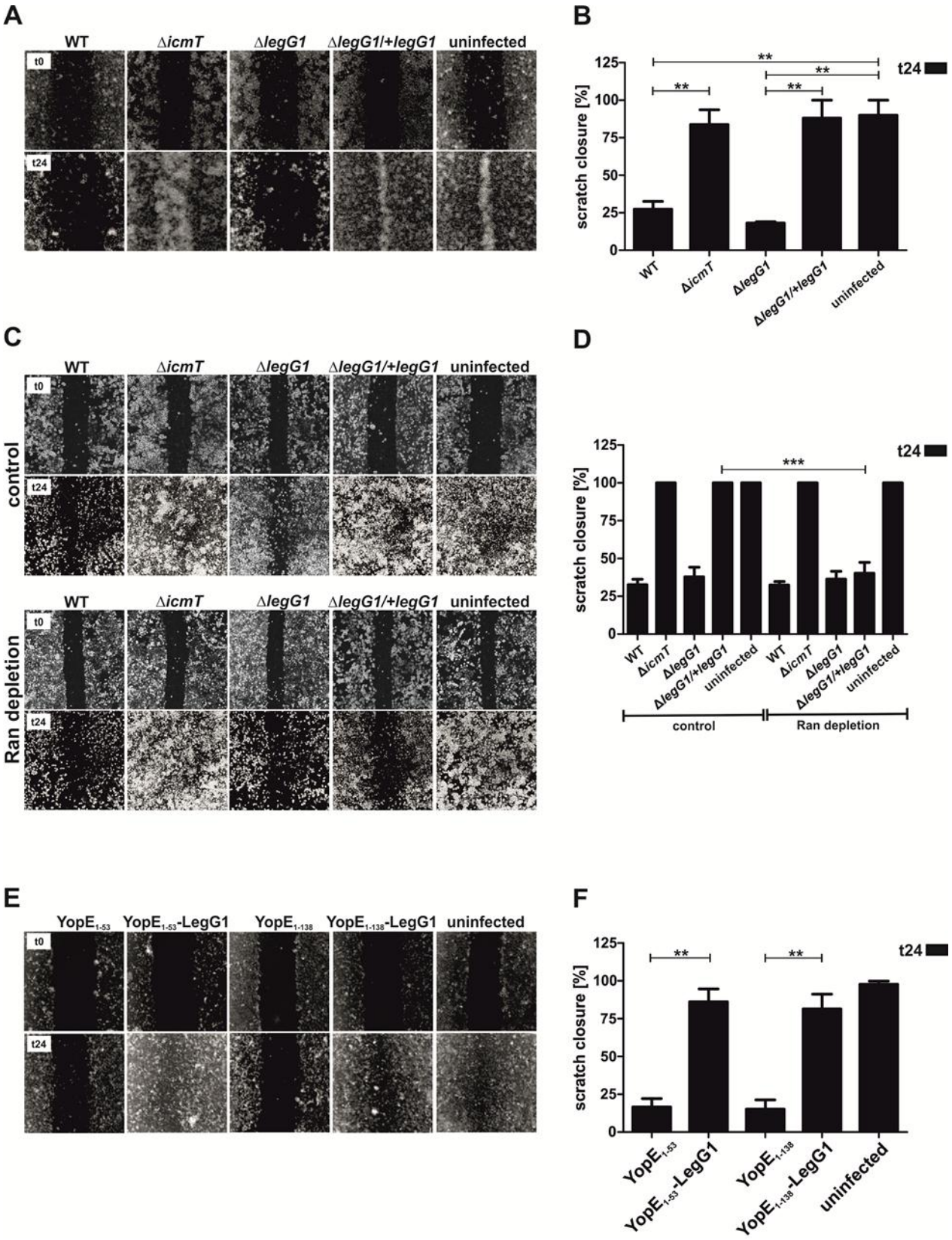
A
WT
ΔicmT
ΔlegG1
ΔlegG1/+legG1
uninfected
t0
t24
B
scratch closure [%]
t24
**
**
**
WT
ΔicmT
ΔlegG1
ΔlegG1/+legG1
uninfected
C
control
Ran depletion
D
***
control
Ran depletion
E
YopE1-53
YopE1-53-LegG1
YopE1-138
YopE1-138-LegG1
F

Figure 18. *L. pneumophila* LegG1 promotes random cell migration dependent on the small GTPase Ran.

A. Confluent cell layers of murine RAW 264.7 macrophages were infected (MOI 10, 90 min) with DsRed-labelled *L. pneumophila* wild-type, Δ*icmT*, Δ*legG1* or Δ*legG1/+legG1*, washed and scratched with a sterile pipette tip. Detached cells were washed away and images of the scratched positions taken 0 h and 24 h after infection.

B. The remaining scratch area (scratch closure) was quantified using the ImageJ software.

C. Confluent layers of A549 cells were treated with RNA interference (siRNA) against Ran for 48 h, infected (MOI 10, 90 min) and scratched as described in (A). Images of the scratched positions were taken after 0 h and 24 h.

D. Quantification of the scratch closure was performed using the ImageJ software.

E. HeLa cells were seeded and infected (MOI 10, 90 min) with *Y. enterocolitica* strains producing $YopE_{1-53}$, $YopE_{1-53}$-LegG1, $YopE_{1-138}$ or $YopE_{1-138}$-LegG1. Scratches and images were made as described in (A-C).

F. Quantification of the remaining scratch area was achieved using the ImageJ software. Student´s t-test; ** $p < 0.01$, *** $p < 0.001$.

5. Real-time analysis of LegG1-dependent cell motility and microtubule polymerization

To address the question, whether LegG1 affects cell motility and subsequent microtubule dynamics, a real-time study was performed. *D. discoideum* cells producing GFP-α-tubulin were infected with *L. pneumophila* wild-type, Δ*legG1* or the complementation strain Δ*legG1/+legG1*. Cells showed a strongly impaired motility and microtubule polymerization after an infection with the Δ*legG1* mutant strain when compared to *L. pneumophila* wild-type. This effect could be complemented by providing the *legG1* gene on a plasmid (Figure 19). These observations are in agreement with those made by Rothmeier *et al.*, where the motility of LCVs harboring Δ*legG1* was found to be abolished [18]. These results indicate that LegG1 specifically promotes microtubule-dependent cell motility.

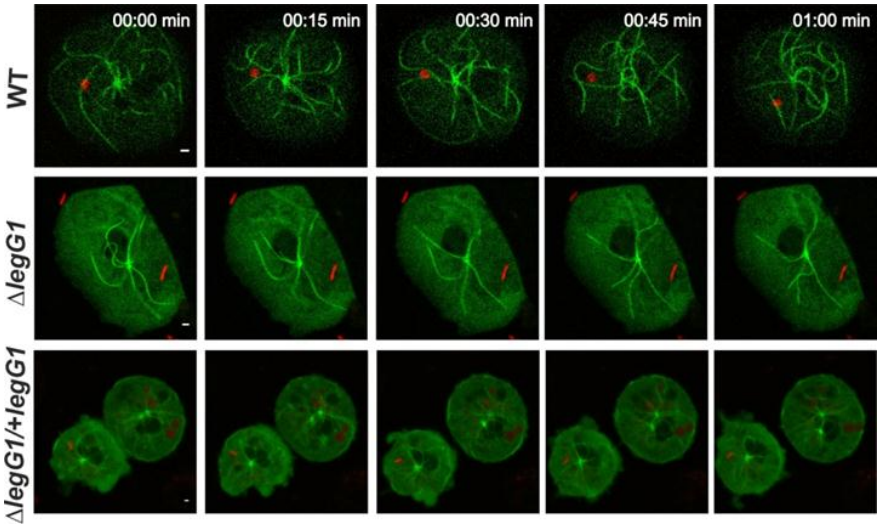

Figure 19. The Ran activator LegG1 promotes microtubule dynamics and cell motility.
Microtubule dynamics and cell motility of *D. discoideum* producing GFP-α-tubulin were observed in real-time fluorescence microscopy. Cells were infected (MOI 10, 2 h) with DsRed-labelled *L. pneumophila* wild-type, Δ*legG1* or Δ*legG1/+legG1*. After 2 h of infection, microtubule polymerization was recorded using confocal microscopy. Images were taken every 15 sec.

In summary, the results of this first section demonstrate that *L. pneumophila* inhibits phagocyte migration in an Icm/Dot-dependent manner. Using several migration assays and host cells, it was shown that the bacterial effector LegG1 and consequent microtubule polymerization antagonizes the migration inhibition caused by *L. pneumophila*.

B. The *L. pneumophila* quorum sensing molecule LAI-1 modulates host cell migration through an IQGAP1-Cdc42-dependent pathway

QS molecules allow the bacteria to perform cell-cell communication, not only amongst each other, but also with their hosts in a process known as inter-kingdom signaling. In *L. pneumophila*, the autoinducer LAI-1 (3-hydroxypentadecane-4-one) is produced by the synthase LqsA, sensed and regulated by LqsS and LqsR, respectively. A novel sensor kinase termed LqsT was recently discovered [105]. Among others, studies on *P. aeruginosa* [102] describing the modulation of host cell migration by QS molecules led us to study the effect of LAI-1 on cell motility and analysis of downstream effects.

1. Quorum sensing regulators and the autoinducer molecule LAI-1 dose-dependently affect host cell migration and chemotaxis

In a first attempt to identify possible effects of QS regulators on host cells, the influence of five *lqs* mutant strains (Δ*lqsS*, Δ*lqsT*, Δ*lqsS-lqsT*, Δ*lqsR* or Δ*lqsA*) on cell motility and chemotaxis was assessed. To this end, *D. discoideum* amoebae were infected for 1 h at an MOI of 10 with these different strains and allowed to migrate in an under-agarose assay towards folic acid (Figure 20A). After 4 h, the migration distance was determined. The migration pattern of cells infected with Δ*lqsR* or Δ*lqsA* mutant strains was similar to uninfected cells and to cells infected with the Δ*icmT* strain, reaching a distance of approximately 1000 µm. An inhibition of migration was visible for the Δ*lqsS*, Δ*lqsT* or Δ*lqsS-lqsT* strains similar to *L. pneumophila* wild-type (Figure 20B).

In a further experiment, murine macrophages (Figure 20C) were infected with the strains listed above. After 4 h of chemotaxis towards CCL5, only the Δ*lqsA* strain did not affect macrophage chemotaxis. The migration distance reached 500 µm, similar to uninfected or cells infected with the Δ*icmT* mutant strain. In contrast, the motility of cells infected with the Δ*lqsS*, Δ*lqsT*, Δ*lqsS-lqsT* or Δ*lqsR* strains was almost completely abolished.

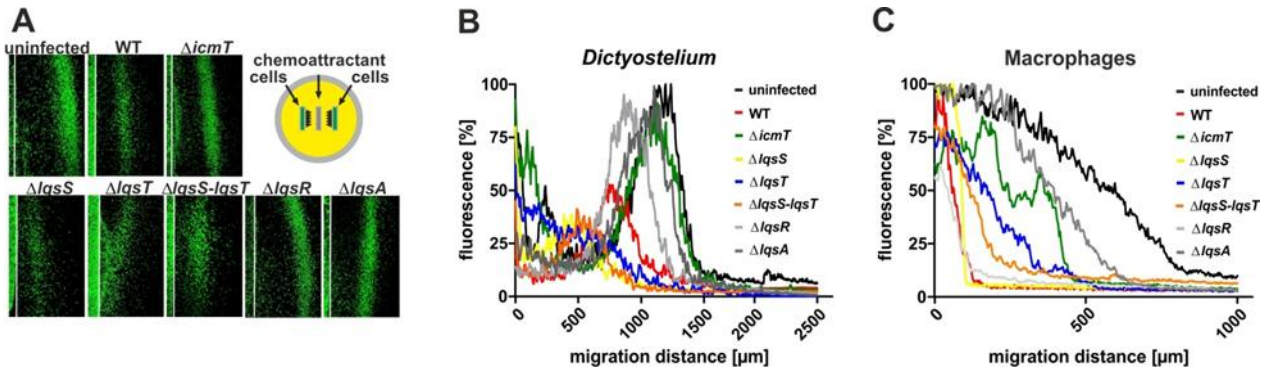

Figure 20. Effect of QS regulators on host cell chemotaxis.
A. *D. discoideum* cells harboring Ax3 pSW102 (GFP) were infected (MOI 10, 1 h) with *L. pneumophila* wild-type, Δ*icmT*, Δ*lqsS*, Δ*lqsT*, Δ*lqsS-lqsT*, Δ*lqsR* or Δ*lqsA* mutant strains. Directed migration towards folic acid (1 mM) was monitored for 4 h in an under-agarose assay. The white lines represent the edge of the well.
B. Graph represents the data from (A) plotted as the percentage of GFP fluorescence intensity versus migration distance.
C. Graph depicts the migration of infected macrophages (same strains and conditions as mentioned in (A)). Cells were stained with a CellTracker Green BODIPY and allowed to migrate towards CCL5 (100 ng mL^{-1}) for 4 h. The percentage of GFP fluorescence intensity versus migration distance is visualized. The data shown are representative of at least three independent experiments.

As there was no inhibition of migration observed for cells infected with the *L. pneumophila* strain lacking the autoinducer LqsA, responsible for the production of LAI-1, a closer look on the effect of LAI-1 on host cell motility was taken.

The influence of different concentrations of racemic LAI-1 (0.5 – 10 µM) was analyzed in a chemotactic under-agarose assay. After LAI-1 treatment, *D. discoideum* amoebae migrated for 4 h towards folic acid (Figure 21A). A dose-dependent inhibition of directed cell migration was revealed with a strong negative effect above a concentration of 3 µM (migration distance of approximately 750 µm instead of 1200 µm for untreated cells). A complete inhibition was observed upon treatment with 10 µM LAI-1.

Likewise, to test which enantiomer of LAI-1 or its amino-derivate is biologically more active, the impact of (R)- and (R)-Am- or (S)- and (S)-Am-LAI-1 was tested in the migration assay. The directed movement of *D. discoideum* cells was distinctly inhibited by the (R)-form; approximately 750 µm of migration distance compared to 1200 µm for amoebae treated with the (S)-form (Figure 21B).

Additionally, the autoinducer molecule CAI-1 of *V. cholerae* was tested at different concentrations and resulted in a similiar dose-dependent inhibition of *D. discoideum* chemotaxis (Figure 21C). The effect was evident at a concentration of 3 µM (migration distance of 1000 µm) and most pronounced at 10 µM (600 µm). However, migration was never completely inhibited.

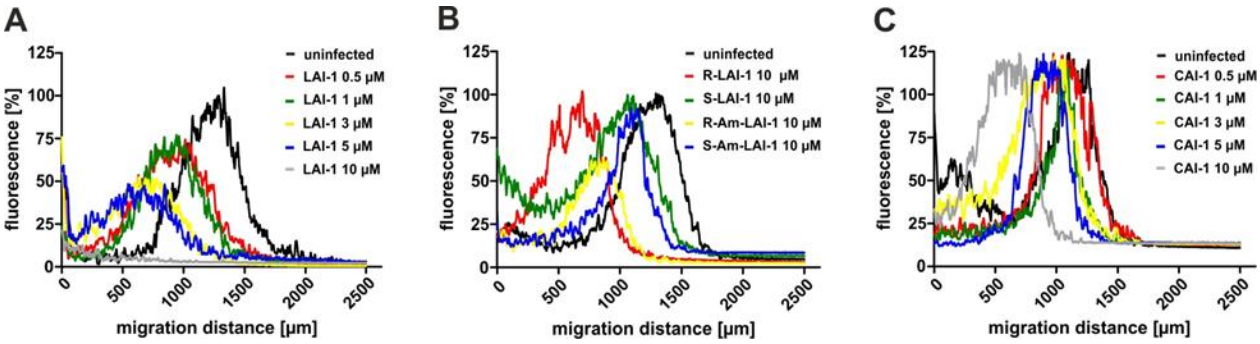

Figure 21. Dose-dependent inhibition of cell migration by LAI-1.
Migration of *D. discoideum* amoebae Ax3 harboring pSW102 (GFP) towards folic acid (1 mM) was followed in an under-agarose assay for 4 h. Cells were treated with racemic LAI-1 (0,5 – 10 µM. (A)), (R)-LAI-1, (S)-LAI-1, (R)-Am-LAI-1 or (S)-Am-LAI-1 (10 µM, B) or with different concentrations of CAI-1 (0,5 – 10 µM, (C)) for 1 h. Graphs represent the percentage of fluorescence intensity versus migration distance. The results are representative of at least three independent experiments.

In order to rule out that the addition of LAI-1 is toxic for cells and therefore causing the observed effect, cytotoxicity of different concentrations of LAI-1 (1, 5 or 10 µM) in combination with *L. pneumophila* infection (wild-type or Δ*icmT*, MOI 10 for 1 h) was evaluated. To this end, cells were stained with PI and analyzed by flow cytometry. The data showed that neither LAI-1 nor *L. pneumophila* infection dramatically influenced the survival of *D. discoideum* amoebae or murine RAW 264.7 macrophages (Figure 22A and B, respectively). The percentage of PI-positive cells was similar with or without LAI-1 and/or in presence of bacteria; approximately 10% for *D. discoideum* and 30% for macrophages.

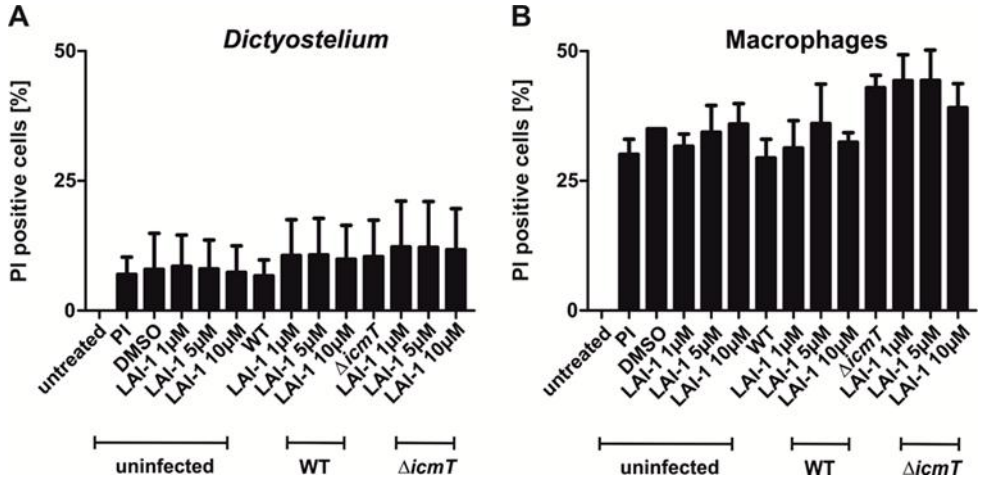

Figure 22. LAI-1 is not toxic for cells.
D. discoideum cells (A) and murine RAW 264.7 macrophages (B) were infected (MOI 10) with *L. pneumophila* wild-type or Δ*icmT* and treated with LAI-1 (1, 5 and 10 µM) for 4 h. Cytotoxicity was determined by flow cytometry following PI staining (2.5 µg mL^{-1}). The percentage of PI positive cells is depicted.

Since LAI-1 negatively influences cell migration, the next aim was to analyze the motility parameters FMI and velocity. First, *D. discoideum* cells, untreated or treated with DMSO or LAI-1 (10 µM), were tracked at a single cell level using a chemotactic migration assay (Figure 23A). The FMI and the velocity were determined (Figure 23B). The addition of LAI-1 significantly reduced the FMI by half but not the velocity, compared to untreated control cells.

A dose-dependent inhibition of murine macrophage migration by LAI-1 was observed (Figure 23C). Therefore, the cells were subsequently used to gain insights into the cellular impact of LAI-1. A closer look revealed that LAI-1 causes microtubule depolymerization (Figure 23D) and dramatic actin destabilization (Figure 23E). The number of microtubule fibers per cell was strongly reduced; from 8 in control cells to about 3 in LAI-1-treated cells. Nocodazole, a microtubule destabilizing compound, was used as a negative control (data not shown). Furthermore, cortical actin was significantly damaged. Over 80% of untreated control cells possess intact actin compared to only 10% of LAI-1-treated cells.

Taken together, these results provided initial insights into the intracellular effect of LAI-1. A dose-dependent inhibition of chemotaxis and reduction in the forward migration of the cell was revealed. Additionally, the impact of LAI-1 was attributable to a direct alteration of the microtubule and actin cytoskeleton.

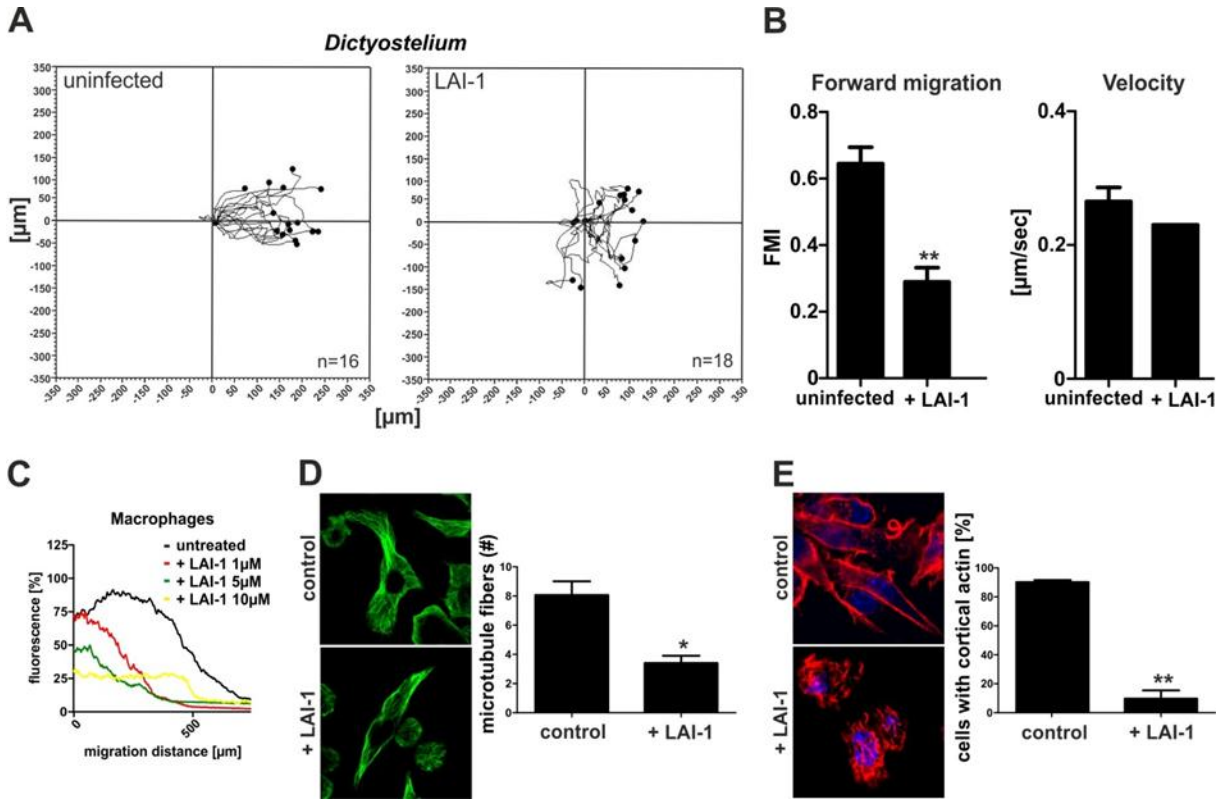

Figure 23. LAI-1 negatively alters directed cell migration by influencing microtubule and actin polymerization.

A. *D. discoideum* Ax3 strain harboring pSW102 (GFP) was treated with LAI-1 (10 µM) for 2 h. Single cell migration towards folic acid (1 mM) was tracked in an under-agarose assay for 15 min. Plots are representative of at least three independent experiments with 15 – 20 cells tracked per experiment.

B. FMI and velocity were analyzed using the ImageJ manual tracker and Ibidi chemotaxis software.

C. Murine RAW 264.7 macrophages were treated with different concentrations of racemic LAI-1 (1, 5 or 10 µM) and chemotaxis towards CCL5 (100 ng mL^{-1}) was documented after 4 h in an under-agarose assay by staining cells with a Cell Tracker Green BODIPY. Graph depicts the percentage of fluorescence intensity versus the migration distance and is representative of at least three independent experiments.

D. Murine RAW 264.7 macrophages were treated with LAI-1 (10 µM, 1 h) and immuno-labeled with α-tubulin (green). Microtubule polymerization was analyzed using confocal fluorescence microscopy by counting the number of microtubules fibers per cell along a cross-section.

E. The effect of LAI-1 (10 µM, 1 h) on actin (phalloidin, red) polymerization in RAW 264.7 macrophages was determined by quantifying the number of cells with cortical actin.

Graphs show means and standard deviations of three independent experiments (n > 25 single cells for one experiment). Student´s t-test; * $p < 0.05$, ** $p < 0.01$.

2. LAI-1-dependent inhibition of cell migration requires IQGAP1 and Cdc42

Possible factors implicated in the LAI-1-triggered host cell signaling pathways were investigated. For this purpose, the effect of LAI-1 on random cell migration was assessed in a scratch/wound healing assay. A549 epithelial cells were used because of their sensitivity to RNA interference (siRNA) treatment, thus allowing the identification of host factors crucial for cell migration.

Confluent layers of A549 cells were treated for 48 h with siRNA against IQGAP1 or the small GTPases Cdc42, RhoA or Rac1 and with LAI-1 (10 µM). After treatment, images of the scratched positions were taken at time points 0 h and 24 h (Figure 24A). The percentage of scratch closures after 24 h is shown in Figure 24B.

Cells treated with LAI-1 alone did not close the scratch in comparison to the scrambled control (100% compared to 25%). For cells treated with siRNA only, the scratches were more or less closed after 24 h. Approximately 80%, 75%, 50% and 80% scratch closure was observed for IQGAP1, Cdc42, RhoA and Rac1, respectively. Upon depletion of IQGAP1, Cdc42 or RhoA and treatment with LAI-1, the scratch closures were about 90%, 80% or 50%, respectively. This was not the case for Rac1, where the scratch remained open (closure below 25%). Since the depletion of Rac1 did not affect the inhibition of random cell migration by LAI-1, this small GTPase is dispensable for LAI-1 signaling. Of note, there was no distinguishable difference in the closure of cells treated with siRNA against RhoA, with or without LAI-1. For both conditions, the scratches were closed to 50%, suggesting that the depletion of RhoA alone reduces random cell migration to some extent. The siRNA depletion efficiencies were determined by Western Blot (Figure 24C).

In summary, these experiments revealed that transduction of LAI-1-mediated inter-kingdom signaling is significantly and specifically promoted by IQGAP1 and Cdc42.

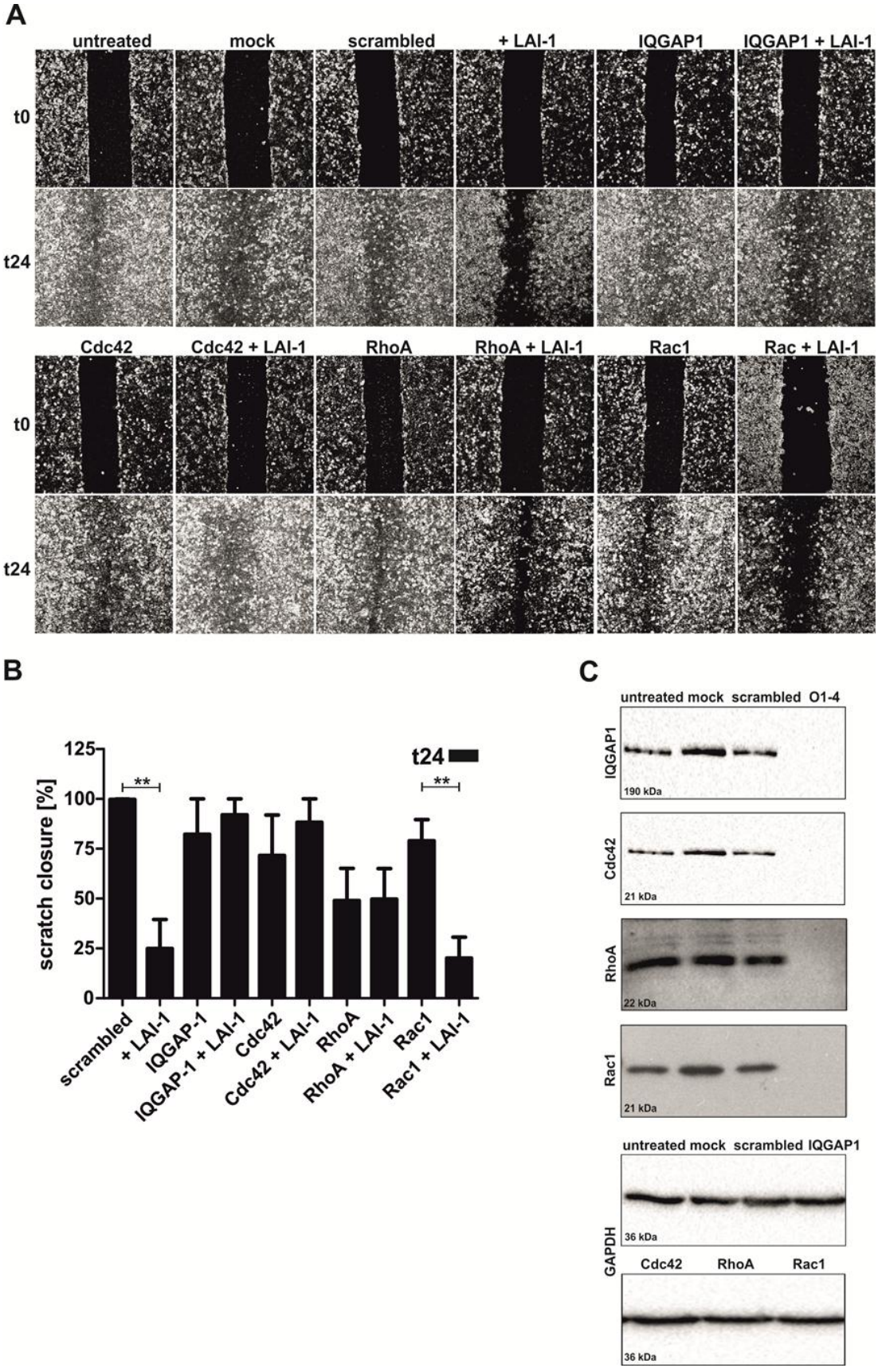
A
untreated
mock
scrambled
+ LAI-1
IQGAP1
IQGAP1 + LAI-1
t0
t24
Cdc42
Cdc42 + LAI-1
RhoA
RhoA + LAI-1
Rac1
Rac + LAI-1
t0
t24
B
scratch closure [%]
125
100
75
50
25
0
t24
**
**
scrambled
+ LAI-1
IQGAP-1
IQGAP-1 + LAI-1
Cdc42
Cdc42 + LAI-1
RhoA
RhoA + LAI-1
Rac1
Rac1 + LAI-1
C
untreated mock scrambled O1-4
IQGAP1
190 kDa
Cdc42
21 kDa
RhoA
22 kDa
Rac1
21 kDa
untreated mock scrambled IQGAP1
GAPDH
36 kDa
Cdc42
RhoA
Rac1
36 kDa

Figure 24. LAI-1-dependent inhibition of cell migration requires IQGAP1 and Cdc42.
A. Confluent layers of A549 epithelial cells were treated for 48 h with siRNA against IQGAP1, Cdc42, RhoA or Rac1. Cells treated only with transfection reagent (mock), LAI-1 (10 µM) or transfected with negative nonsense oligonucleotides (scrambled siRNA) served as controls. The epithelial cells were then treated with LAI-1 (10 µM, 90 min), scratched with a sterile pipette tip and allowed to migrate for another 24 h. After washing detached cells off, images of the scratched position were taken at time point 0 h and after 24 h using confocal microscopy.
B. After 24 h, the percentage of scratch closure was quantified using the ImageJ software. Means and standard deviations from at least three independent experiments are represented (comparison between untreated cells and the corresponding LAI-1 condition).
C. A549 cells were treated with the mentioned siRNA for 48 h and the samples were harvested and prepared for SDS-PAGE. The siRNA efficiency was controlled by Western Blot using the corresponding antibody for each protein. Untreated, mock and scrambled samples served as controls for the siRNA treated sample (O1-4). GAPDH (36 kDa) was used as a positive control. Student´s t-test; ** $p < 0.01$.

3. LAI-1 triggers inactivation of Cdc42 and redistribution of IQGAP1

To determine whether LAI-1 has an impact on the activation of Cdc42, pulldown experiments using A549 epithelial cells treated with LAI-1 (10 µM) and subsequent anti-Cdc42 Western blotting were performed (Figure 25A).

The amount of active Cdc42 was determined using an antibody directed against Cdc42(GTP) and band intensities were quantified by densitometry (Figure 25B). An antibody recognizing both the inactive (GDP) and active (GTP) forms of Cdc42 was used to control the efficiency of the pulldown. An anti-GAPDH control was employed to ensure that an equal amount of protein was present. This examination showed that LAI-1 reduced the amount of active Cdc42(GFP) approximately fourfold. The quantity of Cdc42(GTP/GDP) was unchanged after LAI-1 treatment in comparison to untreated control cells.

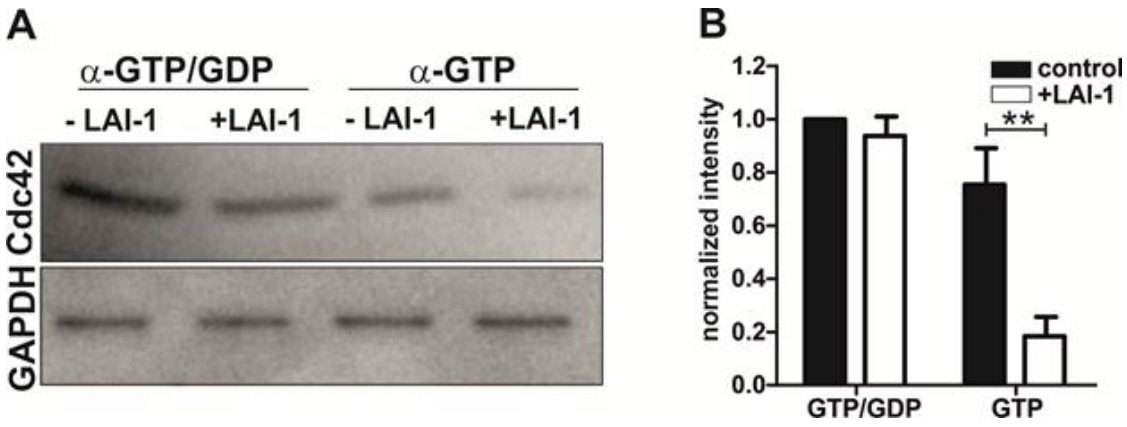

Figure 25. LAI-1 promotes the inactivation of Cdc42.
A. A549 epithelial cells treated with LAI-1 (10 µM, 1 h) were used for pulldown assays and a subsequent Western Blot. The activation state of Cdc42 (21 kDa) was analyzed using antibodies recognizing Cdc42(GTP/GDP) or Cdc42(GTP) only. GAPDH (36 kDa) served as loading control.
B. Graph represents the quantification by densitometry using the ImageJ software (Student´s t-test; ** $p < 0.01$).

Further, the localization of IQGAP1 and Cdc42 in the cell after LAI-1 treatment was studied. A549 cells were incubated with the *L. pneumophila* QS molecule LAI-1 (10 µM, 1 h) and immuno-stained against IQGAP1 (Figure 26A) or Cdc42 (Figure 26C).

Upon addition of LAI-1, a clear relocalization to the cellular cortex was observed for IQGAP1, but not for Cdc42. Quantifications of this redistribution are represented in Figure 26B for IQGAP1 and in Figure 26D for Cdc42. After LAI-1 treatment, nearly 100% of the cells exhibited a relocalization of IQGAP1 from the cytoplasm to the cell cortex. In contrast, the cytoplasmic localization of Cdc42 remained unchanged after LAI-1 addition.

Furthermore, a possible impact of LAI-1 on the phosphorylation status of Cdc42 was assessed by staining A549 cells treated with LAI-1 (10 µM) with an antibody recognizing Cdc42/Rac1-phospho-Ser71. However, no changes were observed in the phosphorylation by fluorescence microscopy (Figure 26E and 26F).

In summary, a LAI-1-dependent inactivation of the GTPase Cdc42 and redistribution of IQGAP1 to the cellular cortex were demonstrated.

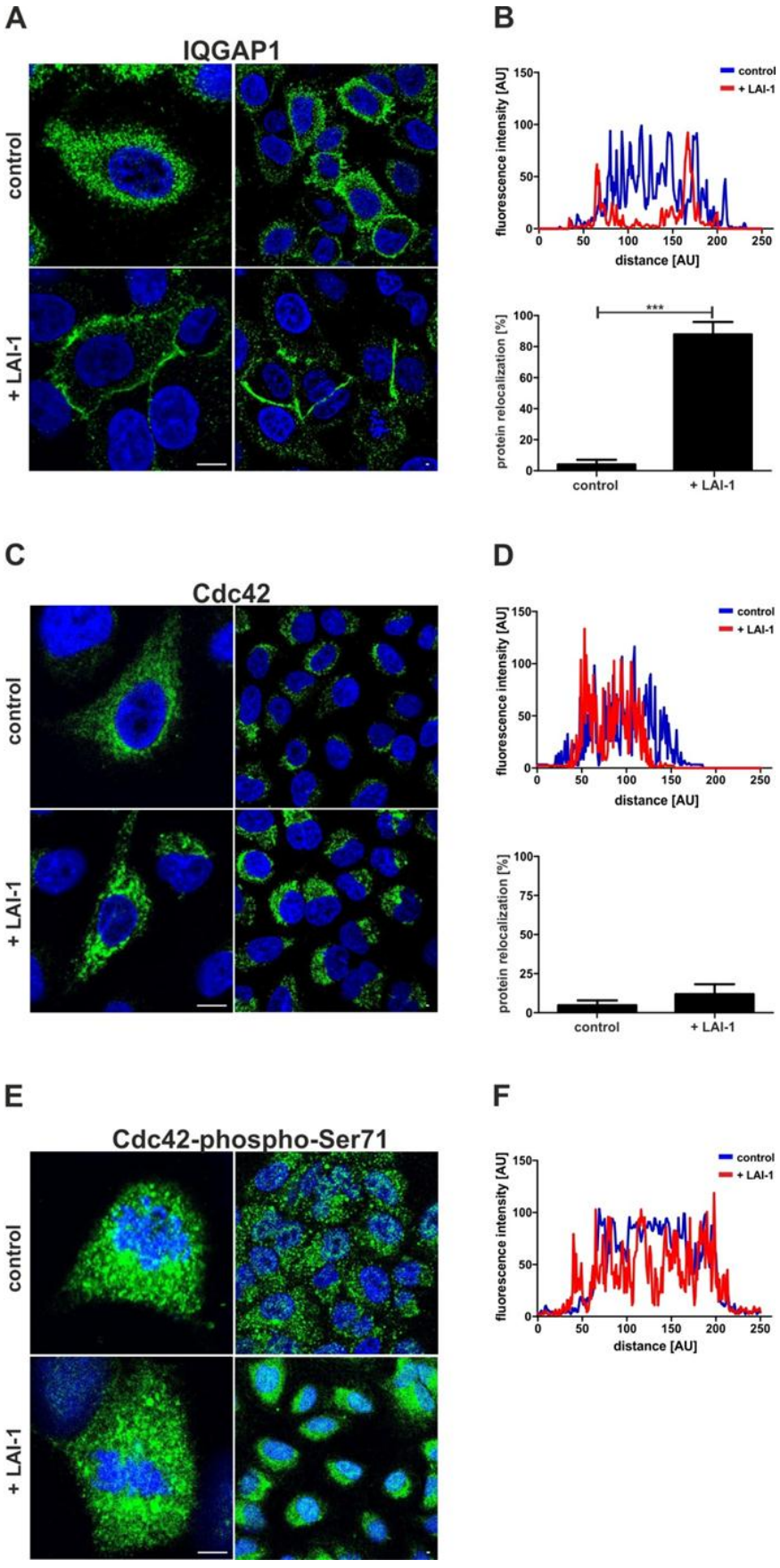

Figure 26. LAI-1 causes a redistribution of IQGAP1 to the cellular cortex.
A549 cells were treated with LAI-1 (10 µM, 1 h), fixed and stained with antibodies (FITC, green) against IQGAP1 (A) or Cdc42 (C). Nuclei were stained with DAPI in blue. Protein localization was analyzed by confocal fluorescence microscopy. Graphs depict the relative fluorescence intensity along a section of a cell (arbitrary units, AU) and the quantification of protein relocalization (B, IQGAP1; D, Cdc42). Redistribution of IQGAP1 was observed in over 50 cells per condition after LAI-1 treatment.
A549 cells were stained with an antibody against Cdc42/Rac1-phospho-Ser71 (FITC, green) and analyzed by confocal fluorescence microscopy (E). Graph (F) illustrates, through the relative fluorescence intensity along a section of a cell (arbitrary units, AU), no difference in the phosphorylation status of Cdc42 after LAI-1 treatment (10 µM, 90 min). Student´s t- test; *** $p < 0.001$.

4. Inhibition of cell migration through LAI-1 requires the Cdc42 GEF ARHGEF9

As LAI-1 causes an inactivation of Cdc42, the activation mechanism of the small GTPase was further investigated. The activation status of Cdc42 is controlled by GEFs or GAPs which appeared to be the next plausible targets to test. Three GEFs (ARHGEF9, FGD1 or DOCK11) and two GAPs (GAP1 or GAP17), specific for Cdc42, were depleted by RNAi in epithelial A549 cells. To test whether these regulators are involved in LAI-1 signaling, a scratch assay was performed.

Confluent cell layers were treated with siRNA against the GEFs and GAPs for 48 h and/or with LAI-1 (10 µM, 90 min). Images of the scratched positions were taken at time points 0 h and 24 h after treatment (Figure 27A) and the scratch closure was evaluated after 24 h of random migration (Figure 27B). The scratches remained open for all cells treated with LAI-1 and depleted for FGD1, DOCK11, GAP1 or GAP17 (around 15-20%), but not GEF9 (closure nearly 100%). Therefore, GEF9 is required for LAI-1-dependent signaling of cell migration inhibition. The scratch closure was approximately 100% for control cells (treated with siRNA only). The siRNA efficiency was controlled by Western Blot using the corresponding antibodies for each protein (Figure 27C). These results implicate that only GEF9 is involved in the activation/inactivation of Cdc42 by LAI-1 as the depletion of this GTPase abrogated the effect of LAI-1.

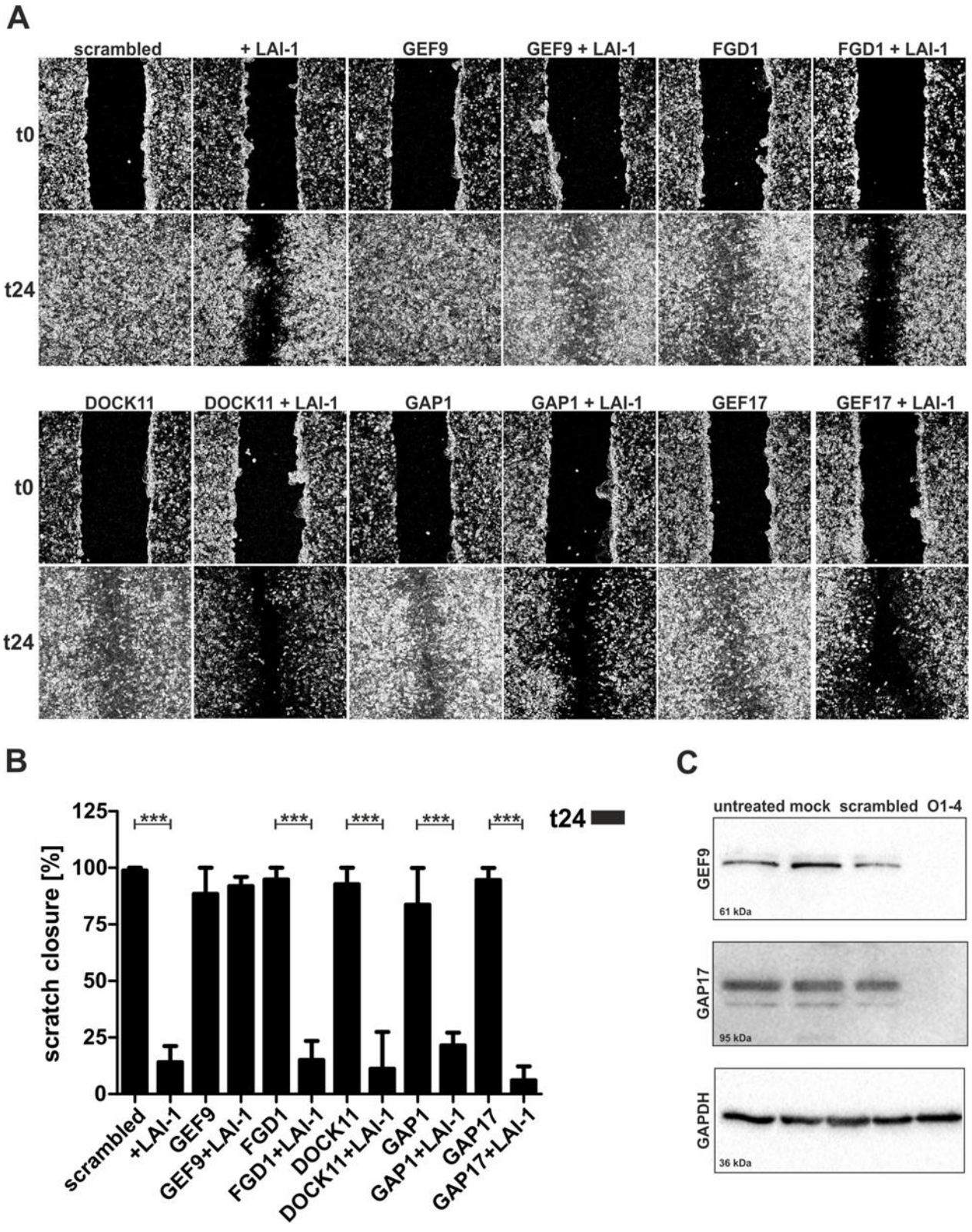
A
scrambled
+ LAI-1
GEF9
GEF9 + LAI-1
FGD1
FGD1 + LAI-1
t0
t24
DOCK11
DOCK11 + LAI-1
GAP1
GAP1 + LAI-1
GEF17
GEF17 + LAI-1
t0
t24
B
scratch closure [%]
125
100
75
50
25
0
***
t24
scrambled
+LAI-1
GEF9
GEF9+LAI-1
FGD1
FGD1+LAI-1
DOCK11
DOCK11+LAI-1
GAP1
GAP1+LAI-1
GAP17
GAP17+LAI-1
C
untreated mock scrambled O1-4
GEF9
61 kDa
GAP17
95 kDa
GAPDH
36 kDa

Figure 27. Cell migration inhibition through LAI-1 requires the Cdc42 GEF9.
A. Confluent layers of A549 cells were treated with siRNA against Cdc42 GEFs (GEF9, FGD1 or DOCK11) or GAPs (GAP1 or GAP17) for 48 h. Cells were additionally treated with LAI-1 (10 µM, 90 min), scratched with a sterile pipette tip and allowed to migrate for another 24 h. Closure of the wound was visualized at time point 0 h and after 24 h.
B. After 24 h, the scratch closure was quantified using the ImageJ software. Means and standard deviations are representative of three independent experiments.
C. The siRNA treatment efficiency was controlled by Western Blot for GEF9 (61 kDa) and GAP17 (95 kDa). GAPDH (36 kDa) served as a loading control. Means and standard deviations of three independent experiments are depicted. Student´s t-test; *** $p < 0.001$.

5. IQGAP1 functions upstream of Cdc42 in the LAI-1 signaling pathway

In order to test whether IQGAP1 is functioning upstream or downstream of Cdc42, A549 epithelial cells were treated with siRNA against IQGAP1 or Cdc42, with or without LAI-1 and immuno-stained for IQGAP1 or Cdc42. The cellular localization of these proteins was determined by fluorescence microscopy (Figure 28A).

IQGAP1 and Cdc42 were visible in the cytoplasm of control cells (untreated, mock or scrambled). In cells treated with siRNA against IQGAP1 (depletion efficiency 100%), Cdc42 was barely produced with only 10% of the protein remaining. In cells treated with siRNA against Cdc42, IQGAP1 was present at almost 100%. The depletion of target proteins was efficient with nearly no proteins being detectable for both conditions (Figure 28B).

A combination of siRNA treatment against Cdc42 and exposure to LAI-1 (10 µM) revealed that IQGAP1 was still present in cells and redistributed to the cell cortex (Figure 28C).

Taken together, this experiment showed that the scaffold protein IQGAP1 functions upstream of Cdc42 and regulates the stability of the small GTPase. Furthermore, the relocalization of IQGAP1 in the LAI-1 signaling cascade is not dependent on Cdc42.

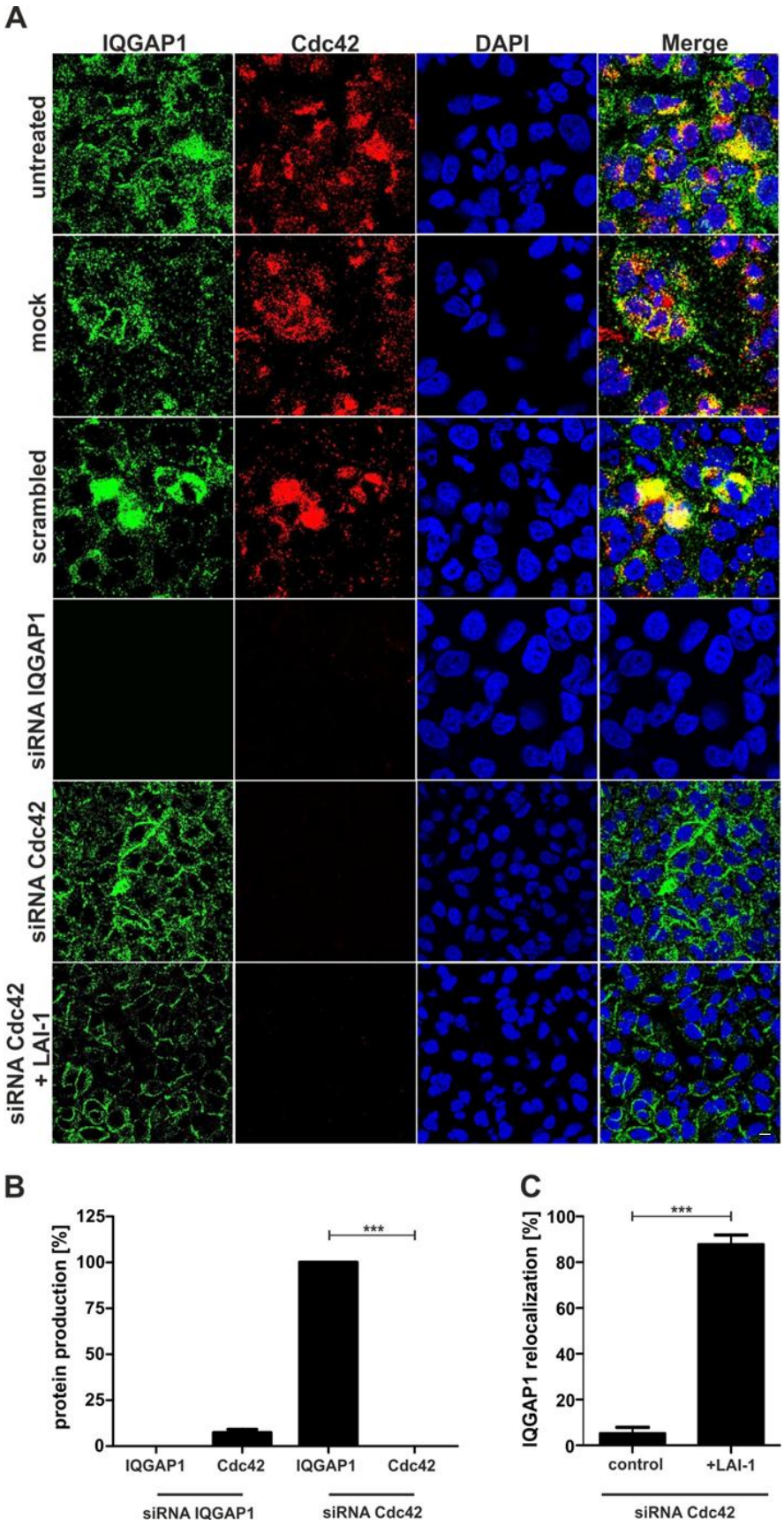

Figure 28. IQGAP1 functions upstream of Cdc42 in the LAI-1 signaling cascade.

A. A549 cells were treated with LAI-1 (10 µM, 1 h) and/or with siRNA against IQGAP1 and Cdc42 for 48 h, fixed and stained with antibodies against IQGAP1 (FITC, green) or Cdc42 (Cy5, red). Protein localization was visualized by confocal fluorescence microscopy. Nuclei were stained with DAPI in blue.

B. Graph represents the quantification of proteins present (IQGAP1 or Cdc42) after siRNA treatment (IQGAP1 or Cdc42).

C. Graph shows the quantification of IQGAP1-redistribution after the depletion of Cdc42 by siRNA.

The protein localization was determined using the relative fluorescence intensity (arbitrary units, AU) along a section of a cell (n > 50). Means and standard deviations of three inde-pendent experiments are shown. Student´s t-test; *** $p < 0.001$.

6. LAI-1 reverses the Icm/Dot-dependent inhibition of migration caused by *L. pneumophila*

L. pneumophila inhibits random and directed cell migration in an Icm/Dot-dependent manner (section A.1. and A.4.). As the bacterial autoinducer molecule LAI-1 negatively alters cell migration, the effect of *L. pneumophila* in combination with LAI-1 treatment was analyzed. To this end, different concentrations of LAI-1 (1, 5 or 10 µM) were added to *D. discoideum* or macrophages infected (MOI 10, 1 h) with *L. pneumophila* wild-type (Figure 29A and 29C) or Δ*icmT* (Figure 29B and Figure 29D). A chemotactic under-agarose assay was used to assess the migration of *D. discoideum* cells or macrophages towards folic acid (1 mM) or CCL5 (100 ng mL^{-1}), respectively. A dose-dependent reversal of the inhibition caused by LAI-1 was observed upon infection with *L. pneumophila* wild-type in both cell types. Cells infected with the wild-type strain did not migrate, whereas a maximum migration distance of 1300 µm or 500 µm for *D. discoideum* cells or macrophages, respectively, was reached after LAI-1 treatment. Furthermore, LAI-1 inhibited directed migration of Δ*icmT*-infected cells, as indicated by 600 µm instead of 1200 µm migration distance for *D. discoideum* cells or nearly zero instead of 500 µm for macrophages.

Since the combination of bacteria and LAI-1 clearly reverses the previously described effects (section A.), a closer look on motility parameters was taken. *D. discoideum* cells were tracked (Figure 29E) after an infection and treatment with LAI-1 (10 µM). The FMI and velocity were investigated (Figure 29F). The FMI of cells infected with wild-type *L. pneumophila* was low (around 0.25) and high (0.65) for Δ*icmT*-infected cells similar to uninfected cells (data not shown). After LAI-1 treatment, the phenotypes were reversed. FMIs of nearly 0.6 and 0.35 were observed for wild-type- and Δ*icmT*-infected *D. discoideum* cells, respectively. No distinguishable differences were detected for the velocity with a value of approximately 0.3 µm sec^{-1} for each condition.

These results suggest that *L. pneumophila* and LAI-1 target at least partly shared signaling pathways involved in chemotactic and random host cell migration.

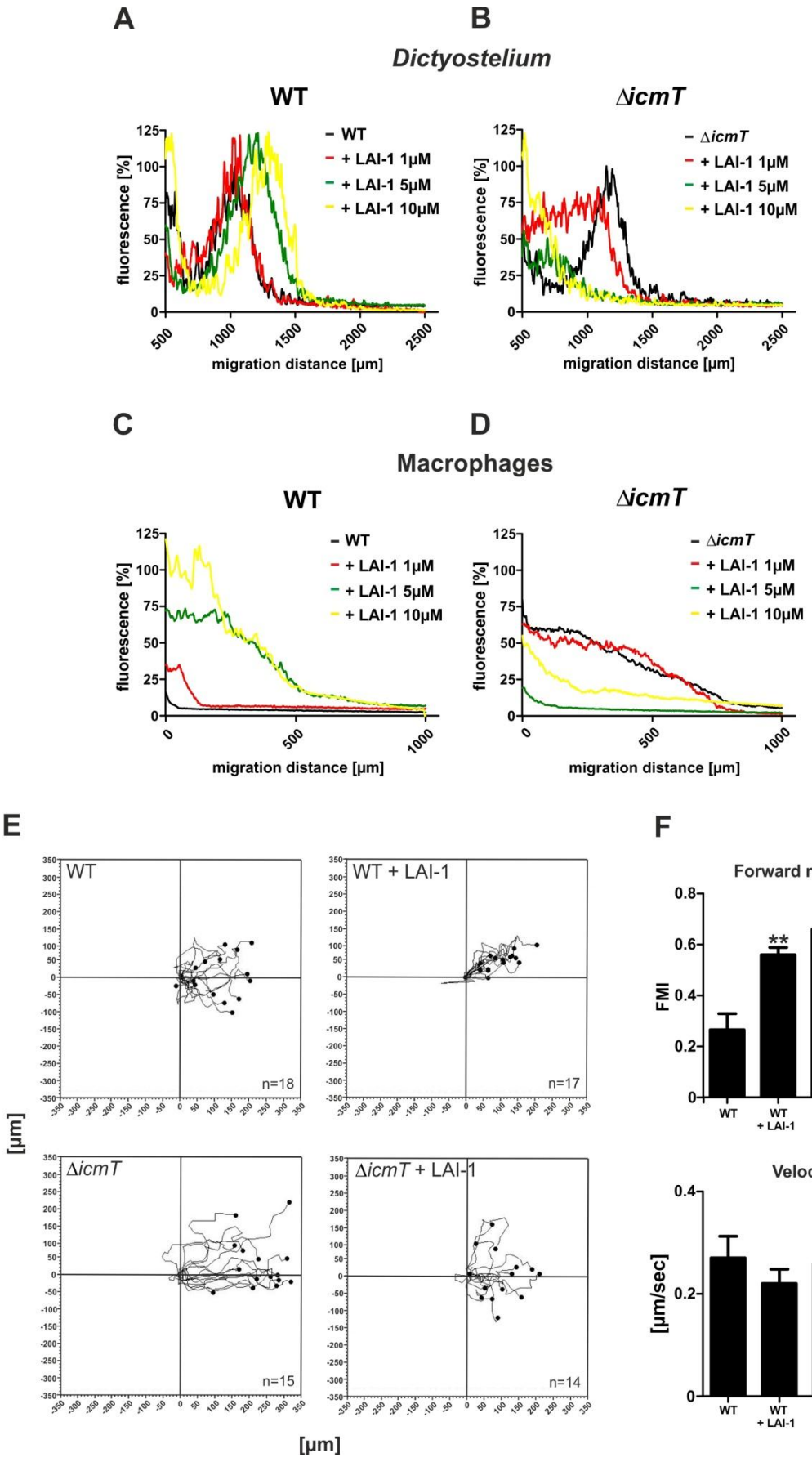
A
B
Dictyostelium
WT
ΔicmT
fluorescence [%]
migration distance [µm]
WT
ΔicmT
+ LAI-1 1µM
+ LAI-1 5µM
+ LAI-1 10µM
C
D
Macrophages
E
F
WT
WT + LAI-1
ΔicmT
ΔicmT + LAI-1
n=18
n=17
n=15
n=14
[µm]
Forward migration
FMI
Velocity
[µm/sec]
**
*
WT
WT + LAI-1
ΔicmT
ΔicmT + LAI-1

Figure 29. LAI-1 reverses the Icm/Dot-dependent inhibition of migration caused by *L. pneumophila*.

The effect of different concentrations of LAI-1 (1, 5 or 10 µM) on *D. discoideum* chemotaxis after infection (MOI 10, 1 h) with *L. pneumophila* wild-type (A) or an Δ*icmT* (B) strain was analyzed in an under-agarose assay. Amoebae harboring pSW102 (GFP) migrated for 4 h towards folic acid (1 mM) and were visualized by confocal fluorescence microscopy. Graphs show the percentage of fluorescence intensity versus migration distance and are representative of at least three independent experiments.

Directed migration of RAW 264.7 macrophages towards CCL5 (100 ng mL^{-1}) after *L. pneumophila* wild-type (C) or Δ*icmT* (D) infection and LAI-1 treatment was monitored in an under-agarose assay for 4 h. Graph depicts the percentage of fluorescence intensity of macrophages, stained with a Green CellTracker BODIPY, versus their migration distance. Results are representative of at least three independent experiments.

D. discoideum Ax3 strain harboring pSW102 (GFP) was infected (MOI 10, 1 h) with *L. pneumophila* wild-type or Δ*icmT* mutant and treated with LAI-1 (10 µM, 1 h). Cells were tracked (n > 50) in an under-agarose assay towards folic acid (1 mM) for 15 min. Tracking plots are representative of at least three independent experiments (E). Motility parameters (FMI and velocity) were analyzed using the ImageJ manuel tracker and the Ibidi chemotaxis software (F). Student´s t-test; * $p < 0.05$ ** $p < 0.01$.

7. Absence of Cdc42 promotes migration inhibition by *L. pneumophila*

A possible hypothesis was that LAI-1 and *L. pneumophila* converge on common pathways or host factors to inhibit cell migration. For this purpose, confluent layers of A549 cells were first treated with siRNA against the small GTPases Cdc42 or Rac1 (as negative control) for 48 h and then infected with *L. pneumophila* wild-type or a Δ*icmT* mutant strain at an MOI of 10 for 90 min. Random migration was analyzed in a scratch assay and images were taken at time points 0 h and 24 h after infection (Figure 30A). The percentage of scratch closure at the end time point is represented in Figure 30B. The scratches of control cells (scrambled or siRNA against Cdc42 or Rac1 only) and Δ*icmT*-infected cells treated or not with siRNA against Cdc42 or Rac1 were closed to 100% after 24 h. Cells infected with *L. pneumophila* wild-type, treated or not with siRNA against Rac1, did not close the scratch (nearly 0%). However, following depletion of Cdc42 and *L. pneumophila* wild-type infection, the failure of closing the scratch was quite dramatic. The scratch was more open than at time point 0 h reaching a closure value of - 80%. Importantly, no increased cytotoxicity was observed under these conditions as cell morphology was unchanged. Moreover, the inhibition of random migration by wild-type *L. pneumophila* was severely and significantly augmented, in comparison to cells treated with siRNA against Cdc42 and infected or not with the Δ*icmT* mutant strain.

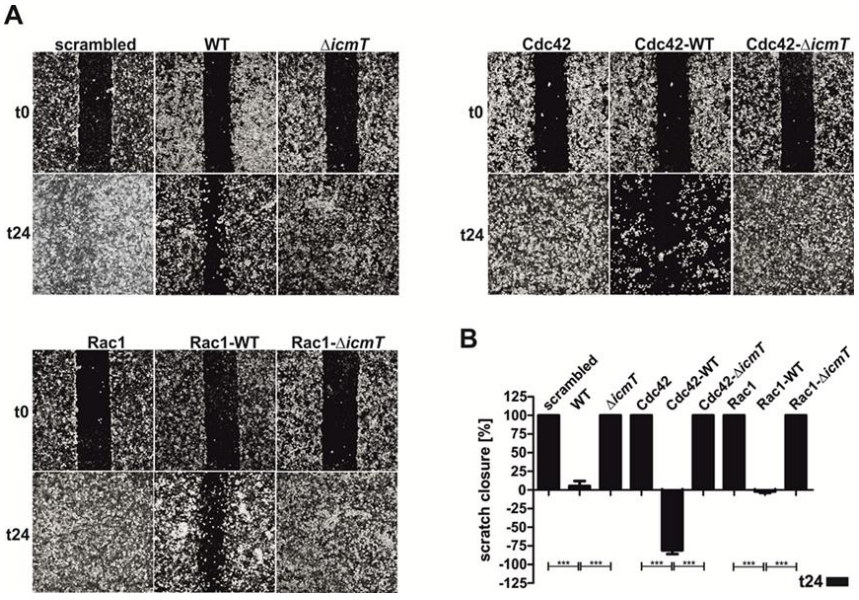

Figure 30. Absence of Cdc42 promotes the inhibition of migration by *L. pneumophila*.
A. Confluent layers of A549 cells were treated with siRNA against Cdc42 or Rac1 (negative control) for 48 h and subsequently infected (MOI 10, 90 min) with *L. pneumophila* wild-type or Δ*icmT*. Cells were scratched and allowed to migrate for another 24 h.
B. After 24 h of migration, the percentage of scratch closure was determined using the ImageJ software. Means and standard deviations of three independent experiments are shown (Student´s t-test; *** $p < 0.001$).

Since the Icm/Dot-dependent inhibition of migration by *L. pneumophila* involves Cdc42, a closer look was taken regarding the cellular localization of the bacteria and the small GTPase. A549 epithelial cells were infected (MOI 10, 1 h) with DsRed-labelled *L. pneumophila* wild-type or a Δ*icmT* mutant strain and treated or not with LAI-1 (10 µM, 1 h). The proteins of interest, IQGAP1 (Figure 31A) and Cdc42 (Figure 31B), were stained with the corresponding antibody and the localization was analyzed by fluorescence microscopy. IQGAP1 as well as Cdc42 colocalized with the bacteria, yet the localization of either protein remained unchanged after LAI-1 addition.

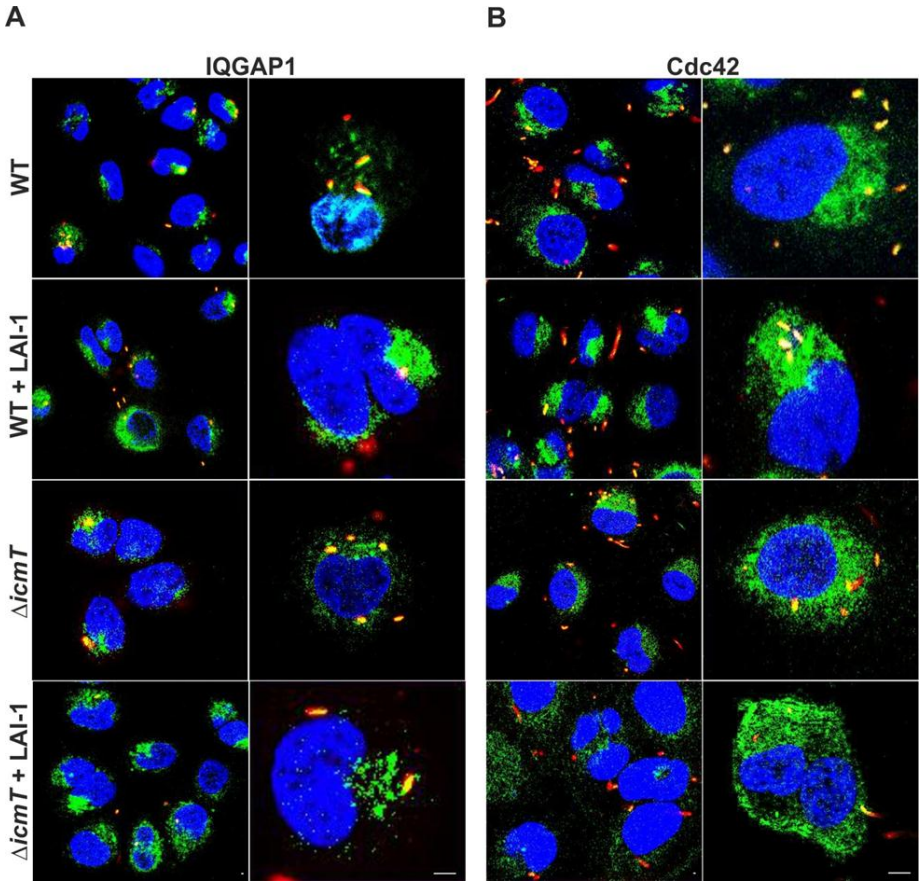

Figure 31. IQGAP1 and Cdc42 colocalize with *L. pneumophila*.
A549 cells were infected (MOI 10, 1 h) with *L. pneumophila* wild-type or a Δ*icmT* mutant strain and treated with LAI-1 (10 µM, 1 h). Cells were fixed, stained with antibodies against IQGAP1 (A) or Cdc42 (B) and analyzed by confocal fluorescence microscopy (IQGAP1 and Cdc42: FITC, green; nucleus: DAPI, blue; *L. pneumophila*: pSW102, red).

Taken together, these results showed that the absence of the small GTPase Cdc42 promoted migration inhibition by *L. pneumophila*. Interestingly, a LAI-1-independent colocalization of IQGAP1 or Cdc42 with the bacteria was observed.

8. IQGAP1, Cdc42 and LAI-1 do not affect uptake and intracellular replication of *L. pneumophila*

To exclude the possibility that the effects observed were caused by an interference between infection and siRNA treatment, intracellular replication assays were performed (Figure 32A). A549 cells were infected with *L. pneumophila* wild-type or Δ*icmT* mutant strains and treated with siRNA against IQGAP1 or Cdc42. Bacterial replication was followed over time (1, 20, 24 and 48 h). After 24 h, the number of wild-type *L. pneumophila* increased while the Δ*icmT* strain did not replicate over 48 h. Therefore, the treatment with siRNA had no effect on intracellular replication of either strain.

Moreover, the effect of different LAI-1 concentrations (1, 5 and 10 µM) on bacterial uptake efficiency was analyzed by flow cytometry. *D. discoideum* cells (Figure 32B) or murine macrophages (Figure 32C) were infected (MOI 10, 1 h) with *L. pneumophilla* wild-type or Δ*icmT* and treated with LAI-1 for 1 h. The addition of the autoinducer molecule did not significantly alter bacterial uptake of wild-type (more efficient than the mutant strain) or Δ*icmT*, either by *D. discoideum* or by macrophages.

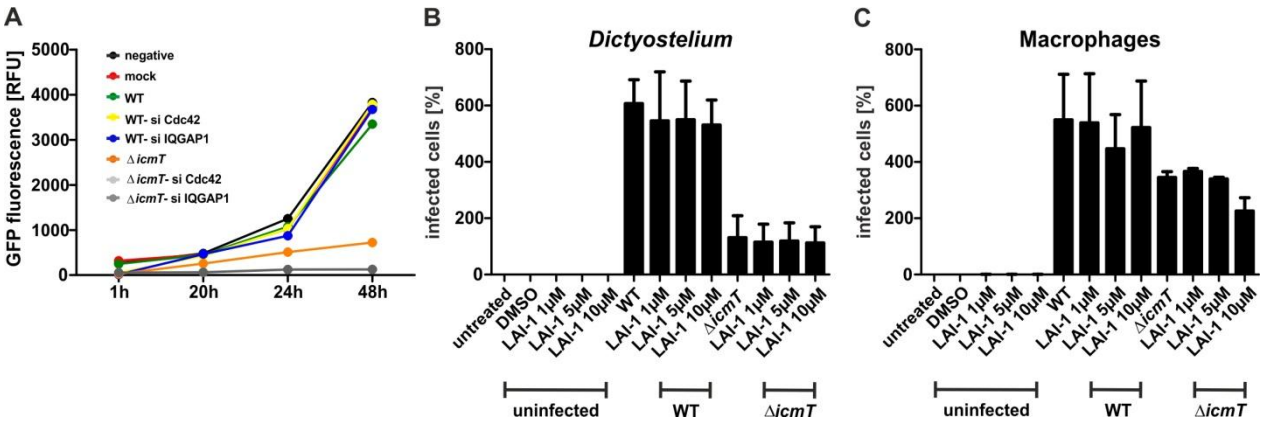

Figure 32. Intracellular replication or bacterial uptake is not affected by siRNA or LAI-1 treatment, respectively.

A549 cells were treated with a mixture of four oligonucleotides for each target (IQGAP1 or Cdc42) for 48 h and subsequently infected with GFP-labeled *L. pneumophila* wild-type or a Δ*icmT* mutant strain. Graph (A) depicts the GFP fluorescence measured at different time points post-infection (1, 20, 24 and 48 h). *D. discoideum* amoebae (B) or murine RAW 264.7 macrophages (C) were infected with the same strains as mentioned in (A) and treated with LAI-1 (1, 5 or 10 µM; 1 h). Uptake efficiency was analyzed by flow cytometry (GFP-positive phagocytes).

9. LAI-1 partially compensates the lack of LqsA for cell migration inhibition

Directed and random migration of free-living amoebae as well as mammalian cells were inhibited by *L. pneumophila* or LAI-1 (section A.1. and B.1.). Previous results showed that no inhibition of directed migration was observed following infection with the bacterial mutant strain lacking the autoinducer synthase LqsA which no longer produces LAI-1. However, it was not known whether LAI-1 would compensate for the lack of LqsA during random cell migration. To this end, confluent layers of A549 epithelial cells were infected (MOI 10, 90 min) with *L. pneumophila* wild-type, Δ*icmT* or Δ*lqsA* strains and treated or not with LAI-1 (10 µM, 90 min). Cell layers were scratched and images of the positions were taken at time points 0 h and 24 h after (Figure 33A). The percentage of scratch closure was 100% for untreated cells as well as for cells infected with the Δ*icmT* or Δ*lqsA* mutant strains after 24 h. Furthermore and in accordance with previous results (B.6.), the inhibition of cell migration caused by the wild-type strain (closure below 10%) was reversed by adding LAI-1 (closure 100%). Also, Δ*icmT*-infected cells did not migrate after LAI-1 treatment, as the scratch remained open with a closure of only 10%. Addition of LAI-1 to Δ*lqsA*-infected cells resulted in scratch closure of only approximately 60% (Figure 33B). Therefore, LAI-1 partially compensated the lack of LqsA for cell migration inhibition.

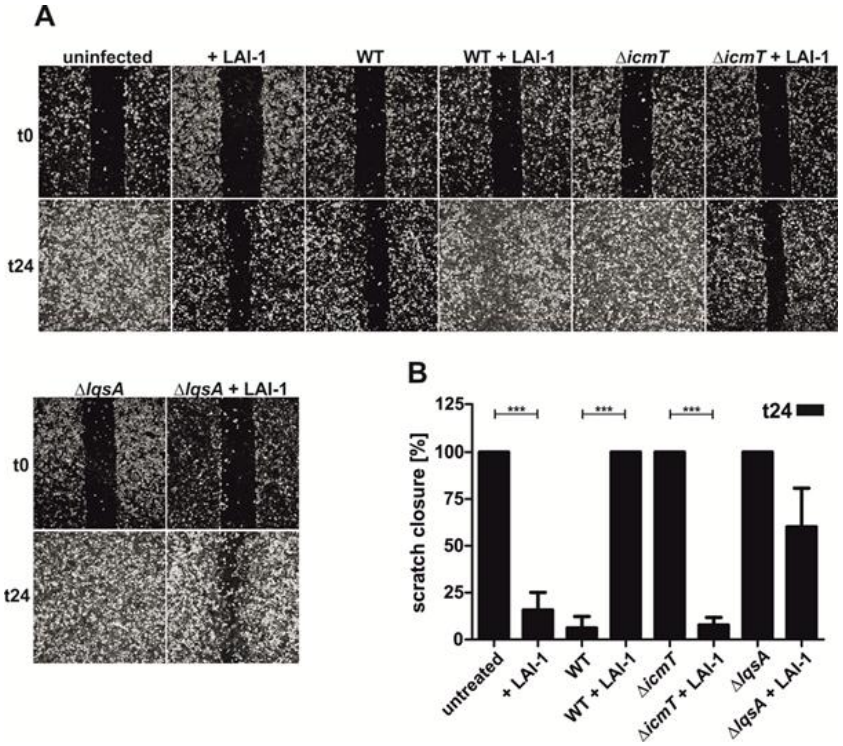

Figure 33. LAI-1 partially compensates the lack of LqsA for cell migration inhibition.
A. Confluent cell layers of A549 were infected (MOI 10, 90 min) with *L. pneumophila* wild-type, Δ*icmT* or Δ*lqsA* and treated with LAI-1 (10 µM). Cells were then scratched with a sterile pipette tip and allowed to migrate for additional 24 h. Images were taken at the time points 0 h and 24 h using confocal microscopy.
B. After 24 h, the scratch closure was determined using the ImageJ software. The data are representative of at least three independent experiments (Student´s t-test; *** $p < 0.001$).

Taken together, LAI-1 partially reversed the lacking effect of *L. pneumophila* Δ*lqsA* on random migration.

In summary, the first part (section A) of this thesis revealed an Icm/Dot-dependent inhibition of phagocyte migration by *L. pneumophila*, which is antagonized by LegG1, a translocated Ran GTPase activator.

The second part (section B) established new insights into the effect of the bacterial autoinducer molecule LAI-1 on host cell migration. Inter-kingdom signaling by the *L. pneumophila* QS compound LAI-1 inhibits directed and random cell migration by involving IQGAP1, Cdc42 and GEF9.

IV. Discussion

A. LegG1 antagonizes the inhibition of phagocyte migration by *L. pneumophila*

L. pneumophila exploits a broad range of host cell processes including cell motility. In this work, an Icm/Dot- and dose-dependent inhibition of amoebae and immune cell chemotaxis by *L. pneumophila* was shown (section A.1.). In previous studies, LegG1 was identified as the first bacterial activator of the small GTPase Ran and described as a modulator of microtubule polymerization and LCV motility [18]. Furthermore, the experiments presented in section A.2. demonstrated that LegG1 influences host cell migration. In absence of the Ran activator, a hyper-inhibition of cell chemotaxis was documented using distinct cell types, migration assays and chemoattractants. Upon infection with *L. pneumophila* lacking LegG1, single cell analysis revealed that the FMI and the velocity of cells was decreased (section A.3.). The phenotype was complemented by providing *legG1* on a plasmid. These results suggest that LegG1 is able to antagonize the *L. pneumophila*-dependent inhibition of cell migration and to stimulate motility of protozoan and mammalian cells. Moreover, *L. pneumophila*- and LegG1-dependent modulation of random cell migration was observed in epithelial scratch assays. Ran activation by LegG1 represents a major downstream effect during *L. pneumophila* infection [18]. The results described in section A.4. and A.5. proved that the modulation of cell migration by LegG1 is dependent on Ran by regulating microtubule polymerization and consequently random as well as directed cell migration. While LegG1 is sufficient to stimulate cell motility, other bacterial effector proteins might target further signaling cascades (section A.1). These data suggest that *L. pneumophila* triggers conserved eukaryotic components to inhibit cell motility rather than targeting distinct signal transduction pathways involved in chemotaxis (Figure 34).

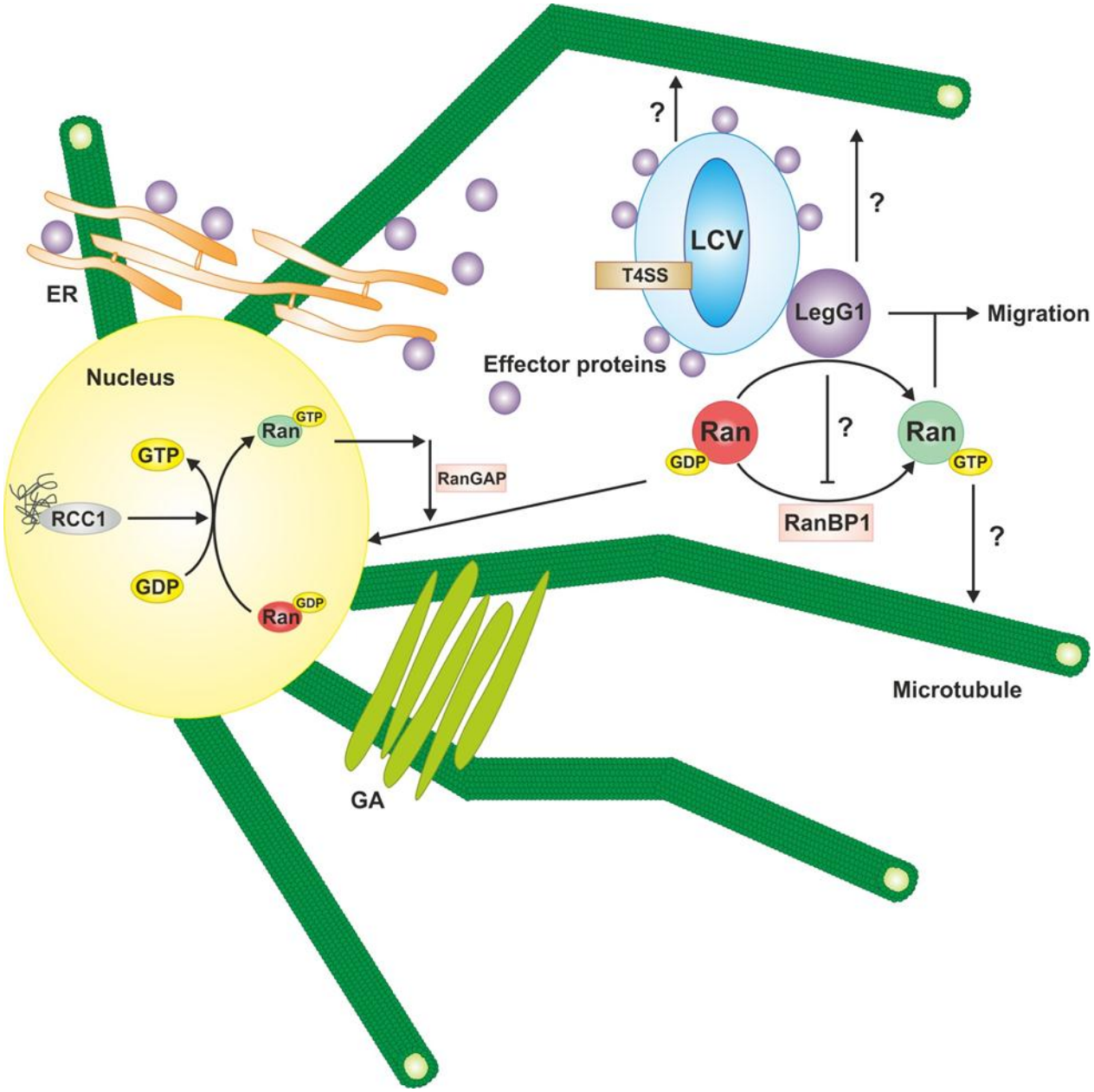

Figure 34. LegG1-dependent modulation of immune cell migration.
L. pneumophila replicates in LCVs and translocates via the T4SS effector proteins which subvert numerous host pathways by targeting the ER and multiple GTPases. The bacterial protein LegG1 activates the GTPase Ran, stabilizes microtubules and promotes cell migration. Ran activation is triggered in the nucleus by the GEF RCC1. It is still unclear how the LCV, LegG1 or RanGTP interact with the microtubule network in *L. pneumophila*-infected cells.
Abbreviations: ER: endoplasmic reticulum; GA: Golgi apparatus; GAP: GTPase activating protein; LCV: *Legionella*-containing vacuole; Ran: Ras-related nuclear protein; RCC1: regulator of chromosome condensation 1; T4SS: type IV secretion system.

1. *L. pneumophila* exploits small host GTPases

LCV formation is governed by the Icm/Dot T4SS which translocates approximately 300 different effectors into the host cell. These proteins target many host cell processes including the regulation of small host GTPases to exploit the secretory or endosomal pathway [53, 155]. Previous studies described a broad range of small GTPases which are recruited to the LCV membrane. One GTPase can be targeted by more than one Icm/Dot-translocated effector protein, e.g., Rab1 which is one of the regulatory host factors involved in membrane trafficking and protein transport from the ER to the Golgi apparatus (GA) [156, 157]. The temporal association of Rab1 to the cytosolic face of the LCV is regulated by the multifunctional protein SidM (DrrA) and the GAP LepB. SidM is only detected during the first 30 min of infection whereas LepB appears and remains for several hours. The Icm/Dot substrate SidM has Rab1 GEF as well as AMPylation activity essential for the recruitment and maintenance to the LCV [158]. In Δ*sidM* mutant strains, a strong decrease in Rab1 on LCVs was observed, suggesting that the GEF and AMPylation reactions are necessary to retain the small GTPase. AMP is removed from the GTPase by the deAMPylase SidD. LepB is able to inactivate Rab1 by acting as a GAP and promoting GTP hydrolysis. The small GTPase is then detached from the LCV by a RabGDI [55, 159, 160].

In addition, the bacterial effector protein AnkX catalyzes the transfer of a phosphocholine group from CDP-choline to a serine/threonine of Rab1 and Rab35. Moreover, Lem3 is able to reverse the AnkX-dependent modification of Rabs by acting as a dephosphocholinase [161]. Thus, these effector proteins interfere with host vesicle trafficking including endocytic and exocytic pathways [162, 163].

Furthermore, recent proteomic analysis of purified intact LCVs from *L. pneumophila*-infected macrophages identified 14 small Rab GTPases (Rab1, Rab2, Rab4, Rab5, Rab6, Rab7, Rab8, Rab10, Rab11, Rab14, Rab18, Rab21, Rab31 and Rab32). Rab5a, Rab14 and Rab21 were described as endocytic GTPases restricting multiplication of *L. pneumophila* and Rab8a, Rab10 and Rab21 as secretory GTPases implicated in Golgi-endosomes trafficking and promoting intracellular growth of the pathogen. Most of the Rab proteins localizing to the LCV are specifically enriched on vacuoles harboring wild-type *L. pneumophila* [149].

2. LegG1-dependent Ran activation is crucial for cell migration

Proteomics revealed the presence of the small GTPase Ran together with its effector RanBP1 on LCVs. LegG1, unique to the *L. pneumophila* Philadelphia strain, functions as a bacterial Ran activator and accumulates in an Icm/Dot-dependent manner on LCVs. The pleiotropic small GTPase Ran is involved in nucleo-cytoplasmic transport as well as in microtubule formation and spindle assembly. Ran activation promotes microtubule stabilization, LCV formation and motility as well as intracellular replication [18]. LegG1 displays amino acid sequence homology to the eukaryotic RanGEF RCC1 and contains a C-terminal CAAX domain. This motif is lipidated by host prenylation allowing to target bacterial effectors to host membranes [40, 89, 91].

LegG1-dependent Ran activation was demonstrated to modulate host cell migration through microtubule stabilization (section A.4. and A.5.). So far, further impacts of LegG1 on cell migration can not be ruled out, although additional experiments could analyze the effects of LegG1 on the actin cytoskeleton and Rho GTPases. Over 20 Rho GTPases have been identified in humans targeting protein kinases and actin binding proteins involved in the assembly of F-actin. Rho GTPases, present in the lamellipodial region of a cell, promote protusive events and motility [164].

It is also unknown, where the putative Ran receptor is localized on LCVs. LegG1 is located on the cytosolic face of the vacuole and colocalizes with the GA without disrupting it. A spatio-temporal regulation of Ran by LegG1 can be in *cis* or in *trans* (in a distance from the LCV). Furthermore, Ran activity was still present in cells infected with the Δ*legG1* mutant strain, suggesting that Ran activation occurs through other eukaryotic GEFs or bacterial effector proteins [18]. Besides RCC1, the cytoplasmic RanBP10 was described as a eukaryotic microtubule modulator which binds to Ran and β1-tubulin and thus might represent a scaffold protein linking Ran activation and microtubules [165].

Two other possible bacterial candidates involved in Ran activation are PpgA (Lpg2224) and LegG2 (Lpg0276). PpgA, predicted to possess RCC1 domains, shares 16% identity and 25% similarity with LegG1 [90]. Furthermore, LegG2 is possibly able to exchange GDP to GTP [89]. However, at this point, no LegG2-effect on cell migration, LCV localization or intracellular replication was observed.

Investigation of a *legG2* mutant strain in combination with siRNA against several RasGTPases (Rho, IQGAP1, Ran, Arf, Rab) might lead to new insights and establish a link between LegG2 and a host GTPase.

Ran activation by LegG1 might also be reverted by a hypothetical bacterial Ran GAP. Analogous processes were described for Rab1 (SidM/LepB as GEF/GAP, SidM/SidD as AMPylase/deAMPylase or AnkX/Lem3 as phosphocholinase/dephosphocholinase) [159, 163]. Furthermore, LegG1 might be degraded to modulate its activity. For instance, the Icm/Dot substrate SidH is polyubiquitinylated by the ubiquitin ligase LubX, thus triggering proteolysis by the proteasome [166].

Microtubule polymerization and polarization represent key processes in cell migration. Their function is mediated by microtubule-associated motors like kinesin, dynein and transport vesicles. Intrinsic dynamics are controlled by microtubule associated proteins (MAPs) [62]. The underlying mechanism for Ran GTPase in the positive regulation of microtubules is still unknown. Moreover, it remains unclear how the LCV is interacting with microtubules or how the movement is established and maintained. Numerous putative scaffold proteins, like RanBP10 might be implicated to link the bacterial vacuole with the microtubule cytoskeleton.

The benefit for *L. pneumophila* from the LegG1-dependent promotion of cell migration is uncertain. One hypothesis is that the effector protein counteracts Icm/Dot-translocated *L. pneumophila* effector proteins which destabilize microtubules. A large number of essential pathways including phagocytosis, vesicle trafficking, cytokinesis and migration might be impaired by these effectors. In such a way, LegG1 may dampen or revert a deleterious impact of other effectors on the host cytoskeleton. Besides, uncontrolled host movement might impede the survival and replication of the bacteria by enhancing energy expenditure necessary for increased migration. Thus, pathogens might benefit from specifically targeting membrane and vesicle trafficking or cell migration and tip the balance in their favors.

B. Inter-kingdom signaling by the *Legionella* quorum sensing molecule LAI-1

The experiments presented in the second part of this thesis (section B.) demonstrated that the autoinducer molecule LAI-1 of *L. pneumophila* modulates host cell motility. A dose-dependent inhibition of directed migration by racemic LAI-1 using the chemotactic under-agarose assay was observed. Furthermore, a pronounced inhibition was documented after addition of the (R)-form of LAI-1 (section B.1.). Single cell tracking (section B.2. and B.6.) revealed that the FMI but not the velocity was affected by LAI-1. The addition of the autoinducer molecule caused microtubule depolymerization and actin destabilization (section B.2.). LAI-1-triggered inhibition of directed and random migration was found to be dependent on IQGAP1 and Cdc42 (section B.3.). Indeed, IQGAP1, which is upstream of Cdc42 (section B.5.), relocalized from the cytoplasm to the cell cortex. Furthermore, an GEF9-dependent inactivation of Cdc42 was observed after LAI-1 treatment (section B.3. and B.4.). Finally, LAI-1 reversed the inhibition of migration caused by *L. pneumophila* infection (section B.6.) and the absence of Cdc42 triggered a pronounced inhibition of cell motility by *L. pneumophila* (section B.7.). Collectively, these results suggest that LAI-1 is a potent agent of inter-kingdom signaling, which affects host cell motility (Figure 35).

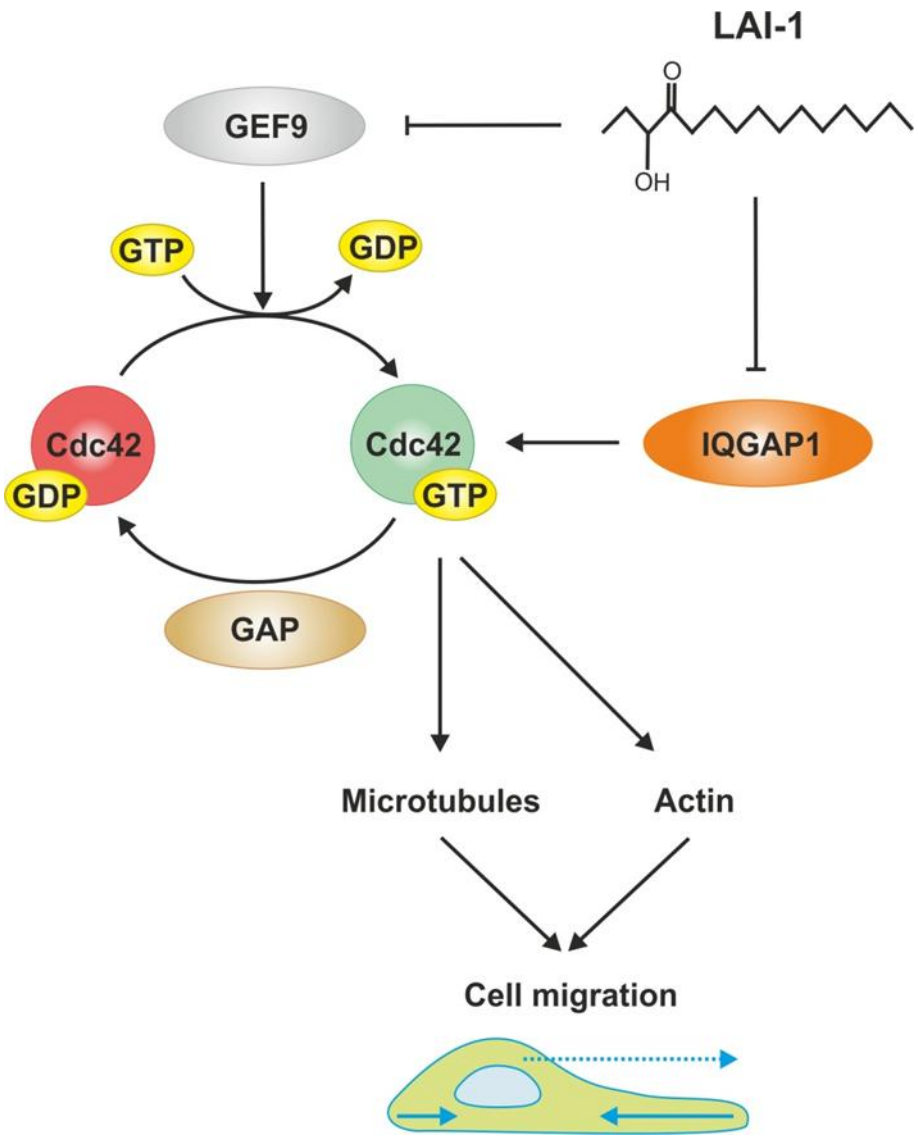

Figure 35. IQGAP1- and Cdc42-dependent modulation of cell migration by LAI-1.
LAI-1 (directly or indirectly) inhibits the activation of the Cdc42-specific GEF9, which in turn obstructs the interaction between IQGAP1 and Cdc42. LAI-1 causes a cellular relocalization of IQGAP1 and might affect its stability. The addition of LAI-1 interferes with host cell migration by destabilizing the microtubule and actin cytoskeleton [206].
Abbreviations: Cdc42: cell division control protein 42; GAP: GTPase-activating protein; GEF: guanine nucleotide exchange factor; IQGAP1: Ras GTPase-activating-like protein.

1. LAI-1-dependent gene regulation in *D. discoideum*

Analysis of cDNA microarrays revealed transcriptional changes of *D. discoideum* genes in response to the *L. pneumophila* signaling molecule LAI-1. The transcriptome study showed that LAI-1 up- or down-regulates 115 and 144 genes, respectively, to an extent of at least 1.5 fold. This number of genes represents approximately 5% of the 5400 genes on the array. 74 up- and 113 down-regulated genes could be functionally categorized based on the yeast classification scheme which was adapted for *Dictyostelium* [167]. Genes involved in vesicle trafficking and signal transduction were mostly up-regulated. By contrast, genes implicated in translation, cell proliferation and movement were down-regulated. These results are in agreement with the notion that LAI-1 directly or indirectly inhibits cell movement.

On a single gene level, the observation was made that several genes of the ubiquitin proteasome system, the „core" autophagy genes *atg8* and *atg16* as well as the autophagy adaptor sequestosome-1, were up-regulated. In addition, gene expression of three members of the ABC transporter G family, a gene named *iliA* (induced after *Legionella* infection) and the gene DDB_G0274423 which encodes a Src homology 3 (SH3) domain-containing protein, was increased. The latter gene is homologous to CD2AP, a scaffold protein modulating actin dynamics and cell migration [168]. However, no difference in migration was observed in A549 cells depleted for CD2AP and treated with LAI-1. Therefore, the LAI-1-dependent inhibition of random cell migration apparently does not require the SH3-domain protein CD2AP. Moreover, down-regulated genes included the aldehyde reductase *arlA* and *arlE* as well as *rliA* (repressed after *Legionella* infection) encoding a putative 12 transmembrane protein of the major facilitator family. Thus, the transcriptome analysis revealed that synthetic LAI-1 in the micromolar concentration range indeed regulates the expression of a number of eukaryotic genes involved in processes like protein homeostasis, vesicle trafficking and cell migration [206].

2. Potential LAI-1 receptors and transporters

This section describes potential interaction partners for LAI-1 including G protein-coupled receptors, outer membrane vesicles, nuclear receptors or GTPases. The possible signaling pathways are summarized in Figure 36.

a. G protein-coupled receptors

G protein-coupled receptors (GPCRs) are seven transmembrane proteins and form the largest group of membrane receptors. The binding of an agonist, orthosterically or allosterically, causes a conformational change and an exchange of GDP to GTP [169]. This leads to the dissociation of the G protein into Gα and Gβγ. Thus, GPCRs function as ligand-regulated GEFs for heterodimeric G proteins and are implicated in canonical (G protein mediated) or non-canonical (β-arrestin-dependent) signaling pathways [170, 171].

The GPCR signaling network is implicated in cell chemotaxis by sensing external stimuli and generation of mechanical forces. Small peptides called chemokines are recognized and trigger directed cell migration. The implication of the GPCR machinery is well described in both humans and *D. discoideum* cells, since the cAMP pathway is essential and ubiquitous in cell communication [172]. Upon extracellular stimulation, cAMP is produced from ATP by adenylate cyclases. The cascade is a GPCR-triggered signaling pathway implicated in various cell processes. Following the dissociation of the G proteins, the Ras GTPase is activated which in turn stimulates the enzyme PI3K. Those kinases then catalyze the phosphorylation of PIP2 into PIP3. Their pleckstrin homology (PH) domains interact with multiple downstream proteins such as GEFs/GAPs, signaling adaptors, tyrosine kinases and serine/threonine kinases. This can lead to the regulation of numerous pathways including migration and chemotaxis, where neutrophils are the first immune cells recruited during infection, known to track and eliminate bacteria [173]. GPCRs include neutrophil and CXC chemokine receptors [174]. CXCR1, CXCR2, CCR1 or CCR2 represent receptors possibly implicated in LAI-1 signaling which can be easily investigated using RNA interference.

So far, only the involvement of CXCR4, important in cell migration in cancer [175], was tested. A random migration assay using A549 epithelial cells showed no differences in the effect of LAI-1 after CXCR4 depletion [206].

Interestingly, oxylipins, involved in QS of *Aspergillus spp*, induce the cAMP pathway through binding to GPCRs called GprC and GprD [176]. Furthermore, a putative GCPR could be confirmed by analyzing the downstream cascade including Ras and PIP3 activation levels. A *D. discoideum* strain producing PH_{Crac}-GFP represents a promising tool, since amoebae and human leukocytes exhibit similar chemotactic behaviors.

A further aspect of GPCRs is their ability to be internalized and redistributed into endosomes [177, 178]. Those membrane-bound compartments represent dynamic sites for GPCR-G protein activation. Additionally, three main GPCR sorting machineries are induced in endosomes. First, the ubiquitin endosome sorting complex required for transport (ESCRT), found in yeast and mammals, which is responsible for re-transport and remodeling of the plasma membrane [179, 180]. Second, the GPCR-associated sorting proteins (GASP) machinery, which reduces the motility of the receptors and targets them to the lysosomal pathway for degradation [181, 182]. Third, the actin sorting nexin 27 retromer tubule (ASRT) system, which recognizes GPCRs via their C-terminal post synaptic density protein (PDZ/PSD) domain and contributes to the selective transport of the endosomes to the plasma membrane (recycling) or the GA (retrograde transport).

Since LAI-1 is a small hydrophobic molecule, one hypothesis is that the autoinducer molecule directly diffuses through the plasma membrane and binds one of the GPCRs in the endosome. Subsequently, LAI-1 may be relocalized in the cell and interacts with the ER or the GA and probably interferes with *L. pneumophila* infection (section B.6.). Studies showed that the autoinducer molecule $3OC_{12}$-HSL of *P. aeruginosa* has an impact on bacterial cell-cell signaling and host cell responses. The QS compound possesses immune-modulatory properties and mobilizes intracellular calcium from the ER which is associated with induction of apoptosis [132]. These findings suggest the existence of more than one receptor for $3OC_{12}$-HSL, a concept which cannot be ruled out for LAI-1. The QS molecule of *P. aeruginosa* influences the migration pattern of primary neutrophils by affecting calcium signaling and actin remodeling [102].

QS molecules like LAI-1 might also interact with calcium-sensing receptors and cause an activation of the phospholipase C (PLC) pathway, which influences the cAMP cascade and cleaves numerous phospholipids [183].

b. Outer membrane vesicles

L. pneumophila is able to release outer membrane vesicles (OMVs) to export proteins, lipids and small molecules. OMVs are spherical bilayer structures with a diameter of 100-200 nm and contain phospholipids, LPS and outer membrane proteins. OMVs are produced extra- and intracellularly during multiple growth phases [184] and are implicated in various processes such as biofilm formation and nutrient acquisition [185]. This mode of contact-free cell communication allows the shedding of many virulence-related proteins within the host cell like, e.g., the zinc metalloprotease ProA and the membrane-associated peptidyl isomerase Mip. Recently, the intrinsic capacity of *L. pneumophila* OMVs to fuse with eukaryotic membrane systems was demonstrated [185]. OMVs inhibit the fusion of phagosomes with lysosomes [42] and exhibit proteolytic and lipolytic activities [186]. OMVs elicit a specific cytokine response in alveolar epithelial cells [184]; IL-1, IL-6, IL-12, IL-17, CXCL1 and TNFα are secreted [187]. Furthermore, a TLR-2-dependent answer via LPS has been described for *L. pneumophila*, whereas more frequently a TLR-4 induced cascade is observed [185]. The release of proteins and molecules by OMVs has also been described for other bacteria. The QS molecule PQS of *P. aeruginosa* is delivered via OMVs, which allows the coordinatination of group behavior [188]. Moreover, the delivery of bacterial components was observed in *Escherichia coli* and *Salmonella enterica* inducing the activation of dendritic cells and influencing B- and T-cell responses [189, 190].

Thus, one hypothesis is that the LAI-1 autoinducer molecule of *L. pneumophila* is delivered and released into host cells by OMVs. Isolation of vesicles and testing in different migration assays should address this question and lead to new insights.

c. Nuclear receptors

The possible binding of LAI-1 to cell surface receptors does not exclude a putative receptor in the cytoplasm or nucleus. The arachidonate metabolite leukotriene B4 (LTB4), which can act as a chemoattractant for leukocytes is able to bind the membrane receptor BLT1/BLT2 or the nuclear peroxisome proliferator-activated receptor (PPAR) [191, 192]. Three isoforms have been identified in mammals, PPARα, PPARβ/δ and PPARγ, exhibiting different expression levels in specific tissues [193]. These ligand-activated transcription factors regulate a broad range of genes involved in metabolism, development and homeostasis. PPARs can interfere with NFκB-driven transcription regulation of inflammatory genes [194]. Furthermore, the specific implication of PPARγ has been described in fibrogenesis, inflammation and wound healing, *in vitro* and *in vivo*. Recent data showed an up-regulation of macrophage-specific PPARγ in a model of pulmonary fibrosis causing an anti-inflammatory effect [195]. Additionally, studies demonstrated that PPARγ functions as a negative regulator of pro-inflammatory cytokines during *Vibrio alginolyticus* infection [196].
The QS molecule $3OC_{12}$-HSL of *P. aeruginosa* acts as an agonist of PPARβ/δ and antagonist of PPARγ transcriptional activities [197]. Interestingly, GPCRs are found on the nuclear membrane and activate similar pathways as the cell surface receptors in various cell types [198]. The autoinducer molecule of *L. pneumophila* might diffuse through the plasma membrane or is delivered in the cytoplasm and targeted to nuclear PPARs for binding and induction of an inflammatory cascade. Further analysis of the signaling and activity cascade of PPARs should lead to a better understanding of the LAI-1 signaling pathway.

d. Interaction with GTPases

LAI-1 might also directly interact with IQGAP1, GEF9 or with other upstream proteins. Due to its small size and hydrophobicity, the molecule can diffuse through the membrane and interact with host factors influencing cell migration. The Vikstrom group suggested that $3OC_{12}$-HSL produced by *P. aeruginosa* could colocalize and interact with IQGAP1 triggering cytoskeleton components.

Yet, in this study, the autoinducer was effective only at very high concentrations (200 µM) and further eukaryotic factors comprising the signaling pathway have not been identified [102].

Data presented in section B. revealed that the *L. pneumophila* autoinducer LAI-1 inhibits chemotactic and random migration of eukaryotic cells in the low micromolar range through a signaling pathway including the host factor IQGAP1, Cdc42 and GEF9. In order to determine a potential interaction partner, LAI-1-biotin probes might be captured with a streptavidin agarose resin in pulldown experiments and analyzed by SDS-PAGE. The protein bands of interest could be analyzed by mass spectrometry. This might shed light onto the dramatic impairment of microtubule polymerization and actin stability triggered by LAI-1.

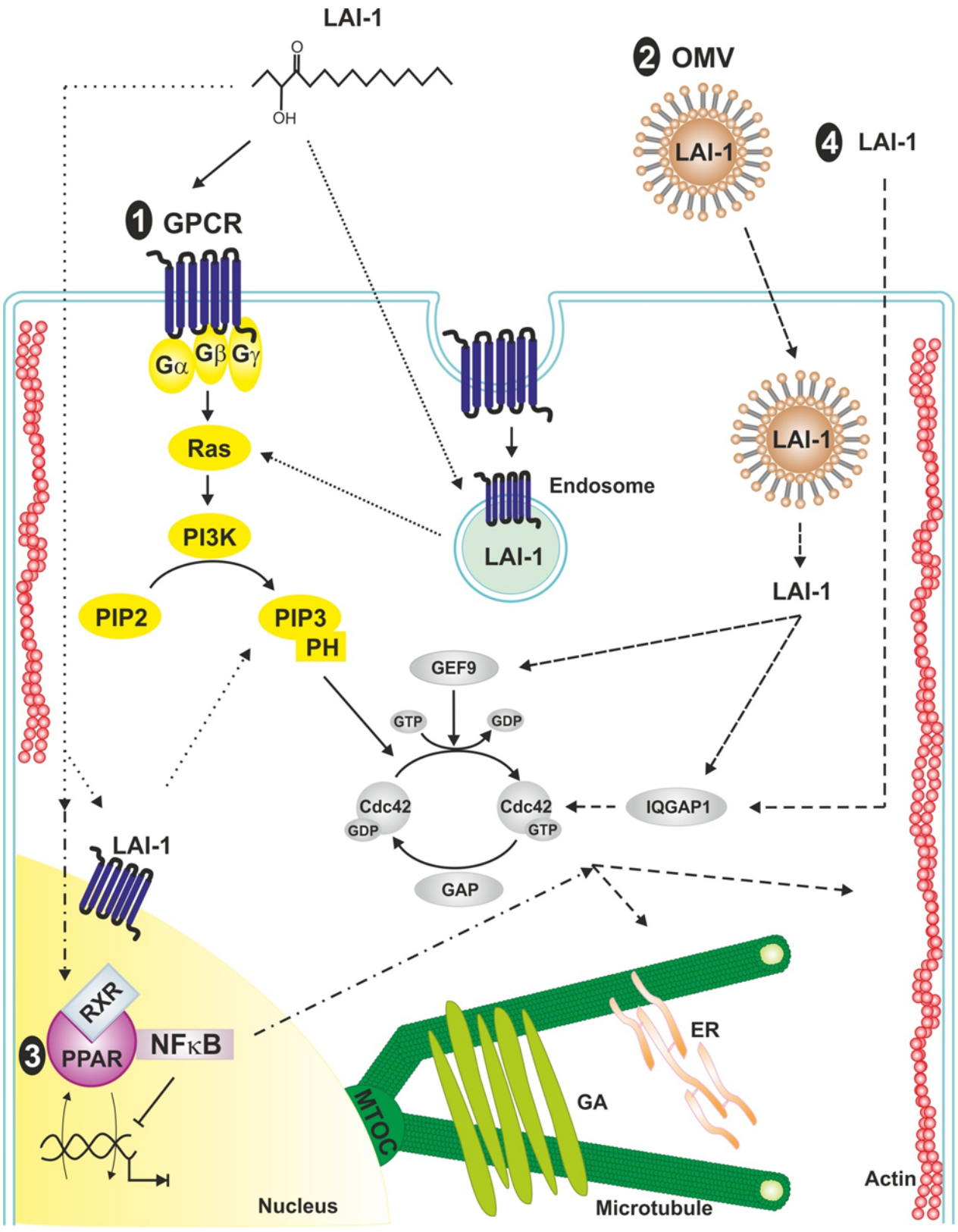
LAI-1
OH
2 OMV
LAI-1
4 LAI-1
1 GPCR
Gα Gβ Gγ
Ras
PI3K
PIP2
PIP3
PH
Endosome
LAI-1
LAI-1
LAI-1
GEF9
GTP
GDP
Cdc42
GDP
Cdc42
GTP
IQGAP1
GAP
LAI-1
RXR
3 PPAR
NFκB
Nucleus
MTOC
GA
ER
Microtubule
Actin

Figure 36. Potential LAI-1 receptors.

1. LAI-1 might bind to G protein-coupled proteins (GPCRs) localized on the cell surface, in endosomes or in the nucleus. Following binding of the autoinducer molecule to the receptor, the G proteins are divided and Gα activates the GTPase Ras as well as PI3K. PIP3 is produced and the PH (pleckstrin homology) domains allow binding to small GTPases, such as Cdc42. which regulate microtubules and actin filaments.
2. LAI-1 localized in OMVs from *L. pneumophila* might be delivered to the host cell and released into the cytoplasm where it could bypass multiple processes.
3. LAI-1 might diffuse through the cell membrane and bind to PPAR in the nucleus. An interaction would cause an inhibition of the transcription factor NF□B, subsequent impairment in gene expression and cytokine production essential for inflammation and migration processes.
4. LAI-1 diffuses and directly interacts with IQGAP1 or the specific Cdc42 GEF9 resulting in destabilization of the microtubule and actin network.

Abbreviations: Cdc42: cell division control protein 42; ER: endoplasmic reticulum; GA: Golgi apparatus; GAP: GTPase activating protein; GEF: guanine nucleotide exchange factor; GPCR: G protein-coupled receptor; IQGAP1: Ras GTPase-activating-like protein; LAI-1: *Legionella* autoinducer 1; MTOC: microtubule organization center; NFκB: nuclear factor kappa-light-chain-enhancer of activated B cells OMV: outer membrane vesicle; PH: pleckstrin homology; PI3K: phosphoinositide 3-kinase; PIP2: phosphatidylinositol (4,5)-bisphosphate; PIP3: phosphatidylinositol (3,4,5)-triphosphate; PPAR: peroxisome proliferator-activated receptor; RXR: retinoid X receptor.

C. Possible *in vivo* analysis of inflammatory processes in the lung after *Legionella* infection

Migration and activation of immune cells are essential during inflammatory processes and disease development. Following inhalation of contaminated aerosols, *L. pneumophila* infects and replicates in phagocytic immune cells in the lung. Alveolar macrophages are killed during the infection, whereas dentritic cells and neutrophils activate natural killer cells through the production of IL-12 and IL-18. In turn, these cells are responsible for the release of IFN-γ [199]. An *in vivo* analysis would give new insights into the chemotactic recruitment of immune cells during the lung inflammation. Furthermore, novel strategies and/or improvement of prevention and treatment could be established.

A/J mice, which support intracellular replication of *L. pneumophila*, would serve as an infection model allowing to study the interactions between the bacteria and host cells as well as host defense mechanisms [200, 201]. A recently described mouse model allows the investigation of pulmonary microcirculation in the ventilated mouse lung through intravital microscopy [202]. Moreover, besides the A/J mice, three other mouse models are available: (i) LysM-eGFP mice with neutrophils producing the fluorescent protein GFP; (ii) CX3CR1gfp/+ mice expressing GFP-labelled monocytes and (iii) the MHC II-GFP model with GFP-producing dendritic cells [203].

In real-time analysis of arterioles, blood vessels and capillaries, adherent and rolling leukocytes can be detected and followed. After an intranasal infection with *L. pneumophila*, intravital microscopy of an infected lung could be established. Following depletion of alveolar macrophages, dendritic cells or neutrophils in the A/J mouse, their implication over time could be analyzed [204, 205]. Furthermore, different *L. pneumophila* mutant strains and cytokine production can be tested.

V. Literature

1. Fraser DW, Tsai TR, Orenstein W, Parkin WE, Beecham HJ, Sharrar RG*, et al.* Legionnaires' disease: description of an epidemic of pneumonia. *N Engl J Med* 1977, 297(22): 1189-1197.

2. McDade JE, Shepard CC, Fraser DW, Tsai TR, Redus MA, Dowdle WR. Legionnaires' disease: isolation of a bacterium and demonstration of its role in other respiratory disease. *N Engl J Med* 1977, 297(22): 1197-1203.

3. Joly JR, Winn WC. *Legionella pneumophila* subgroups, monoclonal antibody reactivity, and strain virulence in Burlington, Vermont. *The Journal of infectious diseases* 1988, 158(6): 1412.

4. Bangsborg JM. Antigenic and genetic characterization of *Legionella* proteins: contributions to taxonomy, diagnosis and pathogenesis. *APMIS Supplementum* 1997, 70: 1-53.

5. Yu VL, Plouffe JF, Pastoris MC, Stout JE, Schousboe M, Widmer A*, et al.* Distribution of *Legionella* species and serogroups isolated by culture in patients with sporadic community-acquired legionellosis: an international collaborative survey. *The Journal of infectious diseases* 2002, 186(1): 127-128.

6. Asare R, Abu Kwaik Y. Early trafficking and intracellular replication of *Legionella longbeachae* within an ER-derived late endosome-like phagosome. *Cellular microbiology* 2007, 9(6): 1571-1587.

7. Fields BS. The molecular ecology of *Legionellae*. *Trends in microbiology* 1996, 4(7): 286-290.

8. Hagele S, Kohler R, Merkert H, Schleicher M, Hacker J, Steinert M. *Dictyostelium discoideum*: a new host model system for intracellular pathogens of the genus *Legionella*. *Cellular microbiology* 2000, 2(2): 165-171.

9. Franco IS, Shuman HA, Charpentier X. The perplexing functions and surprising origins of *Legionella pneumophila* type IV secretion effectors. *Cellular microbiology* 2009, 11(10): 1435-1443.

10. Moliner C, Fournier PE, Raoult D. Genome analysis of microorganisms living in amoebae reveals a melting pot of evolution. *FEMS Microbiol Rev* 2010, 34: 281-294.

11. Taylor M, Ross K, Bentham R. *Legionella*, protozoa, and biofilms: interactions within complex microbial systems. *Microb Ecol* 2009, 58(3): 538-547.

12. Richards AM, Von Dwingelo JE, Price CT, Abu Kwaik Y. Cellular microbiology and molecular ecology of *Legionella*-amoeba interaction. *Virulence* 2013, 4(4): 307-314.

13. Hilbi H, Hoffmann C, Harrison CF. *Legionella* spp. outdoors: colonization, communication and persistence. *Environ Microbiol Rep* 2011, 3(3): 286–296.

14. Burns DL. Type IV transporters of pathogenic bacteria. *Curr Opin Microbiol* 2003, 6(1): 29-34.

15. Christie PJ. Type IV secretion: intercellular transfer of macromolecules by systems ancestrally related to conjugation machines. *Molecular microbiology* 2001, 40(2): 294-305.

16. Vogel JP, Andrews HL, Wong SK, Isberg RR. Conjugative transfer by the virulence system of *Legionella pneumophila*. *Science* 1998, 279(5352): 873-876.

17. Vincent CD, Friedman JR, Jeong KC, Buford EC, Miller JL, Vogel JP. Identification of the core transmembrane complex of the *Legionella* Dot/Icm type IV secretion system. *Molecular microbiology* 2006, 62(5): 1278-1291.

18. Rothmeier E, Pfaffinger G, Hoffmann C, Harrison CF, Grabmayr H, Repnik U*, et al.* Activation of Ran GTPase by a *Legionella* effector promotes microtubule polymerization, pathogen vacuole motility and infection. *PLoS pathogens* 2013, In revision.

19. Finsel I, Ragaz C, Hoffmann C, Harrison CF, Weber S, van Rahden VA*, et al.* The *Legionella* effector RidL inhibits retrograde trafficking to promote intracellular replication. *Cell host & microbe* 2013, 14(1): 38-50.

20. Rolando M, Buchrieser C. Post-translational modifications of host proteins by *Legionella pneumophila*: a sophisticated survival strategy. *Future microbiology* 2012, 7(3): 369-381.

21. Ninio S, Roy CR. Effector proteins translocated by *Legionella pneumophila*: strength in numbers. *Trends in microbiology* 2007, 15(8): 372-380.

22. Hilbi H, Haas A. Secretive bacterial pathogens and the secretory pathway. *Traffic* 2012, 13(9): 1187-1197.

23. Vincent CD, Friedman JR, Jeong KC, Sutherland MC, Vogel JP. Identification of the DotL coupling protein subcomplex of the *Legionella* Dot/Icm type IV secretion system. *Molecular microbiology* 2012, 85(2): 378-391.

24. Ninio S, Zuckman-Cholon DM, Cambronne ED, Roy CR. The *Legionella* IcmS-IcmW protein complex is important for Dot/Icm-mediated protein translocation. *Molecular microbiology* 2005, 55(3): 912-926.

25. Isberg RR, O'Connor TJ, Heidtman M. The *Legionella pneumophila* replication vacuole: making a cosy niche inside host cells. *Nature reviews Microbiology* 2009, 7(1): 13-24.

26. van Schaik EJ, Chen C, Mertens K, Weber MM, Samuel JE. Molecular pathogenesis of the obligate intracellular bacterium *Coxiella burnetii*. *Nature reviews Microbiology* 2013, 11(8): 561-573.

27. De Buck E, Anne J, Lammertyn E. The role of protein secretion systems in the virulence of the intracellular pathogen *Legionella pneumophila*. *Microbiology* 2007, 153(Pt 12): 3948-3953.

28. Gerlach RG, Hensel M. Protein secretion systems and adhesins: the molecular armory of Gram-negative pathogens. *International journal of medical microbiology : IJMM* 2007, 297(6): 401-415.

29. Segal G, Shuman HA. *Legionella pneumophila* utilizes the same genes to multiply within *Acanthamoeba castellanii* and human macrophages. *Infection and immunity* 1999, 67(5): 2117-2124.

30. Albert-Weissenberger C, Cazalet C, Buchrieser C. *Legionella pneumophila* - a human pathogen that co-evolved with fresh water protozoa. *Cellular and molecular life sciences : CMLS* 2007, 64(4): 432-448.

31. Hilbi H, Segal G, Shuman HA. Icm/Dot-dependent upregulation of phagocytosis by *Legionella pneumophila*. *Molecular microbiology* 2001, 42(3): 603-617.

32. Khelef N, Shuman HA, Maxfield FR. Phagocytosis of wild-type *Legionella pneumophila* occurs through a wortmannin-insensitive pathway. *Infection and immunity* 2001, 69(8): 5157-5161.

33. Bardill JP, Miller JL, Vogel JP. IcmS-dependent translocation of SdeA into macrophages by the *Legionella pneumophila* type IV secretion system. *Molecular microbiology* 2005, 56(1): 90-103.

34. Chang B, Kura F, Amemura-Maekawa J, Koizumi N, Watanabe H. Identification of a novel adhesion molecule involved in the virulence of *Legionella pneumophila*. *Infection and immunity* 2005, 73(7): 4272-4280.

35. Liu M, Conover GM, Isberg RR. *Legionella pneumophila* EnhC is required for efficient replication in tumour necrosis factor alpha-stimulated macrophages. *Cellular microbiology* 2008, 10(9): 1906-1923.

36. Newton HJ, Sansom FM, Bennett-Wood V, Hartland EL. Identification of *Legionella pneumophila*-specific genes by genomic subtractive hybridization with *Legionella micdadei* and identification of lpnE, a gene required for efficient host cell entry. *Infection and immunity* 2006, 74(3): 1683-1691.

37. Roy CR, Berger KH, Isberg RR. *Legionella pneumophila* DotA protein is required for early phagosome trafficking decisions that occur within minutes of bacterial uptake. *Molecular microbiology* 1998, 28(3): 663-674.

38. Xu L, Shen X, Bryan A, Banga S, Swanson MS, Luo ZQ. Inhibition of host vacuolar H+-ATPase activity by a *Legionella pneumophila* effector. *PLoS pathogens* 2010, 6(3): e1000822.

39. Bennett TL, Kraft SM, Reaves BJ, Mima J, O'Brien KM, Starai VJ. LegC3, an effector protein from *Legionella pneumophila*, inhibits homotypic yeast vacuole fusion in vivo and in vitro. *PloS one* 2013, 8(2): e56798.

40. de Felipe KS, Glover RT, Charpentier X, Anderson OR, Reyes M, Pericone CD*, et al.* *Legionella* eukaryotic-like type IV substrates interfere with organelle trafficking. *PLoS pathogens* 2008, 4(8): e1000117.

41. Shohdy N, Efe JA, Emr SD, Shuman HA. Pathogen effector protein screening in yeast identifies *Legionella* factors that interfere with membrane trafficking. *Proceedings of the National Academy of Sciences of the United States of America* 2005, 102(13): 4866-4871.

42. Fernandez-Moreira E, Helbig JH, Swanson MS. Membrane vesicles shed by *Legionella pneumophila* inhibit fusion of phagosomes with lysosomes. *Infection and immunity* 2006, 74(6): 3285-3295.

43. Horwitz MA. Formation of a novel phagosome by the Legionnaires' disease bacterium (*Legionella pneumophila*) in human monocytes. *The Journal of experimental medicine* 1983, 158(4): 1319-1331.

44. Kagan JC, Roy CR. *Legionella* phagosomes intercept vesicular traffic from endoplasmic reticulum exit sites. *Nature cell biology* 2002, 4(12): 945-954.

45. Hilbi H, Weber S, Finsel I. Anchors for effectors: subversion of phosphoinositide lipids by *Legionella*. *Frontiers in microbiology* 2011, 2: 91.

46. Machner MP, Isberg RR. Targeting of host Rab GTPase function by the intravacuolar pathogen *Legionella pneumophila*. *Developmental cell* 2006, 11(1): 47-56.

47. Urwyler S, Nyfeler Y, Ragaz C, Lee H, Mueller LN, Aebersold R*, et al.* Proteome analysis of *Legionella* vacuoles purified by magnetic immunoseparation reveals secretory and endosomal GTPases. *Traffic* 2009, 10(1): 76-87.

48. Weber SS, Ragaz C, Reus K, Nyfeler Y, Hilbi H. *Legionella pneumophila* exploits PI(4)P to anchor secreted effector proteins to the replicative vacuole. *PLoS pathogens* 2006, 2(5): e46.

49. Luo ZQ, Isberg RR. Multiple substrates of the *Legionella pneumophila* Dot/Icm system identified by interbacterial protein transfer. *Proceedings of the National Academy of Sciences of the United States of America* 2004, 101(3): 841-846.

50. Ragaz C, Pietsch H, Urwyler S, Tiaden A, Weber SS, Hilbi H. The *Legionella pneumophila* phosphatidylinositol-4 phosphate-binding type IV substrate SidC recruits endoplasmic reticulum vesicles to a replication-permissive vacuole. *Cellular microbiology* 2008, 10(12): 2416-2433.

51. Neunuebel MR, Mohammadi S, Jarnik M, Machner MP. *Legionella pneumophila* LidA affects nucleotide binding and activity of the host GTPase Rab1. *Journal of bacteriology* 2012, 194(6): 1389-1400.

52. Brombacher E, Urwyler S, Ragaz C, Weber SS, Kami K, Overduin M*, et al.* Rab1 guanine nucleotide exchange factor SidM is a major phosphatidylinositol 4-phosphate-binding effector protein of *Legionella pneumophila*. *The Journal of biological chemistry* 2009, 284(8): 4846-4856.

53. Weber SS, Ragaz C, Hilbi H. The inositol polyphosphate 5-phosphatase OCRL1 restricts intracellular growth of *Legionella*, localizes to the replicative vacuole and binds to the bacterial effector LpnE. *Cellular microbiology* 2009, 11(3): 442-460.

54. Newton HJ, Sansom FM, Dao J, McAlister AD, Sloan J, Cianciotto NP*, et al.* Sel1 repeat protein LpnE is a *Legionella pneumophila* virulence determinant that influences vacuolar trafficking. *Infection and immunity* 2007, 75(12): 5575-5585.

55. Neunuebel MR, Chen Y, Gaspar AH, Backlund PS, Jr., Yergey A, Machner MP. De-AMPylation of the small GTPase Rab1 by the pathogen *Legionella pneumophila*. *Science* 2011, 333(6041): 453-456.

56. Donaldson JG. Arfs, phosphoinositides and membrane traffic. *Biochem Soc Trans* 2005, 33(Pt 6): 1276-1278.

57. Nagai H, Cambronne ED, Kagan JC, Amor JC, Kahn RA, Roy CR. A C-terminal translocation signal required for Dot/Icm-dependent delivery of the *Legionella* RalF protein to host cells. *Proceedings of the National Academy of Sciences of the United States of America* 2005, 102(3): 826-831.

58. Lomma M, Dervins-Ravault D, Rolando M, Nora T, Newton HJ, Sansom FM*, et al.* The *Legionella pneumophila* F-box protein Lpp2082 (AnkB) modulates ubiquitination of the host protein parvin B and promotes intracellular replication. *Cellular microbiology* 2010, 12(9): 1272-1291.

59. Choy A, Dancourt J, Mugo B, O'Connor TJ, Isberg RR, Melia TJ*, et al.* The *Legionella* effector RavZ inhibits host autophagy through irreversible Atg8 deconjugation. *Science* 2012, 338(6110): 1072-1076.

60. Chen J, de Felipe KS, Clarke M, Lu H, Anderson OR, Segal G*, et al. Legionella* effectors that promote nonlytic release from protozoa. *Science* 2004, 303(5662): 1358-1361.

61. Molmeret M, Bitar DM, Han L, Kwaik YA. Disruption of the phagosomal membrane and egress of *Legionella pneumophila* into the cytoplasm during the last stages of intracellular infection of macrophages and *Acanthamoeba polyphaga*. *Infection and immunity* 2004, 72(7): 4040-4051.

62. Etienne-Manneville S. Microtubules in cell migration. *Annual review of cell and developmental biology* 2013, 29: 471-499.

63. Gardner MK, Zanic M, Howard J. Microtubule catastrophe and rescue. *Current opinion in cell biology* 2013, 25(1): 14-22.

64. Kaverina I, Straube A. Regulation of cell migration by dynamic microtubules. *Seminars in cell & developmental biology* 2011, 22(9): 968-974.

65. Tropini C, Roth EA, Zanic M, Gardner MK, Howard J. Islands containing slowly hydrolyzable GTP analogs promote microtubule rescues. *PloS one* 2012, 7(1): e30103.

66. Tamura N, Draviam VM. Microtubule plus-ends within a mitotic cell are 'moving platforms' with anchoring, signalling and force-coupling roles. *Open biology* 2012, 2(11): 120132.

67. Tanaka K. Dynamic regulation of kinetochore-microtubule interaction during mitosis. *Journal of biochemistry* 2012, 152(5): 415-424.

68. Parsons JT, Horwitz AR, Schwartz MA. Cell adhesion: integrating cytoskeletal dynamics and cellular tension. *Nature reviews Molecular cell biology* 2010, 11(9): 633-643.

69. Stehbens S, Wittmann T. Targeting and transport: how microtubules control focal adhesion dynamics. *The Journal of cell biology* 2012, 198(4): 481-489.

70. Kay RR, Langridge P, Traynor D, Hoeller O. Changing directions in the study of chemotaxis. *Nature reviews Molecular cell biology* 2008, 9(6): 455-463.

71. Vorotnikov AV. Chemotaxis: movement, direction, control. *Biochemistry Biokhimiia* 2011, 76(13): 1528-1555.

72. Wittmann T, Waterman-Storer CM. Cell motility: can Rho GTPases and microtubules point the way? *Journal of cell science* 2001, 114(Pt 21): 3795-3803.

73. Woodham EF, Machesky LM. Polarised cell migration: intrinsic and extrinsic drivers. *Current opinion in cell biology* 2014, 30: 25-32.

74. Petrie RJ, Doyle AD, Yamada KM. Random versus directionally persistent cell migration. *Nature reviews Molecular cell biology* 2009, 10(8): 538-549.

75. Fukata M, Watanabe T, Noritake J, Nakagawa M, Yamaga M, Kuroda S*, et al.* Rac1 and Cdc42 capture microtubules through IQGAP1 and CLIP-170. *Cell* 2002, 109(7): 873-885.

76. Bonner JT. Evidence for the formation of cell aggregates by chemotaxis in the development of the slime mold *Dictyostelium discoideum*. *The Journal of experimental zoology* 1947, 106(1): 1-26.

77. Loomis WF. Cell signaling during development of *Dictyostelium*. *Developmental biology* 2014, 391(1): 1-16.

78. Wang Y, Chen CL, Iijima M. Signaling mechanisms for chemotaxis. *Development, growth & differentiation* 2011, 53(4): 495-502.

79. Zhang P, Wang Y, Sesaki H, Iijima M. Proteomic identification of phosphatidylinositol (3,4,5) triphosphate-binding proteins in *Dictyostelium discoideum*. *Proceedings of the National Academy of Sciences of the United States of America* 2010, 107(26): 11829-11834.

80. Sasaki AT, Firtel RA. Regulation of chemotaxis by the orchestrated activation of Ras, PI3K, and TOR. *European journal of cell biology* 2006, 85(9-10): 873-895.

81. Parent CA, Blacklock BJ, Froehlich WM, Murphy DB, Devreotes PN. G Protein Signaling Events Are Activated at the Leading Edge of Chemotactic Cells. *Cell* 1998, 95(1): 81-91.

82. Shi C, Iglesias PA. Excitable behavior in amoeboid chemotaxis. *Wiley interdisciplinary reviews Systems biology and medicine* 2013, 5(5): 631-642.

83. Guttler T, Gorlich D. Ran-dependent nuclear export mediators: a structural perspective. *The EMBO journal* 2011, 30(17): 3457-3474.

84. Bischoff FR, Ponstingl H. Mitotic regulator protein RCC1 is complexed with a nuclear ras-related polypeptide. *Proceedings of the National Academy of Sciences of the United States of America* 1991, 88(23): 10830-10834.

85. Li HY, Zheng Y. Phosphorylation of RCC1 in mitosis is essential for producing a high RanGTP concentration on chromosomes and for spindle assembly in mammalian cells. *Genes & development* 2004, 18(5): 512-527.

86. Yudin D, Fainzilber M. Ran on tracks--cytoplasmic roles for a nuclear regulator. *Journal of cell science* 2009, 122(Pt 5): 587-593.

87. Kalab P, Pralle A. Chapter 21: Quantitative fluorescence lifetime imaging in cells as a tool to design computational models of ran-regulated reaction networks. *Methods in cell biology* 2008, 89: 541-568.

88. Yokoyama H, Gruss OJ. New mitotic regulators released from chromatin. *Frontiers in oncology* 2013, 3: 308.

89. de Felipe KS, Pampou S, Jovanovic OS, Pericone CD, Ye SF, Kalachikov S*, et al.* Evidence for acquisition of *Legionella* type IV secretion substrates via interdomain horizontal gene transfer. *Journal of bacteriology* 2005, 187(22): 7716-7726.

90. Ninio S, Celli J, Roy CR. A *Legionella pneumophila* effector protein encoded in a region of genomic plasticity binds to Dot/Icm-modified vacuoles. *PLoS pathogens* 2009, 5(1): e1000278.

91. Ivanov SS, Charron G, Hang HC, Roy CR. Lipidation by the host prenyltransferase machinery facilitates membrane localization of *Legionella pneumophila* effector proteins. *The Journal of biological chemistry* 2010, 285(45): 34686-34698.

92. Hilbi H, Rothmeier E, Hoffmann C, Harrison CF. Beyond Rab GTPases *Legionella* activates the small GTPase Ran to promote microtubule polymerization, pathogen vacuole motility, and infection. *Small GTPases* 2014, 5(3): 1-6.

93. Robinson VL, Buckler DR, Stock AM. A tale of two components: a novel kinase and a regulatory switch. *Nat Struct Biol* 2000, 7(8): 626-633.

94. Verma SC, Miyashiro T. Quorum sensing in the squid-Vibrio symbiosis. *International journal of molecular sciences* 2013, 14(8): 16386-16401.

95. Tiaden A, Hilbi H. alpha-Hydroxyketone synthesis and sensing by *Legionella* and *Vibrio*. *Sensors (Basel)* 2012, 12(3): 2899-2919.

96. Jimenez JC, Federle MJ. Quorum sensing in group A *Streptococcus*. *Front Cell Infect Microbiol* 2014, 4: 127.

97. George EA, Muir TW. Molecular mechanisms of agr quorum sensing in virulent *Staphylococci*. *Chembiochem* 2007, 8(8): 847-855.

98. Gray B, Hall P, Gresham H. Targeting agr- and agr-Like quorum sensing systems for development of common therapeutics to treat multiple gram-positive bacterial infections. *Sensors (Basel)* 2013, 13(4): 5130-5166.

99. Rutherford ST, Bassler BL. Bacterial quorum sensing: its role in virulence and possibilities for its control. *Cold Spring Harbor perspectives in medicine* 2012, 2(11).

100. Holm A, Vikstrom E. Quorum sensing communication between bacteria and human cells: signals, targets, and functions. *Frontiers in plant science* 2014, 5: 309.

101. Miller MB, Bassler BL. Quorum sensing in bacteria. *Annu Rev Microbiol* 2001, 55: 165-199.

102. Karlsson T, Turkina MV, Yakymenko O, Magnusson KE, Vikstrom E. The *Pseudomonas aeruginosa* N-acylhomoserine lactone quorum sensing molecules target IQGAP1 and modulate epithelial cell migration. *PLoS Pathog* 2012, 8(10): e1002953.

103. Kahle NA, Brenner-Weiss G, Overhage J, Obst U, Hansch GM. Bacterial quorum sensing molecule induces chemotaxis of human neutrophils via induction of p38 and leukocyte specific protein 1 (LSP1). *Immunobiology* 2013, 218(2): 145-151.

104. Glucksam-Galnoy Y, Sananes R, Silberstein N, Krief P, Kravchenko VV, Meijler MM*, et al.* The bacterial quorum-sensing signal molecule N-3-oxo-dodecanoyl-L-homoserine lactone reciprocally modulates pro- and anti-inflammatory cytokines in activated macrophages. *Journal of immunology* 2013, 191(1): 337-344.

105. Kessler A, Schell U, Sahr T, Tiaden A, Harrison C, Buchrieser C*, et al.* The *Legionella pneumophila* orphan sensor kinase LqsT regulates competence and pathogen-host interactions as a component of the LAI-1 circuit. *Environ Microbiol* 2013, 15(2): 646-662.

106. Spirig T, Tiaden A, Kiefer P, Buchrieser C, Vorholt JA, Hilbi H. The *Legionella* autoinducer synthase LqsA produces an alpha-hydroxyketone signaling molecule. *The Journal of biological chemistry* 2008, 283(26): 18113-18123.

107. Tiaden A, Spirig T, Sahr T, Walti MA, Boucke K, Buchrieser C*, et al.* The autoinducer synthase LqsA and putative sensor kinase LqsS regulate phagocyte interactions, extracellular filaments and a genomic island of *Legionella pneumophila*. *Environ Microbiol* 2010, 12(5): 1243-1259.

108. Tiaden A, Spirig T, Weber SS, Bruggemann H, Bosshard R, Buchrieser C*, et al.* The *Legionella pneumophila* response regulator LqsR promotes host cell interactions as an element of the virulence regulatory network controlled by RpoS and LetA. *Cellular microbiology* 2007, 9(12): 2903-2920.

109. Schell U, Kessler A, Hilbi H. Phosphorylation signalling through the *Legionella* quorum sensing histidine kinases LqsS and LqsT converges on the response regulator LqsR. *Molecular microbiology* 2014, 92(5): 1039-1055.

110. White CD, Erdemir HH, Sacks DB. IQGAP1 and its binding proteins control diverse biological functions. *Cellular signalling* 2012, 24(4): 826-834.

111. Briggs MW, Sacks DB. IQGAP proteins are integral components of cytoskeletal regulation. *EMBO Rep* 2003, 4(6): 571-574.

112. Shannon KB. IQGAP Family Members in Yeast, *Dictyostelium*, and Mammalian Cells. *Int J Cell Biol* 2012, 2012: 894817.

113. Wu JQ, Ye Y, Wang N, Pollard TD, Pringle JR. Cooperation between the septins and the actomyosin ring and role of a cell-integrity pathway during cell division in fission yeast. *Genetics* 2010, 186(3): 897-915.

114. Lee SE, Sun SC, Choi HY, Uhm SJ, Kim NH. mTOR is required for asymmetric division through small GTPases in mouse oocytes. *Mol Reprod Dev* 2012, 79(5): 356-366.

115. Collins ES, Balchand SK, Faraci JL, Wadsworth P, Lee WL. Cell cycle-regulated cortical dynein/dynactin promotes symmetric cell division by differential pole motion in anaphase. *Mol Biol Cell* 2012, 23(17): 3380-3390.

116. Tian Y, Gawlak G, Shah AS, Higginbotham K, Tian X, Kawasaki Y*, et al.* HGF-induced Asef-IQGAP1 Complex Controls Cytoskeletal Remodeling and Endothelial Barrier. *The Journal of biological chemistry* 2014.

117. Tian Y, Tian X, Gawlak G, O'Donnell JJ, 3rd, Sacks DB, Birukova AA. IQGAP1 regulates endothelial barrier function via EB1-cortactin cross talk. *Molecular and cellular biology* 2014, 34(18): 3546-3558.

118. Filic V, Marinovic M, Faix J, Weber I. The IQGAP-related protein DGAP1 mediates signaling to the actin cytoskeleton as an effector and a sequestrator of Rac1 GTPases. *Cellular and molecular life sciences : CMLS* 2014, 71(15): 2775-2785.

119. Mondal S, Burgute B, Rieger D, Muller R, Rivero F, Faix J*, et al.* Regulation of the actin cytoskeleton by an interaction of IQGAP related protein GAPA with filamin and cortexillin I. *PloS one* 2010, 5(11): e15440.

120. Machacek M, Hodgson L, Welch C, Elliott H, Pertz O, Nalbant P*, et al.* Coordination of Rho GTPase activities during cell protrusion. *Nature* 2009, 461(7260): 99-103.

121. Goicoechea SM, Awadia S, Garcia-Mata R. I'm coming to GEF you: Regulation of RhoGEFs during cell migration. *Cell Adh Migr* 2014, 8(6): 535-549.

122. Yang FC, Atkinson SJ, Gu Y, Borneo JB, Roberts AW, Zheng Y*, et al.* Rac and Cdc42 GTPases control hematopoietic stem cell shape, adhesion, migration, and mobilization. *Proceedings of the National Academy of Sciences of the United States of America* 2001, 98(10): 5614-5618.

123. Nishikimi A, Kukimoto-Niino M, Yokoyama S, Fukui Y. Immune regulatory functions of DOCK family proteins in health and disease. *Exp Cell Res* 2013, 319(15): 2343-2349.

124. Shi L. Dock protein family in brain development and neurological disease. *Commun Integr Biol* 2013, 6(6): e26839.

125. Qin Y, Meisen WH, Hao Y, Macara IG. Tuba, a Cdc42 GEF, is required for polarized spindle orientation during epithelial cyst formation. *The Journal of cell biology* 2010, 189(4): 661-669.

126. Ngok SP, Lin WH, Anastasiadis PZ. Establishment of epithelial polarity--GEF who's minding the GAP? *Journal of cell science* 2014, 127(Pt 15): 3205-3215.

127. Oshima T, Fujino T, Ando K, Hayakawa M. Role of FGD1, a Cdc42 guanine nucleotide exchange factor, in epidermal growth factor-stimulated c-Jun NH2-terminal kinase activation and cell migration. *Biol Pharm Bull* 2011, 34(1): 54-60.

128. Omelchenko T, Hall A. Myosin-IXA regulates collective epithelial cell migration by targeting RhoGAP activity to cell-cell junctions. *Current biology : CB* 2012, 22(4): 278-288.

129. Kooistra MR, Dube N, Bos JL. Rap1: a key regulator in cell-cell junction formation. *Journal of cell science* 2007, 120(Pt 1): 17-22.

130. Machesky LM. Cytokinesis: IQGAPs find a function. *Current biology : CB* 1998, 8(6): R202-205.

131. Mayer ML, Sheridan JA, Blohmke CJ, Turvey SE, Hancock RE. The *Pseudomonas aeruginosa* autoinducer 3O-C12 homoserine lactone provokes hyperinflammatory responses from cystic fibrosis airway epithelial cells. *PloS one* 2011, 6(1): e16246.

132. Shiner EK, Terentyev D, Bryan A, Sennoune S, Martinez-Zaguilan R, Li G*, et al.* *Pseudomonas aeruginosa* autoinducer modulates host cell responses through calcium signalling. *Cellular microbiology* 2006, 8(10): 1601-1610.

133. Paes C, Nakagami G, Minematsu T, Nagase T, Huang L, Sari Y*, et al.* The *Pseudomonas aeruginosa* quorum sensing signal molecule N-(3-oxododecanoyl) homoserine lactone enhances keratinocyte migration and induces Mmp13 gene expression in vitro. *Biochemical and biophysical research communications* 2012, 427(2): 273-279.

134. Feeley JC, Gibson RJ, Gorman GW, Langford NC, Rasheed JK, Mackel DC*, et al.* Charcoal-yeast extract agar: primary isolation medium for Legionella pneumophila. *Journal of clinical microbiology* 1979, 10(4): 437-441.

135. Watts DJ, Ashworth JM. Growth of myxameobae of the cellular slime mould *Dictyostelium discoideum* in axenic culture. *Biochem J* 1970, 119(2): 171-174.

136. Solomon JM, Rupper A, Cardelli JA, Isberg RR. Intracellular growth of *Legionella pneumophila* in *Dictyostelium discoideum*, a system for genetic analysis of host-pathogen interactions. *Infection and immunity* 2000, 68(5): 2939-2947.

137. Sussman M. Some genetic and biochemical aspects of the regulatory program for slime mold development. *Curr Top Dev Biol* 1966, 1: 61-83.

138. Malchow D, Nagele B, Schwarz H, Gerisch G. Membrane-bound cyclic AMP phosphodiesterase in chemotactically responding cells of *Dictyostelium discoideum*. *European journal of biochemistry / FEBS* 1972, 28(1): 136-142.

139. Neujahr R, Albrecht R, Kohler J, Matzner M, Schwartz JM, Westphal M*, et al.* Microtubule-mediated centrosome motility and the positioning of cleavage furrows in multinucleate myosin II-null cells. *Journal of cell science* 1998, 111 (Pt 9): 1227-1240.

140. Cazalet C, Gomez-Valero L, Rusniok C, Lomma M, Dervins-Ravault D, Newton HJ*, et al.* Analysis of the *Legionella longbeachae* genome and transcriptome uncovers unique strategies to cause Legionnaires' disease. *PLoS Genet* 2010, 6(2): e1000851.

141. Segal G, Shuman HA. Intracellular multiplication and human macrophage killing by *Legionella pneumophila* are inhibited by conjugal components of IncQ plasmid RSF1010. *Molecular microbiology* 1998, 30(1): 197-208.

142. Sadosky AB, Wiater LA, Shuman HA. Identification of *Legionella pneumophila* genes required for growth within and killing of human macrophages. *Infection and immunity* 1993, 61(12): 5361-5373.

143. Purcell M, Shuman HA. The *Legionella pneumophila icmGCDJBF* genes are required for killing of human macrophages. *Infection and immunity* 1998, 66(5): 2245-2255.

144. Simon S, Wagner MA, Rothmeier E, Muller-Taubenberger A, Hilbi H. Icm/Dot-dependent inhibition of phagocyte migration by *Legionella* is antagonized by a translocated Ran GTPase activator. *Cellular microbiology* 2014, 16(7): 977-992.

145. Mampel J, Spirig T, Weber SS, Haagensen JA, Molin S, Hilbi H. Planktonic replication is essential for biofilm formation by *Legionella pneumophila* in a complex medium under static and dynamic flow conditions. *Applied and environmental microbiology* 2006, 72(4): 2885-2895.

146. Arnould T, Michiels C, Remacle J. Hypoxic human umbilical vein endothelial cells induce activation of adherent polymorphonuclear leukocytes. *Blood* 1994, 83(12): 3705-3716.

147. Laevsky G, Knecht DA. Under-agarose folate chemotaxis of *Dictyostelium discoideum* amoebae in permissive and mechanically inhibited conditions. *Biotechniques* 2001, 31(5): 1140-1142, 1144, 1146-1149.

148. Heit B, Kubes P. Measuring chemotaxis and chemokinesis: the under-agarose cell migration assay. *Science's STKE : signal transduction knowledge environment* 2003, 2003(170): PL5.

149. Hoffmann C, Finsel I, Otto A, Pfaffinger G, Rothmeier E, Hecker M*, et al.* Functional analysis of novel Rab GTPases identified in the proteome of purified *Legionella*-containing vacuoles from macrophages. *Cellular microbiology* 2014, 16(7): 1034-1052.

150. Tiaden AN, Kessler A, Hilbi H. Analysis of *Legionella* infection by flow cytometry. *Methods in molecular biology* 2013, 954: 233-249.

151. Welkos S, Friedlander A, McDowell D, Weeks J, Tobery S. V antigen of *Yersinia pestis* inhibits neutrophil chemotaxis. *Microb Pathog* 1998, 24(3): 185-196.

152. Velan B, Bar-Haim E, Zauberman A, Mamroud E, Shafferman A, Cohen S. Discordance in the effects of *Yersinia pestis* on the dendritic cell functions manifested by induction of maturation and paralysis of migration. *Infection and immunity* 2006, 74(11): 6365-6376.

153. McLaughlin LM, Govoni GR, Gerke C, Gopinath S, Peng K, Laidlaw G*, et al.* The *Salmonella* SPI2 effector SseI mediates long-term systemic infection by modulating host cell migration. *PLoS pathogens* 2009, 5(11): e1000671.

154. Konradt C, Frigimelica E, Nothelfer K, Puhar A, Salgado-Pabon W, di Bartolo V*, et al.* The *Shigella flexneri* type three secretion system effector IpgD inhibits T cell migration by manipulating host phosphoinositide metabolism. *Cell host & microbe* 2011, 9(4): 263-272.

155. Itzen A, Goody RS. Covalent coercion by *Legionella pneumophila*. *Cell host & microbe* 2011, 10(2): 89-91.

156. Davidson HW, Balch WE. Differential inhibition of multiple vesicular transport steps between the endoplasmic reticulum and trans Golgi network. *The Journal of biological chemistry* 1993, 268(6): 4216-4226.

157. Zhuang X, Adipietro KA, Datta S, Northup JK, Ray K. Rab1 small GTP-binding protein regulates cell surface trafficking of the human calcium-sensing receptor. *Endocrinology* 2010, 151(11): 5114-5123.

158. Hardiman CA, Roy CR. AMPylation is critical for Rab1 localization to vacuoles containing *Legionella pneumophila*. *MBio* 2014, 5(1): e01035-01013.

159. Ingmundson A, Delprato A, Lambright DG, Roy CR. *Legionella pneumophila* proteins that regulate Rab1 membrane cycling. *Nature* 2007, 450(7168): 365-369.

160. Muller MP, Peters H, Blumer J, Blankenfeldt W, Goody RS, Itzen A. The *Legionella* effector protein DrrA AMPylates the membrane traffic regulator Rab1b. *Science* 2010, 329(5994): 946-949.

161. Goody PR, Heller K, Oesterlin LK, Muller MP, Itzen A, Goody RS. Reversible phosphocholination of Rab proteins by *Legionella pneumophila* effector proteins. *The EMBO journal* 2012, 31(7): 1774-1784.

162. Tan Y, Luo ZQ. *Legionella pneumophila* SidD is a deAMPylase that modifies Rab1. *Nature* 2011, 475(7357): 506-509.

163. Mukherjee S, Liu X, Arasaki K, McDonough J, Galan JE, Roy CR. Modulation of Rab GTPase function by a protein phosphocholine transferase. *Nature* 2011, 477(7362): 103-106.

164. Sit ST, Manser E. Rho GTPases and their role in organizing the actin cytoskeleton. *Journal of cell science* 2011, 124(Pt 5): 679-683.

165. Schulze H, Dose M, Korpal M, Meyer I, Italiano JE, Jr., Shivdasani RA. RanBP10 is a cytoplasmic guanine nucleotide exchange factor that modulates noncentrosomal microtubules. *The Journal of biological chemistry* 2008, 283(20): 14109-14119.

166. Kubori T, Shinzawa N, Kanuka H, Nagai H. *Legionella* metaeffector exploits host proteasome to temporally regulate cognate effector. *PLoS pathogens* 2010, 6(12): e1001216.

167. Urushihara H, Morio T, Saito T, Kohara Y, Koriki E, Ochiai H*, et al.* Analyses of cDNAs from growth and slug stages of *Dictyostelium discoideum*. *Nucleic acids research* 2004, 32(5): 1647-1653.

168. Srivatsan S, Swiecki M, Otero K, Cella M, Shaw AS. CD2-associated protein regulates plasmacytoid dendritic cell migration, but is dispensable for their development and cytokine production. *Journal of immunology* 2013, 191(12): 5933-5940.

169. Bhattacharya S, Hall SE, Li H, Vaidehi N. Ligand-stabilized conformational states of human beta(2) adrenergic receptor: insight into G-protein-coupled receptor activation. *Biophysical journal* 2008, 94(6): 2027-2042.

170. Brogi S, Tafi A, Desaubry L, Nebigil CG. Discovery of GPCR ligands for probing signal transduction pathways. *Frontiers in pharmacology* 2014, 5: 255.

171. Shenoy SK, Lefkowitz RJ. Receptor regulation: beta-arrestin moves up a notch. *Nature cell biology* 2005, 7(12): 1159-1161.

172. Xu X, Jin T. Imaging G-protein coupled receptor (GPCR)-mediated signaling events that control chemotaxis of *Dictyostelium discoideum*. *Journal of visualized experiments : JoVE* 2011(55).

173. Hawkins PT, Stephens LR. PI3K signalling in inflammation. *Biochimica et biophysica acta* 2014.

174. Futosi K, Fodor S, Mocsai A. Neutrophil cell surface receptors and their intracellular signal transduction pathways. *International immunopharmacology* 2013, 17(3): 638-650.

175. Proudfoot AE. Chemokine receptors: multifaceted therapeutic targets. *Nature reviews Immunology* 2002, 2(2): 106-115.

176. Affeldt KJ, Brodhagen M, Keller NP. *Aspergillus* oxylipin signaling and quorum sensing pathways depend on g protein-coupled receptors. *Toxins* 2012, 4(9): 695-717.

177. Vilardaga JP, Jean-Alphonse FG, Gardella TJ. Endosomal generation of cAMP in GPCR signaling. *Nature chemical biology* 2014, 10(9): 700-706.

178. Tsvetanova NG, Irannejad R, von Zastrow M. GPCR signaling via heterotrimeric G proteins from endosomes. *The Journal of biological chemistry* 2015.

179. Katzmann DJ, Babst M, Emr SD. Ubiquitin-dependent sorting into the multivesicular body pathway requires the function of a conserved endosomal protein sorting complex, ESCRT-I. *Cell* 2001, 106(2): 145-155.

180. Schuh AL, Audhya A. The ESCRT machinery: from the plasma membrane to endosomes and back again. *Critical reviews in biochemistry and molecular biology* 2014, 49(3): 242-261.

181. Whistler JL, Enquist J, Marley A, Fong J, Gladher F, Tsuruda P*, et al.* Modulation of postendocytic sorting of G protein-coupled receptors. *Science* 2002, 297(5581): 615-620.

182. Moser E, Kargl J, Whistler JL, Waldhoer M, Tschische P. G protein-coupled receptor-associated sorting protein 1 regulates the postendocytic sorting of seven-transmembrane-spanning G protein-coupled receptors. *Pharmacology* 2010, 86(1): 22-29.

183. Alfadda TI, Saleh AM, Houillier P, Geibel JP. Calcium-sensing receptor 20 years later. *American journal of physiology Cell physiology* 2014, 307(3): C221-231.

184. Galka F, Wai SN, Kusch H, Engelmann S, Hecker M, Schmeck B*, et al.* Proteomic characterization of the whole secretome of *Legionella pneumophila* and functional analysis of outer membrane vesicles. *Infection and immunity* 2008, 76(5): 1825-1836.

185. Jager J, Keese S, Roessle M, Steinert M, Schromm AB. Fusion of *Legionella pneumophila* outer membrane vesicles with eukaryotic membrane systems is a mechanism to deliver pathogen factors to host cell membranes. *Cellular microbiology* 2014.

186. Rodgers FG, Davey MR. Ultrastructure of the cell envelope layers and surface details of *Legionella pneumophila*. *Journal of general microbiology* 1982, 128(7): 1547-1557.

187. Kimizuka Y, Kimura S, Saga T, Ishii M, Hasegawa N, Betsuyaku T*, et al.* Roles of interleukin-17 in an experimental *Legionella pneumophila* pneumonia model. *Infection and immunity* 2012, 80(3): 1121-1127.

188. Mashburn LM, Whiteley M. Membrane vesicles traffic signals and facilitate group activities in a prokaryote. *Nature* 2005, 437(7057): 422-425.

189. Kesty NC, Kuehn MJ. Incorporation of heterologous outer membrane and periplasmic proteins into *Escherichia coli* outer membrane vesicles. *The Journal of biological chemistry* 2004, 279(3): 2069-2076.

190. Alaniz RC, Deatherage BL, Lara JC, Cookson BT. Membrane vesicles are immunogenic facsimiles of *Salmonella typhimurium* that potently activate dendritic cells, prime B and T cell responses, and stimulate protective immunity in vivo. *Journal of immunology* 2007, 179(11): 7692-7701.

191. Yokomizo T, Izumi T, Chang K, Takuwa Y, Shimizu T. A G-protein-coupled receptor for leukotriene B4 that mediates chemotaxis. *Nature* 1997, 387(6633): 620-624.

192. Yokomizo T, Masuda K, Kato K, Toda A, Izumi T, Shimizu T. Leukotriene B4 receptor. Cloning and intracellular signaling. *American journal of respiratory and critical care medicine* 2000, 161(2 Pt 2): S51-55.

193. Chen L, Yang G. PPARs Integrate the Mammalian Clock and Energy Metabolism. *PPAR research* 2014, 2014: 653017.

194. Remels AH, Langen RC, Gosker HR, Russell AP, Spaapen F, Voncken JW*, et al.* PPARgamma inhibits NF-kappaB-dependent transcriptional activation in skeletal muscle. *American journal of physiology Endocrinology and metabolism* 2009, 297(1): E174-183.

195. Yoon YS, Kim SY, Kim MJ, Lim JH, Cho MS, Kang JL. PPARgamma activation following apoptotic cell instillation promotes resolution of lung inflammation and fibrosis via regulation of efferocytosis and proresolving cytokines. *Mucosal immunology* 2015.

196. Luo S, Huang Y, Xie F, Huang X, Liu Y, Wang W*, et al.* Molecular cloning, characterization and expression analysis of PPAR gamma in the orange-spotted grouper (Epinephelus coioides) after the Vibrio alginolyticus challenge. *Fish & shellfish immunology* 2015, 43(2): 310-324.

197. Jahoor A, Patel R, Bryan A, Do C, Krier J, Watters C*, et al.* Peroxisome proliferator-activated receptors mediate host cell proinflammatory responses to *Pseudomonas aeruginosa* autoinducer. *Journal of bacteriology* 2008, 190(13): 4408-4415.

198. Campden R, Audet N, Hebert TE. Nuclear g protein signaling: new tricks for old dogs. *Journal of cardiovascular pharmacology* 2015, 65(2): 110-122.

199. Spörri R, Joller N, Albers U, Hilbi H, Oxenius A. MyD88-dependent IFN-gamma production by NK cells is key for control of *Legionella pneumophila* infection. *Journal of immunology* 2006, 176(10): 6162-6171.

200. Schuelein R, Ang DK, van Driel IR, Hartland EL. Immune Control of *Legionella* Infection: An *in vivo* Perspective. *Frontiers in microbiology* 2011, 2: 126.

201. Tateda K, Moore TA, Newstead MW, Tsai WC, Zeng X, Deng JC*, et al.* Chemokine-dependent neutrophil recruitment in a murine model of *Legionella* pneumonia: potential role of neutrophils as immunoregulatory cells. *Infection and immunity* 2001, 69(4): 2017-2024.

202. Khandoga AG, Khandoga A, Reichel CA, Bihari P, Rehberg M, Krombach F. *In vivo* imaging and quantitative analysis of leukocyte directional migration and polarization in inflamed tissue. *PloS one* 2009, 4(3): e4693.

203. Woodfin A, Voisin MB, Beyrau M, Colom B, Caille D, Diapouli FM*, et al.* The junctional adhesion molecule JAM-C regulates polarized transendothelial migration of neutrophils in vivo. *Nature immunology* 2011, 12(8): 761-769.

204. Tateda K, Moore TA, Deng JC, Newstead MW, Zeng X, Matsukawa A*, et al.* Early recruitment of neutrophils determines subsequent T1/T2 host responses in a murine model of *Legionella pneumophila* pneumonia. *Journal of immunology* 2001, 166(5): 3355-3361.

205. Thepen T, Van Rooijen N, Kraal G. Alveolar macrophage elimination *in vivo* is associated with an increase in pulmonary immune response in mice. *The Journal of experimental medicine* 1989, 170(2): 499-509.

206. Simon, S., Schell, U., Heuer, N., Hager, D., Matthias, J., Trauner, D., Eichinger, L., Hedberg, C., Hilbi, H. Inter-kingdom signaling by the *Legionella* quorum sensing molecule LAI-1 inhibits cell migration through an IQGAP1-Cdc42-ARHGEF9 dependent pathway. Submitted.

VI. Appendix

A. Abbreviations

AHL	acyl-homoserine lactone
AI	autoinducer
AYE	ACES yeast extract
CAI-1	cholera autoinducer 1
Cam	chloramphenicol
cAMP	cyclic adenosine 3´, 5´- monophosphate
Cdc42	cell division control protein 42
CHD	calponic homology domain
CYE	charcoal yeast extract
DOCK	dedication of cytokinesis
Dot	defective organelle trafficking
FACS	fluorescence-activated cell sorting
FCS	fecal calf serum
FMI	forward migration index
fMLP	formyl-methyl-leucyl-phenylalanine
GAP	GTPase-activating protein
GDI	GDP dissociation inhibitor
GEF	guanine nucleotide exchange factor
GPCR	G protein-coupled protein
GRD	GTPase activating protein related domain
h	hour
Icm	intracellular multiplication
IFN	interferon
IFNAR	interferon α/β receptor
IL	interleukin

IPTG	isopropyl 1-thio-β-D-galactopyranoside
IQGAP1	Ras GTPase-activating-like protein
Kan	Kanamycin
L	liter
LAI-1	*Legionella* autoinducer 1
LCV	*Legionella* containing vacuole
LegG1	*Legionella* eukaryotic gene 1
LPS	lipopolysaccharide
Lqs	*Legionella* quorum sensing
M	molar
MAPK	mitogen-activated protein kinase
min	minute
MOI	multiplicity of infection
MTOC	microtubule organization center
nm	nanometer
NFκB	nuclear factor kappa-light-chain-enhancer of activated B cells
OD_{600}	optical density at 600 nm
OMV	outer membrane vesicle
PBS	phosphate-buffered saline
PI	propidium iodide
PI3K	phophoinositide-3-kinase
PIP2	phosphatidylinositol (4,5)-bisphosphate
PIP3	phosphatidylinositol (3,4,5)-triphosphate
PMN	polymorphonuclear neutrophil
PPAR	peroxisome proliferator-activated receptor
QS	quorum sensing
^{R}	resistant
Rac1	Ras-related C3 botulinum toxin substrate 1

Ran	Ras-related nuclear protein
RCC1	regulator of chromosome condensation 1
RCG	Ras GAP C-terminal
RhoA	Ras homolog gene family member A
sec	second
SorC	Sörensen phosphate buffer
T1SS	type I secretion system
T2SS	type II secretion system
T3SS	type III secretion system
T4SS	type IV secretion system
T5SS	type V secretion system
TBS	TRIS buffered saline
TCS	two-component system
TLR	Toll-like receptor
WT	wild-type

B. Publications

Publications described in this thesis:

Simon, S., Schell, U., Heuer, N., Hager, D., Matthias, J., Trauner, D., Eichinger, L., Hedberg, C., Hilbi, H. Inter-kingdom signaling by the *Legionella* quorum sensing molecule LAI-1 inhibits cell migration through an IQGAP1-Cdc42-ARHGEF9 dependent pathway. Submitted.

Simon, S., Wagner, MA,, Rothmeier, E., Müller-Taubenberger, A., Hilbi, H.. (2014) Icm/Dot-dependent inhibition of phagocyte migration by *Legionella* is antagonized by a translocated Ran GTPase activator, *Cell. Microbiol. 16*, 977–992. Highlighted as editor´s choice in the issue of July 2014.

Additional publication:

Schell, U., Simon, S., Sahr, T., Hager, D., Trauner, D., Hedberg, C., Buchrieser, C., Hilbi, H. The *Legionella pneumophila* α-hydroxyketone LAI-1 regulates LqsS- and LqsT-dependent phosphorylation signaling and gene expression. In preparation.

C. Danksagung

Zuerst geht ein riesiges Dankeschön an meinen Doktorvater Prof. Hubert Hilbi. Danke für dein Vertrauen und deine Unterstützung. Deine fantastische Betreuung und durchgehend aufbauenden Tipps haben zu einer gelungenen Doktorarbeit geführt. Ich freue mich auf die Zeit in Zürich. Während meiner Zeit am Max von Pettenkofer Institut habe ich viel erlebt, professionell wie privat. Viel habe ich dazu gelernt und neue wichtige Freundschaften geschlossen. Einiges haben wir zusammen erlebt, über Geburtstage, Weihnachtsfeste, Ausflüge sowie tolle Abende in Biergärten oder an der schönen Isar. Danke an Verena, Ursula und Christine, ihr seid für mich zu treuen Freundinnen geworden. Einiges haben wir erlebt, dass uns zusammen geschweißt hat. Zahlreiche Gespräche und sehr witzige Momente haben mir im Labor Alltag Energie und gute Laune gebracht. Vielen Dank für eure Präsenz! Dankeschön auch an Ivo, Chris, Ute und Aline, ihr seid für mich zu sehr guten Freunden geworden mit denen ich sehr viel Spaß hatte, etliche lustige Abende verbracht habe und auf den besten Partys war, Prost!!! Gudrun, einen besonderen Dank für deine Präsenz und zahlreiche aufbauenden Gespräche. Das Gleiche gilt für Ben und Eva L.. Ebenso bei Ina, Maria, Stephen und Steffi für angenehme und erfahrungsreiche Arbeitszeiten. Einen besonderen Dank an Ina für deine Ratschläge und Tipps für meinen kommenden Zürich Umzug. Euch allen viel Erfolg und Glück in der Zukunft. Ein Dankeschön an dich Sandra, mit dir habe ich in den letzten Jahren viel erlebt, ein Großteil Europas durchreist, gefeiert und über die gleichen Sachen gelacht. Flat, depuis les bancs de la fac, de nombreuses années sont passées, durant lesquelles une solide amitié s'est formée, merci pour ta présence! Danke Sebastian, dass du vor Kurzem in mein Leben getreten bist, ich freue mich sehr auf die kommende gemeinsame Zeit.

Wörter scheinen mir nicht genug zu sein um mich bei meiner Mutter zu bedanken. Maman, merci beaucoup, danke, dass du immer für mich da warst, ich konnte mich schon immer auf dich verlassen. Ohne dich hätte ich es niemals so weit geschafft. Deine Unterstützung und Liebe, in schönen wie in schweren Zeiten, hatte keine Grenzen. Merci pour tout, je t'aime énormément. Un grand merci également à ma famille du Canada et de Mothern, tout particulièrement à mes grands-parents inoubliés.

Au revoir

D. Affidavit

I, Sylvia Simon, declare that I have written this thesis entitled „Modulation of host cell migration by *Legionella pneumophila* effectors and signaling compounds“ independently and that I have not used other sources than declared. Furthermore, I confirm that this thesis has not yet been submitted as part of another examination process neither in identical nor in similar form.

_____ _____

Place, Date Signature

Eidesstattliche Versicherung

Hiermit erkläre ich, Sylvia Simon, an Eides statt, die Dissertation “Modulation of host cell migration by *Legionella pneumophila* effectors and signaling compounds“ eigenständig und selbständig verfasst zu haben und mich außer der angegebenen keiner weiteren Hilfsmittel bedient zu haben. Alle Erkenntnisse, die aus dem Schrifttum ganz oder annähernd übernommen sind, wurden als solche kenntlich gemacht und nach ihrer Herkunft unter Bezeichnung der Fundstelle einzeln nachgewiesen. Ich erkläre des Weiteren, dass die hier vorgelegte Dissertation nicht in gleicher oder in ähnlicher Form bei einer anderen Stelle zur Erlangung eines akademischen Grades eingereicht wurde.

_____ _____

Ort, Datum Unterschrift